Removal of Arsenic Species through Coagulation-Flocculation Processes

A Thesis Submitted to the College of

Graduate Studies and Research

In Partial Fulfillment of the Requirements

For the Master's Degree in the Department of Chemistry

University of Saskatchewan

Saskatoon

By

Savi Bhalkaran

Permission to Use

In presenting this thesis in partial fulfillment of the requirements for a Postgraduate degree from the University of Saskatchewan, I agree that the Libraries of this University may make it freely available for inspection. I further agree that permission for copying of this thesis in any manner, in whole or in part, for scholarly purpose may be granted by the professor or professors who supervised my thesis work or in their absence, by the Head of the Department or the Dean of the College in which my thesis work was done. It is understood that any copying or publication or use of this thesis or part thereof for financial gain shall not be allowed without my written permission. It is also understood that due recognition shall be given to me and to the University of Saskatchewan in any scholarly use which may be made of any material in my thesis.

Requirements for permission to copy or to make use of material in this thesis in whole or part should be addressed to:

Head of Department of Chemistry

University of Saskatchewan

Saskatoon, SK (S7N5C9)

Canada

Abstract

Through the traditional water treatment process of coagulation-flocculation, this thesis aims to investigate the effectiveness of the removal of organic and inorganic forms of arsenic using a two-component coagulant-biopolymer flocculant system. Among the metal salts chosen in this study, the optimal dosage required was 30 ppm for alum, and 15 ppm for Fe(II) chloride and Fe(III) chloride metal salts. The dosage of the biopolymers was 2.5 ppm for medium molecular weight chitosan (MMWC) and 10 ppm for high viscosity sodium alginate (HVA). In addition to the optimal dosage parameters, pH effects were evaluated at several values (pH 3, 5, 7 and 9) due to the importance of charge neutralization in coagulation-flocculation processes. The results showed no significant decrease in turbidity removal at variable pH using a Jar test apparatus. The stirring time and speed was optimized at several conditions: 3 minutes (295 rpm) and 20 minutes (25 rpm) and finally, the addition of the polymers was added in a sequential manner rather than as a single step using a premixed polymer system. This last step was chosen because premixed polymers were less effective.

The next stage of research involved the use of an optimized system to study the removal of roxarsone (4-hydroxy-3-nitrobenzene arsonic acid). The use of a coagulant-biopolymer system (Fe(III)-MMWC/HVA) was shown to be effective for the removal of roxarsone at initial concentrations of 30, 40, 50 ppm. Jar test studies reveal that the concentration of free roxarsone decreased when Fe(III) alone was used as a coagulant, in the presence and absence of kaolinite. Addition of biopolymers generally lead to a decrease in roxarsone uptake. Arsenate (V) was studied using a Jar test setup at an initial concentration of 30 ppm. The removal (%) of arsenate (V) was shown to be slightly higher than roxarsone at 42%, as compared to 23% using the metal salt-biopolymer system without kaolinite. Addition of kaolinite to the arsenate (V) caused a 10% increase in removal (%) when using Fe(III) and Fe(III)-HVA system, where no discernible change was found for the Fe(III)-MMWC/HVA system.

The *one-pot* method was used to study the kinetics during floc formation and settling. The removal efficacy (%) was plotted against time and revealed that Fe(III) species were primarily responsible for roxarsone removal, while alginate hinders the roxarsone uptake. Kinetic studies were carried out using the one-pot method and evaluated by two kinetic models, the pseudo-first order (PFO) and pseudo-second order (PSO) models by plotting "arsenic uptake" (Q_t) in mg/g

against time (t). The PFO model was more favorable, indicating reversible binding interactions throughout the coagulation-flocculation process of roxarsone and arsenate (V) with Fe(III), MMWC and HVA. Thermodynamic studies were carried out at variable temperatures (20 ºC, 30 ºC and 40 ºC) using only Fe(III) and the Fe(III)–MMWC/HVA systems, in the presence and absence of a model colloid (kaolinite). All "apparent" E_a values were negative for the removal of As(V), except for the removal of arsenate(V) in the presence of kaolinite with Fe(III)-MMWC/HVA. Thermodynamic activation parameters ($\Delta H^{\ddagger}$, $\Delta S^{\ddagger}$ and $\Delta G^{\ddagger}$) were estimated by Eyring theory, where most $\Delta H^{\ddagger}$ values were negative for the coagulation-flocculation process. A dominant and negative value of $\Delta S^{\ddagger}$ was obtained due to floc formation with arsenic and Fe(III), chitosan and alginate, with a resulting positive $\Delta G^{\ddagger}$ for the process.

Acknowledgements

First and foremost, I would like to thank my supervisor, Dr. Lee D. Wilson, whose guidance, unwavering support and encouragement was integral to the writing and completion of my thesis. I shall forever be grateful for his patience throughout my master's program.

Thanks are extended to my committee member, Dr. Graham George, for his helpful advice. I would also like to thank Dr. Robert Scott. Both professors provided helpful comments and suggestions that helped to improve my research. Thank you to Dr. Joyce McBeth for agreeing to be my external examiner, especially on such short notice.

To the members of my group, I extend my deepest gratitude. Each one of you provided me with support and encouragement that I will always remember. Thank you for all the help you provided in the lab and in the writing of this thesis.

I am deeply appreciative to my mother and family for their unwavering support and guidance throughout the years. Thanks also to my friends, especially my group, for the good times during these two and a half years.

Lastly, I would like to thank the University of Saskatchewan for the funding provided through the Dean's Scholarship and the Government of Saskatchewan through the Ministry of Agriculture (Agriculture Development Fund). I would also like to thank the Fund Management Committee of the University of Saskatchewan for the John Spencer Middleton and Jack Spencer Gordon Middleton bursary.

Dedication

I would like to dedicate this thesis to

my mother, Haymatrie Pattiram

Table of Contents

List of Abbreviations

As(V)	Arsenate (V)
Buff	Buffer solution
DLS	Dynamic Light Scattering
DW	Distilled water
EM	Electrophoretic mobility
FTIR	Fourier Transform Infrared spectroscopy
HVA	High viscosity alginate
ICP-OES	Inductively Coupled Plasma-Optical Emission Spectroscopy
IR	Infrared spectroscopy
LMWC	Low molecular weight chitosan
LVA	Low viscosity alginate
MMWC	Medium molecular weight chitosan
pK_a	Acid Dissociation Constant
ppb	Parts per billion
ppm	Parts per million
ROX	Roxarsone
rpm	Revolutions per minute
SEM	Scanning Electron Microscopy
XAS	X-ray absorption spectroscopy

List of Figures

List of Tables

List of Schemes

Chapter 1 INTRODUCTION

1.1 Arsenic

1.1.1 Physical Characterization of Arsenic

Arsenic is the thirty-third element in the periodic table, with an atomic weight of 74.9 g/mol and comes in three allotrope forms: α-metallic form (steel-gray brittle crystalline metal), β-arsenic (black amorphous vitreous solid) and yellow arsenic. Arsenic is present as the 20th most abundant element in the earth's crust, 14th in sea water and 12th in the human body. It sublimes at 613°C when heated at normal atmospheric pressure and has a melting point of 817°C at 28 atm. Its vapor pressure is 1 mmHg at 372 ºC and it has a specific gravity of 5.73.[1] Arsenic was isolated by Albertus Magnus in 1250 A.D.[2] Arsenic is insoluble in water, caustic soda, hydrogen and hydrochloric acid, unless there is an oxidant present, in which case it will react with concentrated hydrochloric acid.[1]

1.1.2 Arsenic Compounds and their Occurrence

Arsenic is the 20th most abundant element in the earth's crust and is widely distributed globally. It can be found in the earth's crust, in land (soils), bodies of water (fresh and sea water), sediments and the atmosphere. It is usually associated with minerals that contain sulphur and metals. Some of the highest amounts of arsenic occur in marine shale, magmatic sulphides and minerals such as orpiment (As_2S_3), realgar (AsS), niccolite (NiAsS), cobalite (CoAsS) and arsenopyrite (FeAsS).[3] Anthropogenic sources of arsenic include processes such as the smelting of Cu, Pb, Ni and Zn ores, the burning of fossil fuels in households and power plants, in production processes of items such as coloring agents, and it is especially prevalent in chemicals such as herbicides, pesticides and fungicides used in agriculture.[4] Arsenic was used widely in pharmaceuticals before the advent of antibiotics. Ailments including psoriasis, rheumatism, arthritis, asthma, malaria, trypanosomiasis, tuberculosis, to name a few were treated with mixtures that contained arsenic compounds.[4,5]

Arsenic is a metalloid, found in group 15 of the periodic table and it is rarely found in its elemental state. Arsenic occurs in several different oxidation states; +5 (arsenate), +3 (arsenite), 0 (arsenic) and -3 (arsine).[6] The arsine species of arsenic is a gaseous form of arsenic. As such, it can be found in many forms, where it may be combined with carbon in organic compounds and with other elements, such as oxygen and iron,[7] to give inorganic compounds.

1.1.2.1 Organic Arsenic Compounds

Arsenic can combine with carbon to form various organic compounds. Organoarsenical compounds can possess variable oxidation state (+3 or +5), with the general formulae R_3As and R_5As, respectively. Organoarsenical compounds have been known for many centuries. The first organic arsenic compound discovered was tetramethyldiarsine or 'cacodyl' as it was commonly identified. Eventually studies lead to the discovery of Salvarsan by Paul Ehrlich as a treatment for syphilis. It is a mixture of 3- and 5-membered As-As rings with aromatic groups attached.[8]

Many organoarsenicals are used in agriculture, as herbicides, pesticides and feed additives. Examples include roxarsone (4-hydroxy-3-nitrophenylarsonic acid), which was formerly used as a feed additive in poultry and swine farming[9] and monosodium methanearsonate (MSMA), a pesticide used on cotton plants. Roxarsone was banned from use due to the possibility of its breakdown into toxic inorganic arsenic species by bacteria present in soils.[10] There are also microorganisms such as certain bacteria and fungi that can do the reverse; that is, they can convert inorganic arsenic species into organic species, such as monomethylarsonic acid (MMA) and dimethylarsonic acid (DMA).[11]

Organic arsenic compounds occur in water bodies naturally as well as through anthropogenic sources. The concentrations are increased due to biological methylation by microbes such as bacteria, yeasts and algae.[12] Methylation of arsenic species occurs widely, occurring in soil, aquatic environments, plants, and animals, including humans.[13] For instance, *C. humiculus*, which can found on preserved wood, and *Rhodotorula rubra*, a marine yeast, can both methylate arsenic species.[12] In surface waters, dimethylarsinic acid (DMAA) and monomethylarsinic (MMAA) are dominant forms and are found in higher amounts during summer due to increased microbiological activity.[7,14]

1.1.2.2 Inorganic Arsenic Compounds

Inorganic species of arsenic compounds tend to be oxyanions, with variable valence on the arsenic species of +3 and +5. The oxyanion containing arsenic in the +3 state is the arsenite anion (AsO_3^{3-}) and occurs primarily in anaerobic conditions, such as in some well or ground waters.[15] The arsenate species (AsO_4^{3-}) contain arsenic in the +5 state and this occurs under oxygenated conditions, such as in some surface waters and soils.[16] Arsenic in water dissociates into several ionic species based on the pH of the surroundings. The equations below show the dissociation for the arsenite and arsenate species and the associated pK_a values.[17]

$$H_3AsO_3 \underset{}{\overset{-H^+,\ pK_a=9.1}{\rightleftharpoons}} H_2AsO_3^- \overset{-H^+,\ pK_a=12.1}{\rightleftharpoons} HAsO_3^{2-} \overset{-H^+,\ pK_a=13.4}{\rightleftharpoons} AsO_3^{3-} \quad (1\text{-}1)$$

$$H_3AsO_4 \overset{-H^+,\ pK_a=2.1}{\rightleftharpoons} H_2AsO_4^- \overset{-H^+,\ pK_a=6.7}{\rightleftharpoons} HAsO_4^{2-} \overset{-H^+,\ pK_a=11.2}{\rightleftharpoons} AsO_4^{3-} \quad (1\text{-}2)$$

Based on the pH and pE of the environment, the speciation of arsenic oxyanion species shows a wide variation (as shown in Figure 1.1). This diagram shows the conditions under which the arsenic speciation exists in equations 1-1 and 1-2. Studies conducted on arsenic removal have evaluated the removal of arsenate and arsenite species in aqueous environments, particularly because of the ease of mobility of these arsenic species over a wide range of redox conditions, especially at those pH values prevalent in groundwater (6.5 – 8.5).[7]

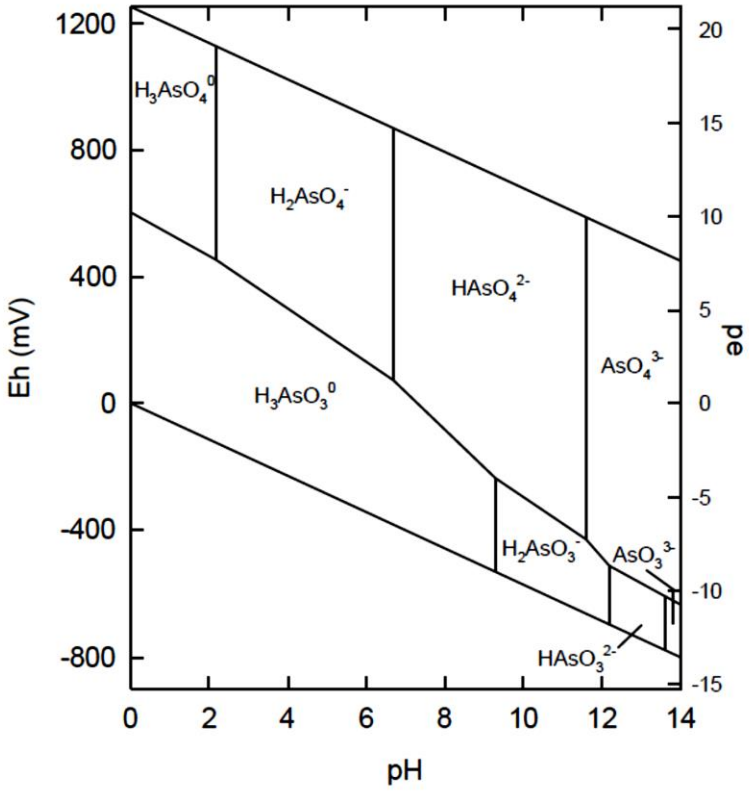

Figure 1.1: Eh-pH diagram for aqueous As species in the system As–O_2–H_2O at 25 ºC and 1 bar total pressure[18] [Reproduced with permission from Ref. 18]

Inorganic forms of arsenic (oxyanion species) exist in many bodies of water. For instance, rain water contains low levels (< 0.14 μgL^{-1}) naturally. When a location is nearer to a copper smelting plant, such as the Tacoma smelter near Seattle, the amount of arsenic increases (16 μgL^{-1}).[7,19] Arsenic can enter the atmosphere through wind erosion, volcanic emissions, low temperature volatilization from soils, marine aerosols and through pollution, as shown in the

previous example. The chemical forms of arsenic will depend on where it originated from; as an example, smelting may produce arsenic (III) oxide (As_2O_3), while arsenic (III) hydride (AsH_3) may be present near landfills. However, exposure to oxygen in the atmospheric, will oxidize some of the As(III) species to their corresponding As(V) forms.[4,7]

Arsenic contamination of rivers is also low naturally (~0.1 – 0.8 μgL^{-1}) and can vary depending on location due to industrial effluents and bedrock composition.[7] Those rivers that contain As-poor bedrocks will also possess less arsenic in the water. High arsenic concentration (190 – 21,800 μgL^{-1}) have been found in the Loa River Basin of northern Chile, which occurs naturally due to water flowing from arsenic-containing rocks to the surface water of the river.[20] The accompanying pH and alkalinity were found to be high as well. For those rivers that are near industrial sources of pollution, arsenic levels can be high as 1,100 μgL^{-1} but will vary quite a lot depending on the source of pollution and other factors, such as surrounding environment.[16] The majority of arsenic species are As(V) vary seasonally; however, biological activity or close proximity to industrial effluents may maintain As(III) levels.[4,7]

The arsenic concentration of lakes tends to be similar or lower than those found in rivers. Azcue and Nriagu found arsenic levels of ~22 and ~62 μgL^{-1} in Lake Moira, Ontario during summer and winter, respectively.[21] The presence of geothermal waters, as well as anthropogenic activities, tends to affect the arsenic levels. These contribute to arsenic pollution that resemble values found in rivers, where the arsenic levels increase with increased level of geothermal water, due to heating effects caused by geothermal energy, and mining activity.[18] Some remediation of lakes contaminated by mining can occur by adsorption of the arsenic to iron oxides under neutral to mildly acidic conditions.[18] Alkaline environments (pH 9.5 – 10) encourage higher concentrations of arsenic, especially in conjunction with increased geothermal activity. For example, Mono Lake in California was found to have 10,000 – 20,000 μL^{-1} dissolved arsenic due to increased evaporation and weathering of volcanic rocks.[18] However, Mono Lake has a higher amount of arsenic compared to other lakes, which is probably due to geothermal activity, as evidenced by geothermal waters having an average arsenic content between 10 to 50,000 μL^{-1}.[18] Lakes show similar proportion of As(III) and (V) as rivers but they show greater variability in stratified lakes owing to their larger difference in redox reactions across strata.[18]

The baseline level of arsenic in seawater is relatively constant, at around 1.5 μgL^{-1}.[7] It is found that in marine oxic waters, the concentration of arsenate decreases with increasing biological

activity in surface waters.[18] This is linked to the similarity in structure of arsenate to phosphate, with both species participating in biological processes. The As(V)/As(III) ratio in open seawater is typically in the range 10-100 and exists mainly as $HAsO_4^{2-}$ and $H_2AsO_4^-$ for As(V) and H_3AsO_3 for As(III).[4,7]

Since the main source of drinking water in most places is groundwater aquifers, arsenic levels in groundwater should be carefully monitored. There is a wide variation of arsenic concentration in groundwater, ranging between 0.5 to 5000 μgL^{-1}.[18] As Figure 1.2 shows, the presence of arsenic is found around the world and present under oxidizing and reducing conditions.[22] A large percentage of these occurrences are from natural sources. Evaporation, leaching from arsenic rich minerals and geothermal waters all contribute to high arsenic levels. In strongly reducing aquifers, (possessing Fe(III)- and sulfate-reducing microbes), As(III) will exist in higher concentration.[18,23] As(V) dominates in oxidizing waters.[7]

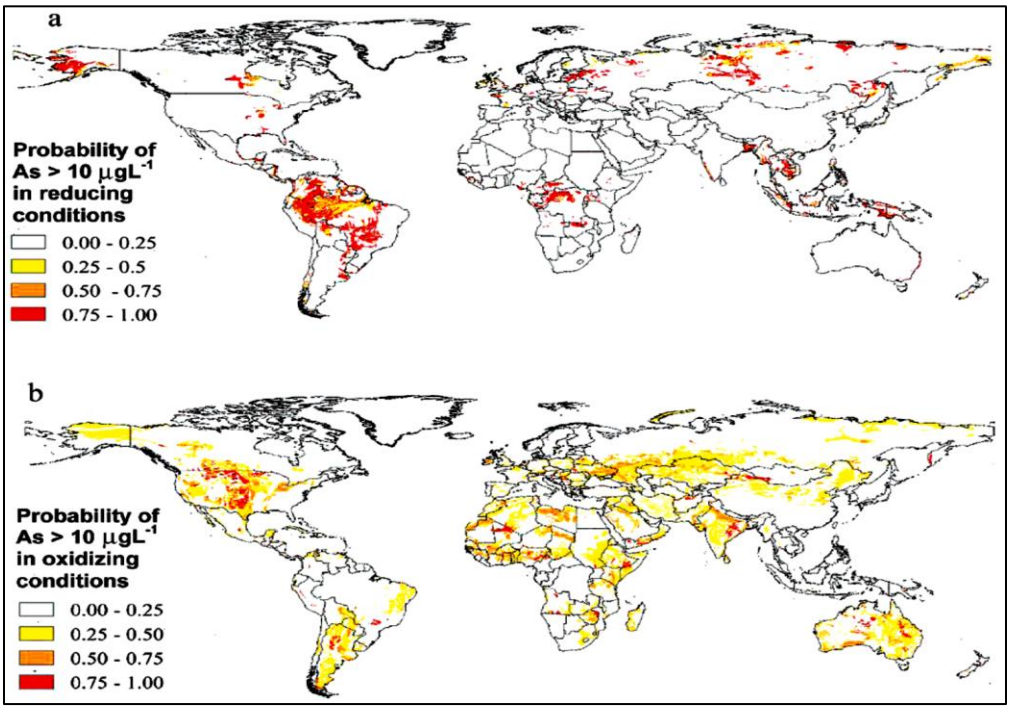

Figure 1.2: Estimated global occurrence of arsenic[24] [Reproduced with permission from Ref. 24]

1.1.2.3 Aqueous Speciation of Arsenic

The distribution of arsenate and arsenite species in aqueous systems depends on the pH and reduction-oxidation (redox) potential of the system. Figure 1.1 shows the species distribution of arsenic in aqueous environment at a range of pH and redox potential conditions. The Eh represents the redox potential of the aqueous environment, where the lower the value, the higher

its reduction potential (ability to be reduced) and the higher the value, the greater is the oxidation potential (ability to be oxidized). The boundaries which contain the various arsenic oxyanion species represent the limit within which water exists. To exceed the Eh of the upper limit means that the water will be oxidized to oxygen, and to go below the lower limit means that the water will be reduced to hydrogen gas. The vertical boundaries illustrate the acid-base equilibria between arsenate and arsenite species, respectively, and are further illustrated using acid-base equations 1-1 and 1-2 in Section 1.1.2.2. The diagonal lines in the diagram represent a combination of acid-base equilibria and redox equilibria. It should be noted that the lines slope diagonally because the basic species favor a more oxidized state.[25] It should be noted that conditions at pH 6.5 – 8.5, the common pH range of natural waters, arsenite species have no ionic charge, while arsenate species are anionic in nature.[18]

1.1.3 Applications of Arsenic Compounds

The uses for arsenic compounds have been, and continue to be, many and varied across diverse industries. Some of those industries include pharmaceuticals, agricultural chemicals, and tailings from mining, metallurgy, glass-making, wood-preservatives and semi-conductor processes. While use of much of the previous arsenic compounds have been discontinued due to human toxicity, complete elimination has not been achieved due to the versatility and favorable properties of certain arsenic species, such as gallium arsenide due to its high-electron mobility.[4,15]

Elemental arsenic is used in the manufacture of alloys, commonly combined with lead and copper.[26] Arsine gas is used in the fibre optic industry and the manufacture of computer chips as a doping agent.[26] The myriad other compounds of arsenic are used in applications such as manufacture of pigments, dyes and soaps, electrophotography, ceramics and many other areas.[7]

1.1.4 Arsenic in the Environment

1.1.4.1 Environmental Arsenic Impacts on Human Health

Exposure to arsenic mainly occurs through the ingestion of food or beverages contaminated with the arsenic species.[26] The other way that humans are exposed to arsenic is through inhalation of arsenic species in air, though this poses a lesser risk due to reduced levels of volatilized arsenic species in the atmosphere and not due to toxicity since arsine gas is the most toxic arsenic species (fatal dose is 250 mg/m^3 at an exposure time of 30 minutes).[4] The trivalent arsenic species poses a greater threat to biological systems, as compared to the pentavalent species due to its ability to be re-absorbed into the system at a faster rate.[4] Both affect the functioning of mitochondria; As(III)

can cause enzymes to become denatured through binding with sulfhydryl groups in proteins and As(V), due to its similarity in structure to phosphate groups, may disrupt binding in adenosine triphosphate during oxidative phosphorylation.[27]

Arsenic toxicity can cause varying effects depending on whether the poisoning is chronic or acute. The long term gradual process of ingesting small amounts of arsenic (chronic) leads to many varied adverse effects. For instance, symptoms can range from mild, such as chronic weariness and hair loss, to severe, such as disturbance in the peripheral vascular and nervous systems and circulatory disorders.[4] Large amounts of arsenic ingested over a short time period (acute) can result in more severe symptoms such as vomiting, dry mouth, abdominal pain, and nervous weakness.[4] These symptoms eventually end in death within 24 h from fatal shock caused by renal failure.[4] Beyond 24 h, severe organ damage will eventually lead to death as well. Arsenic is dangerous because it disrupts the repair process for damaged DNA.[4] For this reason, arsenic is linked to the development of several cancers, including those of the lungs, bladder, skin and liver.[4] Inorganic forms of arsenic have a higher toxicity when compared to organic forms. The lethal dose (LD_{50}) for inorganic sodium arsenite is 4.5 mg/kg and sodium arsenate is 14 to 18 mg/kg, whereas organic monomethylarsonic acid (MMA) requires much higher dosage at 1800 mg/kg and dimethylarsinic acid (DMA) requires 1200 mg/kg.[4]

1.1.4.2 WHO Guidelines for Arsenic

Throughout the world, high levels of naturally-occurring and anthropogenic sources of arsenic in drinking water pose significant health concerns. The map in Figure 1.2 illustrates the worldwide occurrence of arsenic levels that exceed the World Health Organization (WHO) guidelines in regions of high-pH/oxidizing and reducing environmental conditions. This model was obtained by combining arsenic data with data obtained by probability map models.[24] To determine if a region was generally high-pH/oxidizing, it should be arid, have poor drainage conditions and subsoil pH should be high. For reducing regions, the area should be humid, drainage conditions should be poor and organic content of the subsoil should be high. It is quite evident that many countries have arsenic levels in groundwater and surface water that exceeds the safe limit.[22] That limit, set by the WHO, is 10 ppb (μgL^{-1}) and is regarded as the highest level of arsenic that is safe for drinking water to contain.[7] This value was lowered from 50 ppb in 1993, which was primarily due to the advanced analytical capability of instruments for detection of arsenic.[7] As the

sensitivity of arsenic detection further increases, the lower limits of arsenic detection limit will be improved.

1.2 Methods for the Removal of Waterborne Contaminants

Because of the danger posed by arsenic poisoning, many processes have been investigated to lower the levels of arsenic in water. Some of these processes are adsorption, oxidation, ion-exchange, phytoremediation, reverse osmosis, membrane filtration and coagulation-flocculation.[28] Each process has been met with some degree of success. The most widely used methods found in the literature for arsenic removal are adsorption and coagulation-flocculation.[28]

Adsorption is the removal of contaminants using a heterogeneous system, where the species being used for the removal (adsorbent) is in the solid state and the species being removed is either in a gaseous or liquid state. Its advantages include ease of handling, low cost, high removal efficiency and lack of sludge formation.[17]

Oxidation is usually used in conjunction with other removal methods, such as adsorption or filtration. Arsenic removal via oxidation aids in removal by converting soluble As(III) to As(V), which is also soluble but has a greater affinity for sorption onto solid surfaces. In many cases, the oxidation is also for the benefit of forming a suitable species for removal of the arsenic. For instance, the oxidation of Fe(II) to Fe(III), and subsequent iron (III) hydroxide formation provides a surface site for arsenic anions to adsorb.[29–31] There are many ways oxidation can be achieved that include the use of chemical oxidants, photochemical, photocatalytic and biological oxidation.[28]

Ion-exchange involves the adsorption of ions on specially made solid resins with the contaminant ions in solution.[5] Resins usually consist of three-dimensional hydrocarbon networks with pendant ionizable groups. The ions to be removed need to have a stronger affinity for the resin as compared to the ionizable groups. Arsenate removal works well with strong-base anion resins such as, $HCrO_4^-$ and ClO_4^-, suitable for arsenate removal.[5]

Phytoremediation utilizes certain plant species for their natural metal ion uptake ability. The plants usually hyperaccumulate the ions in areas such as plant roots or like the *Pteris vittata* (Chinese brake fern) in fronds.[32]

Reverse osmosis is excellent for arsenic removal on the small scale. It uses membranes with pore sizes <0.001 μm and high pressures that force water through the membrane and leaves the arsenic trapped on the influent side of the membrane.[32] Membrane filtration works in the same

way but depending on the type of membrane, the pore sizes will be different. For instance, microfiltration, ultrafiltration and nanofiltration require membranes of pore sizes 0.1 – 10 μm, 10 – 1000 Å and ~1 nm, respectively.[32]

Coagulation-flocculation is a very common water treatment method. This approach is especially useful for the removal of colloidal species; however, it has been used for the removal of many other types of contaminants, including arsenic.[32] It involves the addition of a coagulant, which works by reducing the charge repulsion of the surface of the charged species to be removed by allowing them to self-assemble into flocs. Further addition of a polymer flocculant allows for bridging of the flocs formed into larger sizes which undergo colloidal destabilization.[33]

1.2.1 General Removal Methods for Organic Arsenic Species

Many studies have focused on the removal of inorganic arsenic species from water and wastewater. However, the widespread occurrence of arsenic in nature, bacterial and fungal species can convert many of the arsenic species into organic forms. Of the four most reported arsenic species in water (arsenite, arsenate, MMA, DMA), two of these are organic forms of arsenic.[34]

Thirunavukkarasu *et al.*[34] studied DMA removal using manganese greensand (MGS), iron oxide-coated sand (IOCS-1 and IOCS-2) and an ion-exchange resin activated with Fe^{3+} ions. IOCS-2 and the ion-exchange resin performed better than IOCS-2 and MGS, both of which showed poor uptake. IOCS-2 had an uptake of 8μg/g after 7 h and the ion-exchange resin had an uptake of 5.7 μg/cm^3.[34] Ramesh *et al.*[35] also studied the removal of DMA using adsorption onto polymeric Al/Fe modified montmorillonite. The maximum uptake for DMA on the montmorillonite was 18.8 mg/g, which was lower than the uptake of As(III) and (V) with the same adsorbent.[35] This work also made reference to other studies[34,36,37] that investigated DMA removal, of which it had the highest uptake.

1.2.2 General Removal Methods for Inorganic Arsenic Species

Inorganic arsenic species are abundant in natural waters due to natural weathering processes, the dissolution of As-bearing minerals and anthropogenic activities such as mining and pesticide use.[38] Most of the inorganic arsenic species are in the +3 and +5 oxidation state. The characteristics of As(III) and (V) differ from each other and leads to differing binding affinity for the two types of As species by removal agents. Leupin and Hug[39] investigated the removal of As (III) species using filtration through sand and zero-valent iron in a column in the presence of phosphate and silicate.[39] The process worked by passing 1 L of synthetic As(III) spiked-water

through the column that becomes re-aerated between each filtration cycle. The mechanism suggested by the authors is that of oxidation of zero-valent iron to Fe(II), which is leached into the water; this is followed by further oxidation to Fe(III) as the water passes through the column in the various columns. The Fe(III) is converted to hydrous ferric oxides (HFO), which adsorb As(III) and As(V). As(V) comes from the concomitant oxidation of As(III) during the wash cycles.[39] Studies by Meng *et al.*[40] on As(III) and As(V) also indicated that the removal of arsenic was due to adsorption and co-precipitation on ferric hydroxides formed from ferric chloride. These studies highlight the interference effects caused by silicates present in the water.[40]

Another removal method used for inorganic arsenic was nanofiltration (NF) and reverse osmosis (RO) membranes. Košutić *et al.*[41] investigated arsenate and pesticide removal using two commercial NF membranes and a reverse osmosis membrane. It was found that NF membranes were highly effective in rejecting arsenate from passing the filter; however, this was not significantly different from the RO membrane. The NF membrane mechanism of action relates to charge exclusion. In the case of the RO membrane, it was simply based on size.[41]

The use of coagulation-flocculation for the removal of arsenic has been primarily done using alum and ferric salts, such as ferric chloride and sulphate. More recently synthetic and natural biopolymers have been incorporated into studies of the process with the regular coagulants or have replaced them as substitutes. Hering *et al.*[42] investigated As(III/V) removal using both alum and ferric chloride with sourced and artificial freshwaters.[42] Both coagulants were found to be effective at removing As(V) (from 20 µg/L up to 2 µg/L) at pH 7. Fe(III) proved to be active over a wider pH range with co-removal of As(III). Alum proved ineffective at removal of As(III) from source waters and it was more negatively influenced by the presence of natural organic matter (NOM) and sulphates, whereas Fe(III) was not affected. Hesami *et al.*[43] employed chitosan along with ferric chloride in the removal of As(III/V). It was determined that the addition of chitosan hindered removal slightly but caused less Fe(III) to be required. As(V) removal was ~95%, while As(III) was 70% using the Fe(III)-chitosan system. There was a 50% drop in dosage of Fe(III).[43] The coagulation process can be coupled to other processes for enhanced contaminant removal; for example, Zouboulis and Katsoyiannis[44] studied arsenate removal using coagulation-direct filtration. The coagulant system was alum or ferric chloride, and organic polymers (cationic and anionic polyelectrolytes) were used to enhance the process in some cases. The coagulation-flocculation process occurred in stages and finally filtered by use of a sand bed filtration system.

The combined metal ion coagulant with cationic polymer proved to be better at removing As species. However, all systems were able to reduce As(V) from an initial concentration of 400 µg/L to below 10 µg/L.[44]

1.2.3 Colorimetric Methods for Determination of Arsenic

Oxyanion arsenic species are colorless in aqueous solution and the measurement of arsenic levels is essential to maintaining proper levels in the environment. For this reason, it has garnered some importance in the literature for finding simple and inexpensive arsenic determination methods.[16,45,46] This is especially relevant for field testing water samples in remote rural areas in affected countries such as India and Bangladesh. There are several very accurate instrumental methods that can be used for arsenic determination such as atomic absorption spectroscopy (AAS), inductively coupled plasma mass spectrometry (ICP-MS) and inductively coupled plasma atomic emission spectroscopy (ICP-AES). However, while these methods possess low and accurate detection limits, they are quite expensive and unsuitable for field use due to instrument size and specialized conditions required. Field kits for arsenic determination have mainly utilized the Guzeit method,[7] which is also the basis for many colorimetric methods for arsenic concentration determination. It works by generation of arsine gas. The arsine gas is produced by the addition of zinc powder and the reduction of arsenic under acidic conditions. The evolved gas is then trapped by silver diethyldithiocarbamate solution or mercuric bromide, which has been impregnated on paper. The detection limit was determined to be 100 μgL^{-1}. This is problematic since many of those contaminated areas have arsenic levels that are below this value. Also, workers in poorly ventilated areas were exposed to dangerous levels of arsine gas. In 1979, Johnson and Pilson modified the standard molybdate-based method, used to determine phosphate concentration in water, for arsenic determination as well.[46] The method works by taking advantage of the blue color formed when arsenate or phosphate react with a reduced molybdate species to form an arseno-molybdate complex. Since the As(V) species can form the complex while the As(III) cannot, an oxidation step is required to determine the total arsenic concentration in water. The detection limit for this method is usually quoted at ~20 μgL^{-1} and the reaction time is about 1 h.[46] Dhar *et al.*[46] proposed a modification of the Johnson and Pilson method.[46] Their modification included an increase to the reaction rate by increasing the amount of potassium antimony tartrate, and using optimized amounts of potassium iodate and ascorbic acid. The result was a rate of color development reduced to 10 minutes, while a new detection limit below the 10 μgL^{-1} threshold set by the WHO.[46] This

modified molybdate arsenic (As) determination method has been used by other researchers. Chun *et al.*[47] used this method when studying the removal of arsenic using a magnetite-loaded mesocellular carbonaceous material, Fe_3O_4/MSU-F-C,[47] Yoon *et al.*[48] utilized it for the monitoring of As(III) concentrations after photocatalytic oxidation with TiO_2,[48] and Fe(III)-treated biomass of *Staphylococcus xylosus* was used to biosorb arsenic by Aryal *et al.*[49] and the molybdenum blue method was also used.[49] Such studies represent only a fraction where arsenic levels were analyzed by this method.

1.3 Coagulation-Flocculation

1.3.1 Introduction

The advantages of using coagulation-flocculation comes from its simplicity as a process. While there are many processes for contaminant removal in water, most cannot be used on an industrial scale without considerable cost.[28] Compared to other methods, coagulation-flocculation offers lower cost, even on an industrial scale, and very efficient when properly optimized.[50] It is also very effective for several different contaminant species, making it quite versatile. Coagulation-flocculation is used for the removal of colloidal species, usually quantified by measurement of turbidity, organic matter, dissolved ionic species, industrial effluents and dyes (anionic, cationic and neutral).[28,33]

Coagulation occurs when the added coagulant combines with a dispersed particle system, allowing it to aggregate and settle. The dispersed particles, most often colloidal in nature, tend to be suspended due to strong repulsive forces amongst the particles. The addition of a coagulant causes the destabilization of the system by compressing the electric double layer surrounding the dispersed particles, reducing repulsion and allowing them to aggregate into larger particles (microflocs).[51] Flocculation is the process of binding the formed microflocs into even denser particles (macroflocs) that can be removed by simpler separation techniques. Polymers are well suited to this due to their large molecular weight and long chains.[51]

1.3.2 Types of Coagulants and Flocculants

Because coagulation is such an extensively used process there are many types of coagulants employed in water treatment. These may be organic or inorganic species. Mineral additives (e.g. lime, calcium salts), hydrolyzing metal salts (e.g. alum, ferric chloride), pre-hydrolyzed metals (e.g. polyaluminum chloride) and polyelectrolytes (coagulant aids) are used for such processes.[28]

Flocculants are usually organic polymeric or inorganic species, where the use of inorganic flocculants has widely been curtailed due to their numerous disadvantages such as high dosage requirements and high sludge production volume.[52] Organic polymer flocculants may be anionic, cationic, amphoteric or non-ionic and can be synthetic or naturally sourced.[28]

It is more common to use ionic species such as aluminum sulphate (alum, $Al_2(SO_4)_3$) and iron (III) chloride ($FeCl_3$) to act as coagulants. They are favored due to their low cost and high effectiveness. However, because of metal toxicity of alum and the formation of high sludge volumes, the use of polymers has become more widespread.[52] Commercial polymers used for water treatment are usually polyacrylamides (PAM). Their potential drawbacks include higher cost and the potential health risks due to acrylamide oligomers remaining in the treated water.[28] Natural polymers, such as chitosan and alginate, have been considered as replacement alternatives for commercial polymers due to their low cost, biodegradability, ease of availability and their relatively low toxicity.[52]

1.3.3 Coagulation-Flocculation Mechanisms

The process of coagulation-flocculation occurs via several mechanisms based on the chemicals used in the process and the system being targeted, such as clay colloidal systems or ionic systems. Two of the main mechanisms are charge neutralization and electrostatic bridging.[53] To explain how these two mechanisms work, let us consider a colloidal clay system, which often requires the use of coagulation-flocculation for turbidity removal. Colloids are substances that scatter light due to their particle size being on the same order of magnitude as the scattered light. They are dispersed within a medium due to charge repulsion among the particles. They tend to be negatively charged and possess a tightly bound counter ion layer followed by another layer of more diffuse counter ions. These layers make up the electrical double layer.[28] When an oppositely (positive in this case) charged species is added (coagulant), electrostatic attraction occurs among the coagulant and colloid, allowing for a decrease in repulsion due to the double layer being compressed. This allows for aggregation of the particles into microflocs which some may settle out of solution. The other mechanism is electrostatic bridging, which as the name implies, works by forming a bridge between and among microflocs to form macroflocs.[54] The process of flocculation tends to occur by this mechanism.[55]

Figure 1.3 shows the mechanism of charge neutralization and electrostatic bridging mentioned previously. Patch bridging was proposed for chitosan as a coagulant/flocculant. When

chitosan is used for coagulation/flocculation (in acidic media), its positive charges are found at smaller distances to each other than compared to those distances between particles of the species to be removed (colloid or dispersed species).[50] This gives rise to 'patches' of charge neutralization, bridged by the rest of the polymer.[50]

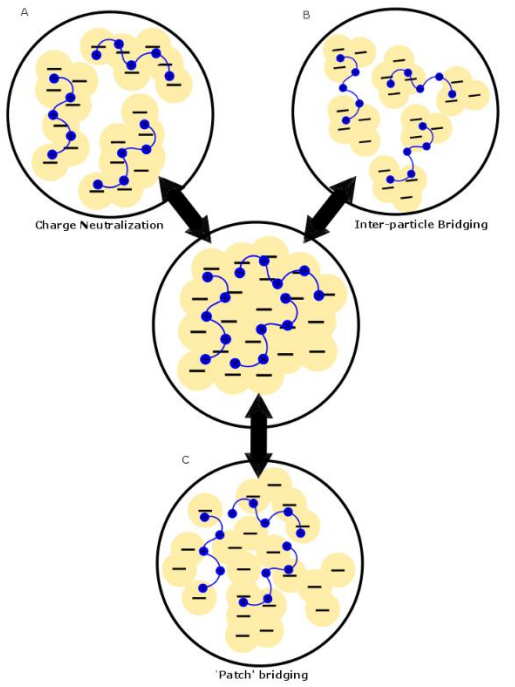

Figure 1.3: Proposed mechanisms of coagulation-flocculation

1.3.4 Jar Test Apparatus Method

Jar tests are an important tool for water treatment and have been used extensively.[56,57] The Jar test method allows for simulating a full-scale water treatment process used in water plants, and allows for the investigation of new chemicals for treating raw water. It provides an opportunity for the small-scale testing in the laboratory for specific water treatment chemicals with a particular raw water system before moving to full scale operations.[58] Jar testing begins by adding identical amounts of raw water to the jars, followed by the addition of water treatment chemicals to assess parameters such as dosage, chemical types, mixing rate, aeration level/time, filtration type, optimum pH and others.[58] The jar test allows for the mixing of the chemicals with raw water in a similar manner as in the water treatment plant but on a much smaller scale. This allows for the observation of floc formation, development and settlement in a simple and cost effective manner.[58]

1.3.5 *One-Pot* Method Kinetics Studies

The *one-pot* method was reported in detail elsewhere,[59] and was used for the study of kinetics of adsorption as an alternative to batch experiments, particularly for heterogeneous sorption systems (e.g. solid-solution systems). The *one-pot* method works for heterogenous systems by separating the solid phase from the solution with adsorbate (substance being adsorbed) using a semi-permeable barrier, such as dialysis membrane or filter paper. Sampling can be done via two methods, *in-situ* or *ex-situ*. In the *in-situ* method, sampling occurs within the membrane, while the adsorbate and adsorbent (substance doing adsorbing) interact outside of the membrane in solution. *Ex-situ* sampling occurs when the solid adsorbent is enclosed within the membrane and immersed in the adsorbate solution; where the samples are taken from the adsorbate solution that lie external to the membrane.

Advantages of the *one-pot* method include the use of less adsorbent material, which can be used with highly dispersed and colloidal material, whilst allowing for studies at variable temperature conditions. Mohamed and Wilson[59] compared the *one-pot* method to conventional batch kinetic methods for the removal of two dyes (*p*-nitrophenol and phenolphthalein) using powdered adsorbents that included cyclodextrin-based polyurethane materials. The method comparison illustrated the difference in the type of experimental design for such kinetic studies. *Ex-situ* sampling showed the slowest kinetics, while batch method showed the fastest uptake. These results highlight the utility of both types of methods, especially in the case of reactions with faster kinetic profiles. The barrier slows the reaction down. Both *in-situ* and *ex-situ* sampling *one-pot* methods allow for comparison of adsorbent species because even if the absolute kinetic parameters (Q_t and k) cannot be determined, the relative parameters provide a relative comparison.[59]

The development of the *one-pot* method began with the study of the kinetics of roxarsone removal using iron oxide composites on activated carbon supports.[60] The use of the *in-situ* sampling *one-pot* method was further enhanced through studies on the kinetics of urea uptake by Xue and Wilson.[61] The choice of the *one-pot* method for the investigation of the utility of chitosan-based materials for uptake of urea was due to the normally rapid kinetics of biological systems and the narrow concentration range of urea in the environment.[61] The use of the *one-pot* method allowed for modeling of kinetics through the pseudo-first order (PFO) and pseudo-second order (PSO) models.

The versatility of this method continues to be highlighted by studies such as those that look at the kinetics of processes at take up differing species, e.g. phosphate[62] and methylene blue dye.[63] Mahaninia and Wilson[62] used the *in-situ* sampling *one-pot* method to not only determine kinetic parameters, but thermodynamic adsorption values by using the Arrhenius equation and the Eyring method.[62] Dolatkhah and Wilson[63] employed the *ex-situ one-pot* method for the study of the kinetics of methylene blue dye uptake with magnetite/polymer brush nanocomposites.[63] These studies illustrate the versatility of the method and how it can be applied to heterogeneous systems.

1.4 Biopolymers

A polymer is defined as a series of repeating chemical units (monomers) that are covalently bonded.[51] Polymers may be further divided into homopolymers that consist of only one type of monomer, and copolymers that consist of more than one type of monomer unit. Many polymers, including chitosan and alginate used herein are special types of biopolymers that possesses ionizable groups, and are referred to as polyelectrolytes. Polyelectrolytes can be cationic, anionic or ampholytic by possessing positive, negative or both types of ionic charge. Non-ionic polymers do not have any ionizable groups. Polyelectrolytes are endowed with hydrophilic properties due to these ionizable groups, which becomes charged with certain pH values.[51]

Natural polyelectrolytes or biopolymers are polymers whose origins are natural sources such as the plant or animal sources from the environment. Their use as flocculants can be traced back for many years, as evidenced by mention of the use of nuts of the Nirmali tree for water treatment (Sanskrit text ca. 2000 BC).[51] The use of biopolymers for water treatment has improved over the years but similar to using synthetic polymers, the biopolymers must be studied (using jar test analyses) to determine suitability for a particular water system. The advantages of using biopolymers include them being of low toxicity and biodegradable.[28] They also tend to be more readily available, and may be locally sourced in some cases and are often inexpensive. Sources of natural polyelectrolytes are diverse, ranging from starch derivatives, cactus plants (*Opuntia*), alginate from seaweed and many others.[28,64]

1.4.1 Chitosan

1.4.1.1 Extraction and Production of Chitosan

Chitosan refers to a group of biopolymers obtained from the deacetylation of chitin. Chitin naturally occurs in nature and is found to be the second most abundant biopolymer, after

cellulose.[65] Chitin, first identified in 1884, is found in many invertebrates such as nematodes, molluscs, in the exoskeletons of arthropods and insects and the cell walls of fungi and yeast.[65] Chitosan is obtained by deacetylation of chitin; chitosan is characterized by its degree of acetylation (DA), which can be expressed as a mole percent (mol%). Those biopolymers derived from chitin and its deacetylated form below 50 mol% are referred to as chitosan.[65] One of the major differences between chitosan and chitin lies in the solubility. Chitin, found abundantly in crab and shrimp shells, has a limited solubility, being soluble in strong polar protic solvents such as trichloroacetic acid.[66] In fact, it is less soluble than cellulose as well due to hydrogen bonding of the acetylamide group; this makes chitin highly crystalline.[65,66] Loss of about two-thirds of these groups, when the amide is converted to amine to form chitosan, causes chitosan to be of a higher solubility than chitin in dilute acids.[66]

The main commercial source of chitin is crab and shrimp shells. In these exoskeletons chitin exists as crystalline microfibrils that can be extracted and deacetylated by enzymatic or chemical means to chitosan.[65] Commercial preparation of chitosan tends to rely on chemical methods of lower cost and more suited to an industrial scale process.[65] Alkali N-deacetylation is preferred because it is less likely to cleave glycosidic linkages as compared to acid extraction.[65] Alkali deacetylation may be heterogeneous or homogeneous, depending on the degree of deacetylation required. In the heterogeneous method, hot concentrated alkali (often NaOH) solution is combined with the chitin and left to stand for a few hours.[65] This process results in a chitosan with ~85 – 99% DA, which is formed as an insoluble residue. A 48 – 55% DA is obtained when homogeneous N-deacetylation is used. This method also employs the use of concentrated NaOH. The chitin is reacted with the NaOH for upwards of 3 h, and then dissolved in crushed ice. Chitosan formed by this process is soluble with uniform distribution of acetyl groups. Studies have shown that the morphology of chitosan, particularly MW and DA, are affected by the concentration and nature of alkali, reaction time, temperature, number of alkaline hydrolysis steps, atmospheric conditions and the use of a reducing agent, such as sodium borohydride ($NaBH_4$).[65] The MW is more influenced by concentration and nature of the alkali, while DA is more influenced by reaction time, temperature, number of alkaline hydrolysis steps, atmospheric conditions and reducing agent.[65]

Enzymatic deacetylation of chitin has the advantage of being less energy consuming and does not require large amounts of alkali solution.[65] It takes advantage of chitin deacetylases, which

can be found in fungi and some insect species.[67] Some common fungal species used are *Mucor rouxii*, *Absidia coerulea*, *Aspergillus nidulans* and *Colletotrichum lindemuthianum*.[67] These species work by hydrolyzing the N-acetamide bonds in chitin.[67]

1.4.1.2 Applications of Chitosan

Chitosan is non-toxic, non-immunogenic, biodegradable and biocompatible in animal tissues. It has a low cost and high availability; as such, it is applicable to many fields of use. For instance, in the field of biomedical applications, it is used in wound dressings, tissue engineering, blood anticoagulants, implant coatings, and therapeutic agent delivery systems.[68] Park *et al.*[69] studied chitosan oligosaccharides (CTS-OS) and their anti-tumor activity.[69] The various CTS-OS were shown to cause 50% cancer cell death (CC_{50}). For example, 25 μgL^{-1} CTS-OS concentration was required for CC_{50} of A549 (lung cancer cell).[70] Chitosan has been shown quite often to have anti-microbial activity, where Zheng *et al.*[71] studied the effect of chitosan MW on *Staphylococcus aureus* (gram-positive) and *Escherichia coli* (gram-negative).[71] An increase of MW caused an increase in antimicrobial activity for the former but a decrease for the latter.[71]

Other applications of chitosan include usage as a food thickener, paper and textile adhesive, membrane and film formation, chelating agent for metals and flocculant.[72,73] Chitosan is used in microbial, animal plant cell immobilization, by providing a solid support on which to mount them.[73] The textile industry takes advantage of the antimicrobial properties of chitosan by using it to create medically related sutures, threads and fibres.[73] Due to its structural similarity to cellulose, chitosan is used in the paper industry extensively.[73] Uses include, but are not limited to, strengthening recycled paper, and increasing its biodegradability, increasing water resistance and aiding in the production of paper with a smoother surface.[73]

Chitosan is highly applicable to many biomedical applications. Chitosan membranes have been proposed for the manufacture of artificial kidneys, due to their excellent tensile strength and permeability.[68] Zhang and Zhang synthesized microporous chitosan/calcium phosphate composite for tissue engineering.[73] Chitosan has been used often in the manufacture of various wound dressings; for example, chitosan films may be used in ocular bandage lens.[73] Another biomedical application where chitosan is employed includes the development of drug delivery systems.[73] Jain and Banerjee investigated the use of chitosan as a delivery system for ciprofloxacin hydrochloride. Chitosan proved to be promising for this purpose.[74]

Investigations have been done on the use of chitosan as a coagulant or coagulant aid, in conjunction with common salts used for coagulation to remove turbidity, color and ionic species such as arsenic.[28] One of the disadvantages of chitosan is its lack of stability, which is due to its hydrophilic nature and pH sensitivity.[65] However, this also makes it easier to modify to enhance properties it lacks in its pristine form. Chitosan may be crosslinked to form beads, fibres, films and hydrogels. Common modifiers are organic reagents such as epichlorohydrin, chloroacetic acid, 3-chloro-2-hydroxypropyl trimethyl ammonium chloride and others,[65] as described further in Section 1.4.5.

1.4.1.3 Functional Characteristics

Chitosan is a linear polysaccharide composed of glucosamine and N-acetyl-glucosamine monomers linked by β(1→4) glycosidic bonds. Figure 1.4 shows the structural differences between chitin and chitosan.[75] Primarily, the acetamido groups have been replaced with amino groups. The DA and distribution of acetyl groups along the biopolymer exert strong influence on the physical properties of chitosan, when in solution. When the acetyl groups are distributed in a non-uniform manner in blocks that lead to a greater ease of aggregation of particles due to increased chain association. With the amino groups present on the chitosan, in acidic media (pK_a 6.5)[75] these groups become protonated and chitosan adopts a positive charge. The protonated amino groups provide the positive charge sites to neutralize negatively charged species.

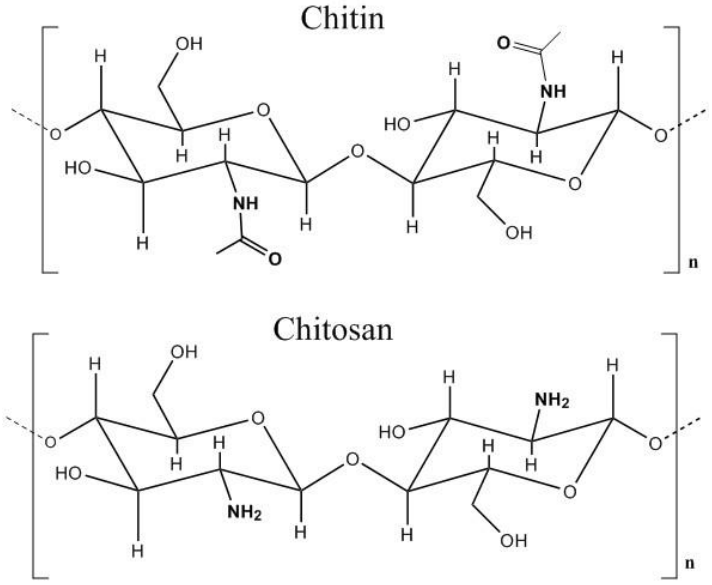

Figure 1.4: Structure of chitosan and chitin, where n denotes the degree of polymerization

Since it is a linear polymer, it can also partake in bridging via loops and tails that extend out of the microflocs.[76] This should highlight the importance of the configuration of the biopolymer in water. Configuration is also influenced by the charge density of the polymer. Firstly, the greater the level of charge density of chitosan, the greater its viscosity in solution at a given MW.[51] Secondly, an increase in viscosity is linked to an increase in molecular chain length. This indicates that as the charge density is increased, the electrostatic repulsion with the chain increases.[51] It can be concluded that as the charge density of the biopolymer increases, the chain goes from tightly coiled (low charge density), to kinked coils (medium) and extended filament-like chains (high), and is accompanied by an increased solution viscosity. It may also be inferred that as the viscosity increases with chain length or MW, the viscosity increases proportionately. Hence, ionic strength of the medium is important since greater ionic strength reduces the influence of charge on the polymer (less charge repulsion), resulting in a tighter coiled configuration.[51]

The pH of the solution also influences the conformation of the polymer just as the MW and charge density affect polymer conformation. This relates to the effect of pH on charge density of chitosan. At pH values below 6.5 (pK_a of chitosan), the amine groups are protonated and positively charged. Chitosan often has a more extended structure in acidic media due to electrostatic repulsion of these ammonium cations. At pH values above the pK_a, chitosan becomes neutralized and has a more coiled conformation since there is less charge repulsion and hydrophobic effects play a role.[28]

1.4.1.4 Removal of Arsenic using Chitosan/Chitosan Based Materials

Investigation of the removal of arsenic by chitosan are extensive and varied in terms of the process used, where adsorption has been highly favored and reviewed.[32,77–79] As previously discussed, the process of coagulation-flocculation is highly applicable to many types of contaminants, dissolved species like arsenic being one such species. The potential of this area has not been fully explored but studies have been carried out using coagulation-flocculation for the removal of arsenic, where most studies use traditional coagulants such as alum and Fe(III).[28,30] The latter is particularly favored because of its natural occurrence in water bodies which has been linked to lower arsenic levels, as supported by numerous studies.[30,31] Hesami *et al.*[43] investigated the removal of arsenite and arsenate with an Fe(III)-chitosan system, with chitosan as a coagulant aid.[43] Optimal removal of As(III) (80%–100%) was achieved at pH 7 using Fe(III) by itself at a dosage of 60 mg/L. The advantage of chitosan as an aid resulted in less Fe(III) required. Chitosan addition also affected As(V) removal, but to a lesser degree, where the removal was ca. 5%–10%

and less than that observed for As(III).[43] This study showed that while chitosan was responsible for less Fe(III) being required, the Fe(III) itself was mainly responsible for arsenic removal. The suggested mechanism for removal of arsenic using Fe(III) deals with soluble arsenic being converted to insoluble arsenic. The soluble arsenic species are converted through three major steps: (1) formation of solid iron arsenate ($FeAsO_4$) through precipitation; (2) co-precipitation of arsenic species along with solid metal hydroxides through inclusion, occlusion or adsorption; and (3) removal of soluble arsenic species via adsorption onto pre-formed solid hydroxide precipitates.[29–31] Chitosan addition resulted in the use of lower Fe(III) levels used through the bridging of flocs formed from iron and arsenic. Since the study was done at pH 7 at levels above the pK_a of chitosan, precipitation would likely occur between chitosan, arsenic species and Fe(III) hydroxides from solution. Bridging with chitosan occurs through dispersion forces rather than electrostatic attractions.[43] Arsenite species had a noticeable drop in removal due to competition between arsenite and chitosan for Fe(III). Arsenite and chitosan are non-ionized at this condition, where favourable association occurs via dispersion forces.[43]

Organoarsenical removal by coagulation-flocculation has not been widely evaluated but since they are formed through bacterial and fungal action on inorganic arsenic species, they should be considered. Biomethylation of arsenite and arsenate may yield methylated species such as monomethyl arsenate (MMA) or dimethyl arsenate (DMA). In a study done by Hu *et al.*[11], Fe(III) performed better than aluminum, when the two and polyaluminum chloride were compared.[11] The removal efficiency (%), As(V) > MMA > DMA, showed that methyl groups hinder removal. The ionic binding of As species onto the surface of the Fe/Al hydroxide illustrates the key mechanism of As removal. The authors suggested that the binding changed based on available groups on the arsenic species, with less available groups for binding being present with increasing methylation.[11]

The lack of research on the use of chitosan for the removal of arsenic using coagulation-flocculation has led to the investigation reported in this thesis.

1.4.2 Alginate

1.4.2.1 Extraction and Production of Alginate

The two main sources of alginate are marine brown algae (*Phaeophyceae*) and bacterial biosynthesis.[80] It acts as a structural component with the alginate-gel matrix giving the algae mechanical strength and flexibility. In a way, it is like the cellulose of ocean plants. Brown

seaweed species used for alginate harvesting include *Ascophyllum*, *Durvillaea*, *Ecklonia*, *Laminaria*, *Lessonia*, *Macrocystis* and *Sargassum.*[80]

Alginate extraction is fairly simple, but the difficulty lies in removing gelatinous precipitates and slimy residues that resist filtration and centrifugation.[81] The extraction of alginate first involves the seaweed being cut into tiny pieces. An alkaline solution (usually NaOH) is then used to separate the alginate from the insoluble seaweed residues. The extracted alginate is in the form of a very dilute sodium alginate solution in water. From this stage, separation may occur by two pathways: calcium alginate process or alginic acid process.[81]

In the former process, calcium chloride is added to the alginate solution and converted to the insoluble calcium alginate (equation 1-3) and filtered out. After this, further separation occurs by addition of acid to form alginic acid fibres (equation 1-4) and finally sodium carbonate or sodium hydroxide is added and sodium alginate is obtained (equation 1-5).

$$Ca^{2+}(aq) + 2NaAlg(dilute, aq) \rightarrow Ca(Alg)_2(s) + 2Na^{+}(aq) \quad (1\text{-}3)$$

$$Ca(Alg)_2(s) + 2H^{+}(aq) \rightarrow 2HAlg(aq.) + Ca^{2+}(aq) \quad (1\text{-}4)$$

$$HAlg(aq) + Na^{+}(aq) \rightarrow NaAlg(conc., aq) + H^{+}(aq) \quad (1\text{-}5)$$

The latter process produces sodium alginate via alginic acid, where the addition of acid followed by addition of alcohol and sodium carbonate firstly produces alginic acid then sodium alginate.[81] This results in similar compound formation as that shown in the previous equations, without the added step of adding calcium chloride.[82]

1.4.2.2 Functional Characteristics

Alginate is composed of two major monomer units: β-D-mannuronate (M) and α-L-guluronate (G). The monomers are bound through (1→4) linkages that form block copolymers, with an M:G ratio that depends on the alginate source. The alginate blocks are either in groups of M residues (MMMMM), groups of G residues (GGGGG) or alternating M and G residues (MGMGMG).[83] The alginate monomer residues do not have a regular repeating pattern and as such, its sequential structure is not easily determined. As previously mentioned with chitosan, the conformation of the alginate polymer is very important in understanding its functionality. Alginate has interesting properties due to its copolymer blocks. For those homopolymer blocks, the G-blocks were in a $^{1}C_4$ conformation and the M-block, in a $^{4}C_1$ conformation (see Figure 1.5(A)). The blocks also differ in viscosity and chain stiffness, where the stiffness is listed in ascending order: MG < MM < GG. The diaxial linkage in the G-block causes hindered rotation around the

glycosidic linkage and this leads to the G-block being stiffer than the M- and MG-block. The Mark-Houwink-Sakurada equation shows the relationship between intrinsic viscosity ([η]) and MW (M); where the parameter (a) shows the extent of chain stiffness and extension. As a increases, the stiffness increases.[80] Both a and K are constants, which are linked to the type of solvent and temperature conditions,[84] according to equation (1-6).

$$[\eta] = K.\ M^{a} \qquad (1\text{-}6)$$

Equation (1-6) shows that the MW influences the viscosity of the alginate in solution since the viscosity increases as the molecular weight increases. Since alginate is a linear polymer as shown in Fig. 1.5 (A), alginate possesses multiple carboxylate groups on the monomer residues since it is an anionic polyelectrolyte above its pK_a value. The charge repulsion of the anionic groups cause, the polymer adopts a more extended conformation with greater intrinsic viscosity. The pK_a of the M and G residues are 3.38 and 3.65,[85] respectively. Depending on the composition of the alginate, the pK_a of the polymer will fall between the two individual pK_a values. This is an important factor because the presence of anionic groups lead to its solubility in water at pH values below the pK_a of the alginate. At pH values below the pK_a, the alginate will precipitate out or gel depending on how gradually the pH changed. Gel formation occurs with a more gradual pH change. The composition of the polymer chains also matter, where the homopolymer blocks precipitate faster due to the presence of hydrogen bonds that stabilize the crystalline polymer domains. MG-blocks tend to lack these domains and precipitate at more acidic pH values.[80] Aside from pH in water, the solubility of alginate is affected by two other factors: i) ionic strength and ii) the nature of the ions in water also affect solubility. Particularly, Ca^{2+} ions in 'hard' water react with the alginate to form gels (see Fig. 1.5(B)).[80]

The nature of the blocks of copolymers is responsible for the physical properties shown by alginate, and especially affect gelling phenomena with divalent metal ions. More specifically, the G residues contribute significantly to the formation of alginate gels.

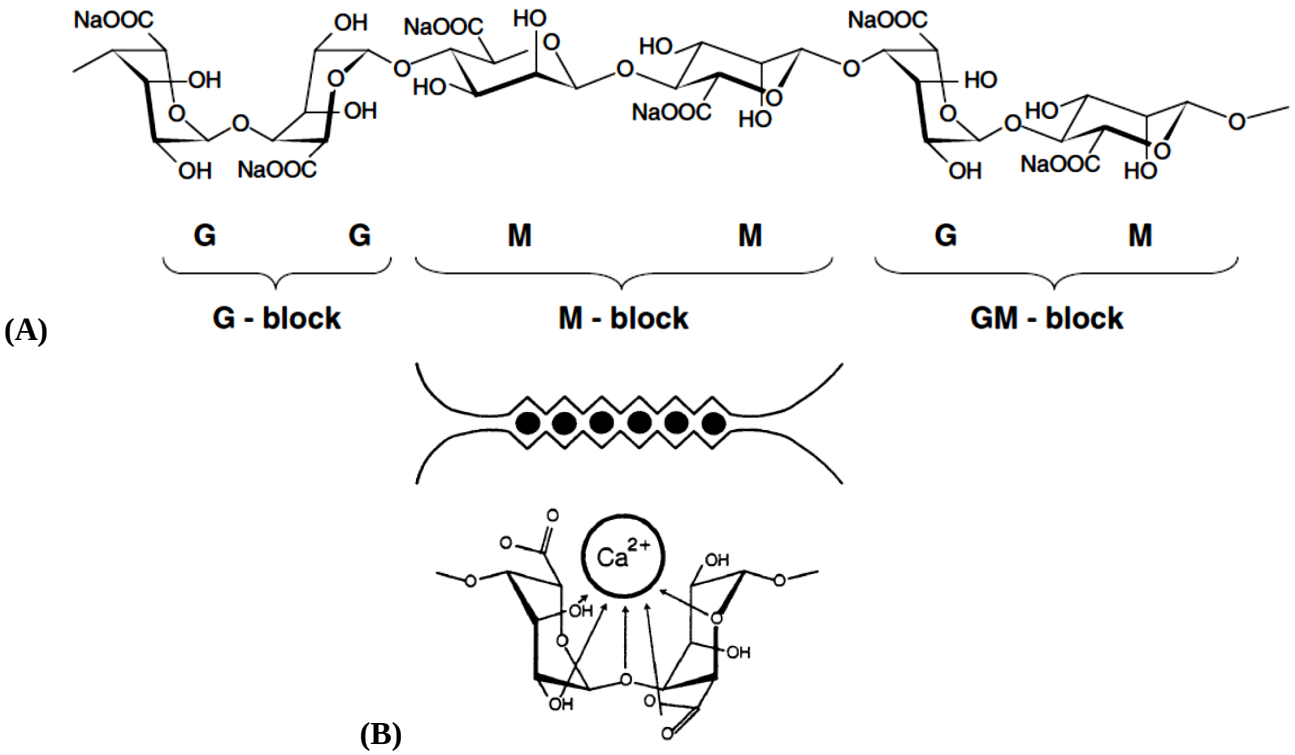

Figure 1.5: (A) Structure of sodium alginate and (B) Egg-box model for binding of Ca^{2+} ions with G residues[80] [Reproduced with permission Ref. 80]

1.4.2.3 Applications of Alginate

Alginate possesses three properties that make it a very versatile biopolymer. This includes its ability to act as a thickener in aqueous solutions, along with its gelling ability and the ability to form films and fibres. These properties are widely exploited across many industries such as the food, textile and pharmaceutical industries, to name a few.[86]

In the textile industry, alginate can be used to decolorize dyes such Amaranth and Reactive Red 22. The former was done using *Trametes versicolor* immobilized on the alginate[87] and the latter, immobilized *Pseudomonas luteola* [88] onto an alginate-silicate sol-gel. The fibre-forming ability of alginate was used extensively for the manufacture of wound dressings. Qin compared the performance capability of several of these dressings for absorbency capacities, gel swelling ratios in water and normal saline, wicking of fluid, and dry and wet strengths.[89] The findings highlighted the difference in functional abilities with variation in alginate composition (M:G ratio) and the amounts of calcium and sodium present in the fibres. For instance, the gelling ability of the fibres increased as the amount of M was increased, and the addition of sodium ions increased the absorbency of the fibres. Qin *et al.*[89] studied the transformation of calcium alginate fibres into

alginic acid fibres and sodium alginate fibres and also found that the sodium ions increased absorbency, while the alginic acid fibres were less absorbent than both calcium and sodium fibres.[89]

The use of alginate in the pharmaceutical industry is variable, where alginate interactions with polycation species have been studied in the manufacture of drug delivery devices such as insulin delivery microcapsules. Thu *et al.*[90] studied the interaction of alginate with poly-L-lysine (PLL), a polymer containing multiple cationic amine groups.[90] Enhanced binding of PLL was found with alginate containing higher amounts of M residues. Microencapsulation is also used in food biotechnology, where bioactive ingredients may be coated with materials that allow for several beneficial outcomes. Alginate can be used for the coating of probiotic microorganisms; this allows for the microorganisms to be released into favorable environments when digested.[91]

1.4.2.4 Removal of Arsenic using Alginate/Alginate-based Materials

The use of alginate for the removal of arsenic is infrequent, especially on its own. However, with its gelling abilities, it makes for a good support material to attach other more traditional arsenic removing materials; one of the most widely used species being Fe (III). Escudero *et al.*[92] entrapped waste Fe (III) and Ni (II) (hydr)oxides from an electroplating industrial plant into calcium alginate beads for the removal of arsenate and arsenite species. These novel materials helped to increase uptake of arsenic by 60% when compared to using the hydr(oxides) only.[92] A calcium alginate entrapped material was made by Lim *et al.*[93] and used for the removal of arsenate. The material encapsulated into the calcium alginate was magnetite, a magnetic Fe compound.[93] The research showed that the lattice oxygen in magnetite and the oxygen in hydroxyl groups of the calcium alginate are important for the uptake of arsenate.[93,94]

While alginate has been studied for the removal of contaminants using coagulation-flocculation,[95] it has so far not been studied on the removal of arsenic by this process. The previous examples show its utility when alginate acts as a biosorbent. Further studies are needed to investigate its activity as a bioflocculant.

1.4.3 Polyelectrolyte Complexes

Polyelectrolyte complexes (PECs) are formed when two oppositely charged polymers (polyanions and polycations) are mixed together and stabilized by electrostatic forces. At certain optimum pH ranges, the polymers will have opposing charges and be able to come together to form the complex. Bungenberg de Jong and coworkers were some of the earliest scientists to study

these macromolecules in the 1930's and 1940's. An example of a PEC is the combination of gelatin (polycation) and gum arabic (polyanion). PECs may come from natural sources, as seen in the previous example, where a combination of synthetic polymers, such as sodium poly(styrene sulfonate) and poly(vinyl methyl pyridinium) are used.[96] Saether *et al.*[97] mention entropy gain through release of counter-ions as a major driving force for PEC formation.[97] Michaels explains this further as an 'escaping tendency'; each polymer has with it accompanying micro counterions, which are limited in mobility due to electrostatic attraction. When a PEC is formed, the counterions are released and diffuse into the solution and increase the entropy of the system. The entropy is the driving force for the reaction provided that it is larger than the entropy decrease caused by the formation of the PEC since PEC formations results in a more ordered structure. Evidence for entropy as the driving force comes from observable swelling of the PEC in concentrated electrolyte solutions.[96] Flocs are thought to be formed by either having one polymer act as a charge neutralization facilitator and then the other polymer bridges the microflocs together by electrostatic attraction to the first polymer. Or if pre-mixed, having both bridge simultaneously the particles in the system.[98]

Chitosan, due to its cationic polyelectrolyte nature can for complexes with synthetic and natural anionic polyelectrolytes such as alginate at certain pH values. The complex formation of such polymer species to form a PEC has been studied by Saether *et al.*[97] by investigation of the size, zeta potential and pH of the chitosan-alginate PEC using Dynamic Light Scattering (DLS). It was reported that the two most influential parameters related to net charge ratio and MW of the biopolymers.[97] Another study looked at the M/G ratio of alginate in the formation of the chitosan-alginate PEC system. The complex formed was non-stoichiometric and independent of alginate composition and the MW of chitosan.[99] Stoichiometric complexes are those that exhibit 1:1 binding between poly-ions, while non-stoichiometric complexes bind in a more haphazard manner. The binding affects their swelling ability, where non-stoichiometric PECs can absorb around ten times their dry weight in water and only about 30% water by weight for stoichiometric PECs due to their "tighter" binding.[96] Li *et al.*[100] also studied the characterization of chitosan-alginate PECs. This study helped to determine that there was partial protonation of the amine groups of chitosan and these groups bonded electrostatically with the carboxylate groups of the alginate to give a strong PEC.[100] Han *et al.*[101] showed that the chitosan-alginate PEC can also be modified to adjust various properties. A chitosan/hydroxyapatite solution was incorporated into an alginate scaffold

to form a PEC and its microstructure, porosity, mechanical strength and thermal stability were investigated. This PEC showed good mechanical strength and thermal stability and it exhibited good pore structure (after freeze drying) with pore sizes ranging from 80 to 200 μm.[101] This study shows the utility of chitosan-alginate PECs and how it can be further modified for many applications.

In terms of applications, PECs may be used for dialysis and ultrafiltration membranes, fuel cell membranes, moisture-breathable plastic composites, electrically conductive and anti-static coatings, medical and surgical prosthetic materials, environmental sensors and chemical detectors.[96] Chitosan-alginate PECs may be considered for specific types of drug or gene delivery systems in biomedical science, immune stimulating properties, tissue engineering and other applications including wastewater treatment.[97,102]

1.5 Summary

The removal of arsenic from water and wastewater is of immense importance due to its toxicity and widespread occurrence across the globe. The use of biopolymers such as chitosan and alginate, along with traditional metal salt coagulants, in the coagulation-flocculation process is a promising avenue of study. The biopolymers themselves are advantageous due to their 'green' nature, since they could be and have been used without toxic side effects. The low cost of these biopolymers adds to their desirability since both come from natural, abundant sources and studies have shown that using flocculants reduces the amount of traditional coagulant required, while requiring a small dosage itself.

The use of these biopolymers has been studied and shown to be effective at water remediation involving a variety of colloidal materials and dissolved particles but their use in arsenic removal either separately or together is sparse or non-existent when compared with other structurally related inorganic oxyanions such as phosphate. The utility of coagulation-flocculation using biopolymers will be explored in this thesis and is of great interest due to the simplicity of the process and the self-assembly of the flocculants. This means that the polymers arrange themselves in an optimal configuration based on the environmental conditions, pH for instance, and their intrinsic parameters such as MW and charge density. Both chitosan and alginate are polyelectrolytes, with the former being cationic at pH values below its pK_a at 6.5. Alginate forms anion species at pH conditions above its pK_a, especially at pH conditions above 3.38 to 3.65. At the appropriate pH conditions, chitosan and alginate may form a PEC, which is posited to enhance

arsenic uptake into flocs through precipitation and/or extended flocculation since there are two polymers instead of one.

1.6 Research Objectives

This thesis aimed to answer the following questions by addressing several research objectives:

1. Do the parameters of dosage, metal salt type, pH conditions, MW and viscosity affect the removal of colloidal materials using a metal salt-chitosan/alginate system? To address this objective, Jar test studies were performed using a model kaolinite suspension to test the removal efficiency of the metal salt-chitosan/alginate. Speed and time of stirring using the Jar test was also studied.
2. How does the addition of colloidal materials affect the removal of roxarsone using the metal salt-chitosan/alginate system? To address this objective, Jar tests were performed both with and without kaolinite suspension at ambient pH conditions and pH 7 to determine removal efficiency.
3. How does the addition of colloidal materials affect the removal of arsenate using the metal salt-chitosan/alginate system? To address this objective, Jar tests were performed both with and without kaolinite suspension at ambient pH conditions and pH 3 to determine removal efficiency.
4. Which of the components are responsible for roxarsone removal and how do they affect the kinetics of the reaction? To address this objective, a novel *one-pot* method was used to determine the change in roxarsone removal, with and without kaolinite, at variable time and temperature conditions.
5. Which of the components are responsible for arsenate removal and how do they affect the kinetics of the reaction? To address this objective, a *one-pot* method was used to determine the change in roxarsone removal, with and without kaolinite, at variable time and temperature conditions.

The following hypotheses were investigated in this thesis:

1. The coagulation flocculation of a model kaolinite suspension will be improved by using a metal salt-chitosan/alginate at optimized conditions.
2. Arsenic (roxarsone and arsenate) removal will be enhanced by addition of chitosan/alginate biopolymers to iron (III) and further enhanced with kaolinite present.

3. Variable kinetic models (e.g. pseudo-first order and pseudo-second order kinetic models) can be used to analyze coagulation flocculation of roxarsone and arsenate using iron (III) and iron (III)-chitosan/alginate systems.

Each of the following chapters of this thesis will address the questions proposed above and are chapters outlined, as described below:

- Chapter 1 provides an introduction of the topics addressed in this thesis, along with the relevant literature survey herein.
- Chapter 2 provides a description of materials and methods used for Jar test and *one-pot* studies are described, including other experimental methods used herein.
- Chapter 3 describes the results and data analysis of the optimization of the metal salt-chitosan/alginate system using the Jar test method for model kaolinite suspension removal.
- Chapter 4 describes the results and data analysis for the Jar test studies of roxarsone and arsenate (V) removal using iron (III)-chitosan/alginate system described herein.
- Chapter 5 describes the results and data analysis of the removal of roxarsone and arsenate using the *one-pot* method. The results and data analysis of the kinetic and thermodynamic studies are described herein.
- Chapter 6 provides a conclusion and suggestions for future work. Further experiments are proposed to further enhance the removal of arsenic species from water and also, experiments for the use of the metal salt-chitosan/alginate system for removal of arsenic samples from *ex-situ* sources are proposed to demonstrate *proof-of-concept* in practical applications.

Chapter 2 EXPERIMENTAL METHODS

2.1 Material and Methods

This chapter encompasses the list of materials used in the research, methods used for coagulation-flocculation and analysis of the process by instrumental techniques.

2.1.1 Materials

Low molecular weight chitosan (LMWC, 75-85% deacetylation; MW range 50,000-190,000 kDa) and medium molecular weight chitosan (MMWC, 75-85% deacetylation; MW range 190,000-310,000 kDa), potassium antimony (III) tartrate hydrate, antimony molybdate tetrahydrate were purchased from Sigma-Aldrich Canada (Oakville, ON). High viscosity alginate (viscosity range 1000-1500 cps, 1% aq. soln.), low viscosity alginate (viscosity range 40-90 cps, 1% aq. soln.), aluminum sulfate hydrate and sodium hydrogen arsenate heptahydrate were obtained from Alfa Aesar (Ward Hill, MA). Roxarsone was obtained and purified according to method in reference 45. Kaolinite, NaOH, HCl, H_2SO_4, potassium phosphate monobasic, iron (II) chloride tetrahydrate, iron (III) chloride hexahydrate were all obtained from Sigma-Aldrich Canada (Oakville, ON). Potassium phosphate dibasic was obtained from Fisher Scientific (Fair Lawn, NJ). L-ascorbic acid was obtained from BDH Chemicals Canada (Toronto, ON). All materials were used as received without further purification unless specified otherwise. All stock solutions were prepared using 18 MΩ.cm Millipore water and pH was adjusted with 2.5 M HCl and NaOH solutions. Unless stated otherwise, all experiments were carried out at room temperature, 20 ± 1 ºC.

2.2 Spectroscopic Techniques

2.2.1 Ultraviolet-Visible (UV-vis) Spectroscopy

2.2.1.1 Measurement of Transmittance

A Varian Cary-100 Scan UV-Vis spectrophotometer was used in the transmittance mode to indirectly measure the turbidity of kaolinite suspensions in water at 800 nm.

2.2.1.2 Measurement of Absorbance

A Varian Cary-100 Scan UV-Vis spectrophotometer was used to measure the absorbance spectra of roxarsone (λ_{max} = 244 nm) directly in aqueous solution, buffered to pH 7 using phosphate buffer. The Beer-Lambert law was used to quantitatively determine the concentration of roxarsone at pH 7.

A Varian Cary-6000i Scan UV-Vis-NIR spectrophotometer was used to measure arsenate ion levels, which were indirectly estimated by colorimetric detection of the formation of an arseno-molybdate complex using a colorimetric method (adapted from reference Dhar *et. al.* (2004) and explained in further detail in Section 2.5.1)[46] where the absorbance of the dye complex (λ_{max} = 900 nm) was monitored at steady-state conditions. The Beer-Lambert law was used to quantitatively determine the concentration of this dye complex and hence the arsenate ion concentration at pH 3 and 6.5.

2.3 Optimization Coagulation-Flocculation Studies with Kaolinite Suspensions

2.3.1 Dosage of Coagulant/Flocculant Solutions

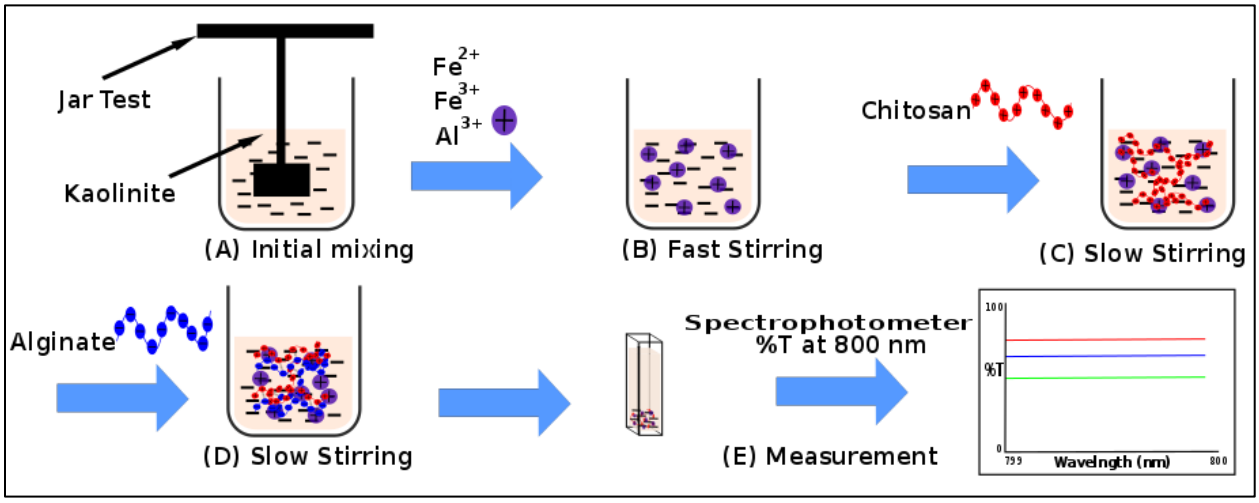

Scheme 2.1: Illustrated scheme for the kaolinite removal procedure

2.3.1.1 Metal Salt Solution

With reference to Scheme 2.1, a single jar of a six-gang Phipps & Bird jar test apparatus was filled with 1 L of 400 ppm kaolinite solution and stirred for 1 min. at 50 rpm to ensure uniform colloid distribution (Step A) for one metal salt experiment and this was repeated for the other metal salts. Just after colloid was mixed, a solution of metal salt (alum, iron (II) and (III) chloride) at variable concentrations (15 – 60 ppm) was added to the kaolinite suspension and stirred for 3 min. at 295 rpm (Step B, fast mixing). Immediately after this, 2.5 ppm MMWC solution (dissolved in 1% HCl solution) was added and stirred for 10 minutes at 50 rpm (Step C). HVA was then added at a concentration of 10 ppm and stirred for a further 10 min. at 50 rpm (Step D, total slow mixing 20 min.). When the stirring had been completed, the suspension was allowed to settle for 30 min.,

with 3 mL aliquots removed initially and subsequently at 5 min. intervals after for transmittance to be measured using the spectrophotometer at $\lambda = 800$ nm (Step E).

2.3.1.2 Chitosan Solution

The procedure in Section 2.3.1.1 was repeated with the addition of fixed amounts of metal salt solution (30 ppm alum, 15 ppm iron (II) and (III) chloride) to the various kaolinite suspensions during step B. During step C, MMWC solution (dissolved in 1% HCl solution) was added at variable concentrations (2.5 – 10 ppm). The remainder of the procedure is repeated as indicated in Section 2.3.1.1 (step E).

2.3.1.3 Alginate Solution

The procedure in Section 2.3.1.1 was repeated with the addition of fixed amounts of metal salt solution (30 ppm alum, 15 ppm iron (II) and (III) chloride) to the various kaolinite suspensions at step B. Then 2.5 ppm MMWC solution (dissolved in 1% HCl solution) was added at step C. At step D, HVA was then added at variable concentrations (2.5 ppm – 10 ppm) and stirred for a further 10 min. at 50 rpm (total slow mixing 20 min.). This was followed by step E.

2.3.2 Effect of pH on Coagulation-Flocculation

The procedure in Section 2.3.1.1 was repeated by first adjusting the various kaolinite suspensions to the desired pH (3, 5, 7, 9) using HCl or NaOH solution. Step B was done with fixed amounts of metal salt solution (30 ppm alum, 15 ppm iron (II) and (III) chloride). Step C was done with 2.5 ppm MMWC solution (dissolved in 1% HCl solution) and step D with 10 ppm HVA, followed by step E.

2.3.3 Molecular Weight of Chitosan

The procedure in Section 2.3.1.1 was repeated with fixed amounts of metal salt solution (30 ppm alum, 15 ppm iron (II) and (III) chloride) added to the various kaolinite suspensions in step B. For step C, chitosan of varying MW (MMWC or LMWC) solutions (dissolved in 1% HCl solution) in variable concentrations (2.5 – 10 ppm) were added. Step D used 10 ppm alginate (HVA or LVA) followed by step E. The error bars for the corresponding figure denote the standard error of the instrument (5%).

2.3.4 Viscosity of Alginate

The procedure in Section 2.3.1.1 was repeated with fixed amounts of metal salt solution (30 ppm alum, 15 ppm iron (II) and (III) chloride) added to the kaolinite suspension in step B. For step C, chitosan (MMWC or LMWC) solutions (dissolved in 1% HCl solution) at a concentration

of 2.5 ppm were added. Various concentrations (2.5 – 10 ppm) of alginate at varying viscosities (HVA or LVA) were then added in step D, followed by step E. The error bars for the corresponding figure denote the standard error of the instrument (5%).

2.3.5 Order of Polymer Addition

Using scheme 2.1 as a reference, the procedure in Section 2.3.1.1 was repeated with fixed amounts of metal salt solution (30 ppm alum, 15 ppm iron (II) and (III) chloride) added to the kaolinite suspensions in step B. Step C involved 2.5 ppm MMWC solution (dissolved in 1% HCl), step D, 10 ppm HVA, and finally step E.

The process was repeated; however, HVA (10 ppm) was added directly after stirring of metal salt was completed and stirred for 10 min. at 50 rpm. MMWC (2.5 ppm) was added after stirring of HVA was finished and it was stirred for 10 min. at 50 rpm. When the stirring had been completed, the suspension was allowed to settle for 30 min., with 3 mL aliquots removed initially and subsequently at 5 min. intervals after for transmittance to be measured using the spectrophotometer at $\lambda = 800$ nm.

The process was repeated a third time with MMWC (2.5 ppm) and HVA (10 ppm) pre-mixed then added directly after stirring of metal salt was completed. They were stirred for 10 min. at 50 rpm. When the stirring had been completed, the suspension was allowed to settle for 30 min., with 3 mL aliquots removed initially and subsequently at 5 min. intervals after for transmittance to be measured using the spectrophotometer at $\lambda = 800$ nm.

2.3.6 Mechanical Aspects of Jar Test Studies

2.3.6.1 Effect of Stirring Time

The procedure in Section 2.3.1.1 was repeated with fixed amounts of metal salt solutions (30 ppm alum, 15 ppm iron (II) and (III) chloride) added to the kaolinite suspensions in step B. Immediately after this, MMWC solution (dissolved in 1% HCl solution) at a concentration of 2.5 ppm was added and stirred for 10 minutes at 50 rpm (step C). HVA was then added at a concentration of 10 ppm and stirred for a further 10 min. at 50 rpm (Step D, total slow mixing 20 min.). When the stirring had been completed, the suspension was allowed to settle for 30 min., with 3 mL aliquots removed initially and subsequently at 5 min. intervals after for transmittance to be measured using the spectrophotometer at $\lambda = 800$ nm (Step E).

The process was repeated with the metal salt solution being stirred at 295 rpm for 1 min. (fast mixing) and MMWC stirred at 50 rpm for 10 min. and HVA was added after this and stirred at 50 rpm for 5 min. (total slow mixing 15 min.).

A final repetition was done with the metal salt solution being stirred at 295 rpm for 5 min. (fast mixing) and MMWC stirred at 50 rpm for 10 min. and HVA added after this and stirred at 50 rpm for 15 min. (total slow mixing 25 min.).

2.3.6.2 Effect of Stirring Speed

The procedure in Section 2.3.1.1 was repeated with fixed amounts of metal salt solutions (30 ppm alum, 15 ppm iron (II) and (III) chloride) added to the kaolinite suspensions at step B. Immediately after this, MMWC solution (dissolved in 1% HCl solution) at a concentration of 2.5 ppm was added and stirred for 10 minutes at 50 rpm (step C). HVA was then added at a concentration of 10 ppm and stirred for a further 10 min. at 50 rpm (Step D, total slow mixing 20 min.). When the stirring had been completed, the suspension was allowed to settle for 30 min., with 3 mL aliquots removed initially and subsequently at 5 min. intervals after for transmittance to be measured using the spectrophotometer at $\lambda = 800$ nm (Step E).

The process was repeated with the metal salt solution being stirred for at 150 rpm for 3 min. (fast mixing) and MMWC stirred at 50 rpm for 10 min. and HVA was added after this and stirred at 50 rpm for 10 min. (total slow mixing 20 min.).

A final repetition was done with the metal salt solution being stirred at 295 rpm for 3 min. (fast mixing) and MMWC stirred at 25 rpm for 10 min. and HVA added after this and stirred at 50 rpm for 10 min. (total slow mixing 20 min.).

2.4 Coagulation-Flocculation Studies with Roxarsone Solution

2.4.1 Preparation of Phosphate buffer

A 500 mL 0.1 M phosphate buffer was prepared by combining 307.5 mL 0.1 M K_2HPO_4 and 192.5 mL 0.1 M KH_2PO_4 solutions in a beaker and mixing together. Both solutions were prepared in Millipore water.

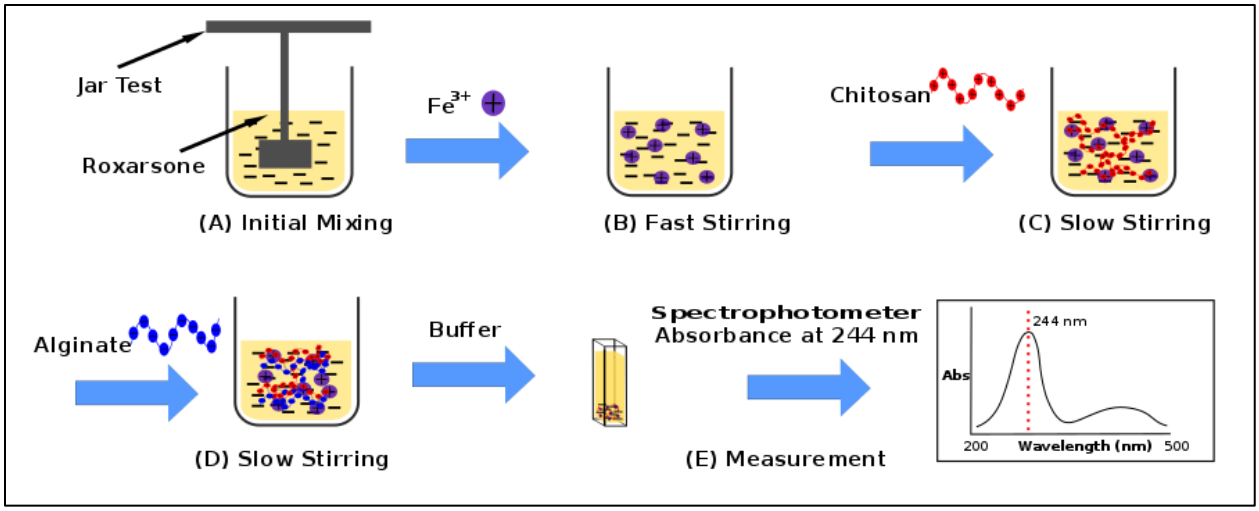

Scheme 2.2: Illustrated scheme for the roxarsone removal procedure

2.4.2 Roxarsone System at ambient pH

With reference to Scheme 2.2, the six jars of a six-gang Phipps & Bird jar test apparatus were each filled with 1 L of variable concentrations (30 – 50 ppm) of roxarsone solution (in Millipore water) and stirred for 1 min. at 50 rpm to ensure uniform distribution (Step A). The pH of roxarsone was then measured and recorded as ~3.5. Just after solution was mixed, 15 ppm of iron (III) was added to all of the jars and stirred for 3 min. at 295 rpm (Step B, fast mixing). Immediately after this, all jars were mixed for 10 min. at 25 rpm. However, jars 1 – 4 only contained the salts previously administered, while MMWC solution (dissolved in 1% HCl solution) at a concentration of 2.5 ppm was added to jars 5 and 6 (Step C). After this mixing period, HVA was then added at a concentration of 10 ppm to jars 3 – 6 and all six jars were stirred for a further 10 min. at 25 rpm (Step D, total slow mixing 20 min.). When the stirring had been completed, the contents of the jars were allowed to settle for 30 min., with 8 mL aliquots being removed initially and after settling and diluted to 25 mL with Millipore water. From this diluted sample, 1.5 mL was taken and added to 1.5 mL 0.1 M phosphate buffer pH 7 and analyzed using a UV-Vis spectrophotometer at $\lambda = 244$ nm (Step E). Table 2.1 gives an overview of the contents of the various jars used in the experiment (jars labelled 1 to 6).

Table 2.1: Overview of the contents of the jars for each separate coagulant-flocculant system

Jar	System	Replicate	Salt added	Chitosan added	Alginate added
1	Metal ion only	1	✓		
2		2	✓		
3	Metal ion/Alginate	1	✓		✓
4		2	✓		✓
5	Metal ion/Chitosan-Alginate	1	✓	✓	✓
6		2	✓	✓	✓

2.4.3 Kaolinite Suspended Solids with Roxarsone System at ambient pH

The procedure in Section 2.4.2 was repeated with the addition of 400 ppm kaolinite suspensions added to the roxarsone in step A.

2.4.4 Roxarsone System pH 7

The procedure in Section 2.4.2 with the adjustment of the pH of roxarsone adjusted to pH 7 using HCl and NaOH solutions.

2.4.5 Kaolinite Suspended Solids with Roxarsone System pH 7

The procedure in Section 2.4.2 was repeated with the addition of 400 ppm kaolinite suspensions added to the roxarsone, and the pH of roxarsone/kaolinite mixture adjusted to pH 7 using HCl and NaOH solutions in step A.

2.5 Coagulation-Flocculation Studies with Arsenate (V) Solution

2.5.1 Preparation of Molybdate Color Reagent

Solutions of L-ascorbic acid (613 mM), ammonium molybdate (24 mM), antimony potassium tartrate (8 mM) and H_2SO_4 (2.5 M) were prepared in Millipore water. The solutions were combined in the previous order and a mixing ratio of 2:2:1:5, taking special care to add the H_2SO_4 immediately after the antimony potassium tartrate to avoid the solution turning turbid. The reagent was a yellow, transparent solution and is stable for up to 6 h.

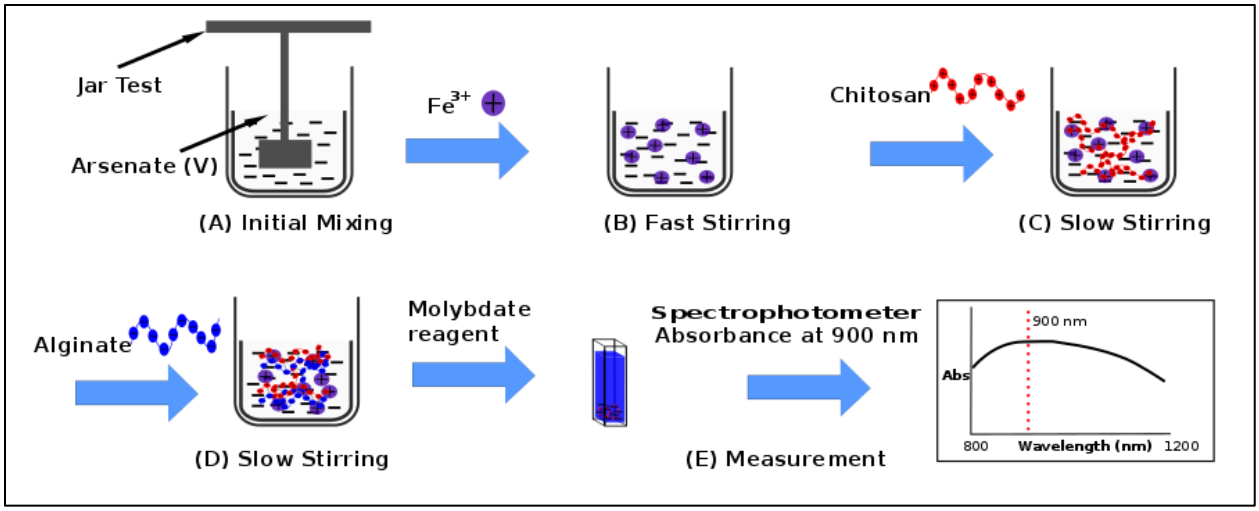

Scheme 2.3: Illustrated procedure for arsenate (V) removal

2.5.2 Arsenate System at ambient pH

With reference to Scheme 2.3, the jars of a six-gang Phipps & Bird jar test apparatus were each filled with 1 L of 30 ppm arsenate solution (in Millipore water) and stirred for 1 min. at 50 rpm to ensure uniform distribution (Step A). The pH of arsenate was then measured and recorded as ~6.5. Just after the solution was mixed, 15 ppm iron (III) was added to all of the jars and stirred for 3 min. at 295 rpm (Step B, fast mixing). Immediately after this, all jars were mixed for 10 min. at 25 rpm. However, jars 1 – 4 only contained the salts previously administered, while the MMWC solution (dissolved in 1% HCl solution) at a concentration of 2.5 ppm was added to jars 5 and 6 (Step C). After this mixing period, HVA was then added at a concentration of 10 ppm to jars 3 – 6 and all six jars were stirred for a further 10 min. at 25 rpm (Step D, total slow mixing 20 min.). When the stirring was complete, the contents of the jars were allowed to settle for 30 min., with 3 mL aliquots being removed initially and after settling. These aliquots were placed into 4 dram vials and 0.5 mL of color reagent was added. The vials were left undisturbed for 15 min. to ensure adequate color development and were analyzed using a UV-Vis spectrophotometer at $\lambda = 900$ nm (Step E).

2.5.3 Kaolinite Suspended Solids with Arsenate System at ambient pH

The procedure in Section 2.5.2 was repeated with the addition of 400 ppm kaolinite to the 30 ppm arsenate (V). Analysis was done using the UV-vis spectrophotometer at $\lambda = 900$ nm.

2.5.4 Arsenate Solution pH 3

The procedure in Section 2.5.2 was repeated; however, the pH of arsenate was adjusted to pH 3 using HCl and NaOH before the addition of the iron (III) solution. The UV-vis spectrophotometer was used to do analysis at $\lambda = 900$ nm.

2.5.5 Kaolinite Suspended Solids with Arsenate System pH 3

The procedure in Section 2.5.2 was repeated with the following changes: 400 ppm of kaolinite suspension was added to the 30 ppm solution of arsenate (V) and the pH of the arsenate (V)/kaolinite mixture was adjusted to pH 3 using HCl and NaOH before the addition of the iron (III) solution.

2.6 *One-Pot* Kinetic Studies

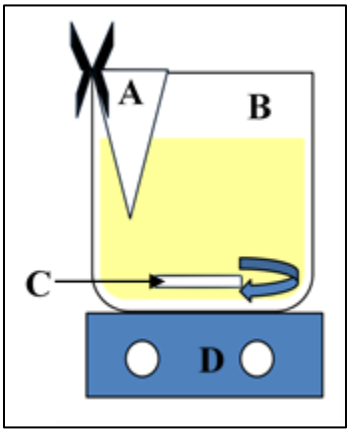

Figure 2.1: Illustration of the experimental setup for the *One-pot* method, where A is the filter barrier, B is the coagulant-flocculant system of interest, C is the Teflon stir bar, and D is the stir plate with temperature control.

2.6.1 Roxarsone Removal

2.6.1.1 Roxarsone System at ambient temperature

An 800 mL beaker was filled with 500 mL of 30 ppm roxarsone solution (in Millipore water) and placed on a magnetic stir plate (D) with a stir bar (C). A Whatman no. 40 filter paper was folded into a cone (A) and attached to the beaker (B) as shown in Fig. 2.1. The cone was allowed to fill up with solution and stirring was carried out at approx. 25 rpm. An initial 3 mL aliquot was taken from within the cone and placed into a 1 dram vial. Sampling within the cone began at time (t) = 0, when the first coagulant or flocculant was added and continued for 10 min. at 1 min. intervals, for a further 10 min. at 2 min. intervals and finally for 40 min. at 5 min.

intervals. At this point, stirring was stopped (t = 60 min.) and sampling continued for a further 55 min. at 5 min. intervals. All 3 mL aliquots were placed into 1 dram vials and centrifuged. After centrifugation, 1.5 mL aliquots were removed and placed into plastic cuvettes with 1.5 mL of 0.1 M phosphate buffer at pH 7. They were then analyzed using a UV-Vis spectrophotometer. Table 2.2 details the coagulants and flocculants used in the various experiments.

Table 2.2: Coagulant/flocculant systems used in *one-pot* experiments

System	Iron (III) added	Chitosan added	Alginate added	Time of addition
1	✓			0 min.
2		✓		0 min.
3			✓	0 min.
4	✓	✓		Fe (III) 0 min.; Chit. 3 min.
5	✓		✓	Fe (III) 0 min.; Alg. 4 min.
6	✓	✓	✓	Fe (III) 0 min.; Chit. 3 min.; Alg. 4 min.

2.6.1.2 Kaolinite Suspended Solids with Roxarsone System at ambient temperature

The procedure in Section 2.6.1.1 was repeated with the following change: 400 ppm of kaolinite suspension was added to the 30 ppm roxarsone solution before coagulants/flocculants were added. The table (Table 2.2) above details the coagulants and flocculants used in the various experiments.

2.6.1.3 Roxarsone System at higher temperature

A circulating bath system was used to maintain a constant temperature of the roxarsone throughout the experiment. 250 mL of 30 ppm roxarsone solution (in Millipore water) was poured into the liquid-jacket glass vessel attached to the circulating bath and placed on a magnetic stir plate with a stir bar. The bath was turned on and the solution heated to the desired temperature (30 or 40 ºC). A Whatman no. 40 filter paper was folded into a cone (A) and attached to the side of the vessel (B), in a similar manner to Figure 2.1. The cone was allowed to fill up with solution and stirring was carried out at approx. 25 rpm. An initial 0.5 mL aliquot was taken from within the cone and placed into a 1 dram vial. Sampling within the cone began at time (t) = 0, when the first

coagulant or flocculant was added and continued for 10 min. at 1 min. intervals, then for a further 10 min. at 2 min. intervals and finally for 40 min. at 5 min. intervals. At this point, stirring was stopped (t = 60 min.) and sampling continued for a further 55 min. at 5 min. intervals. All 0.5 mL aliquots were placed into 1 dram vials and at the end of the sampling, 2.5 mL of 0.1 M phosphate buffer pH 7 was added and the samples were analyzed using a UV-Vis spectrophotometer. The table (Table 2.3) below details the coagulants and flocculants used in the various experiments.

Table 2.3: Types of coagulant and flocculant systems used for temperature studies

System	Iron (III) added	Chitosan added	Alginate added
1	✓		
2	✓	✓	✓

2.6.1.4 Kaolinite Suspended Solids with Roxarsone System at higher temperature

The procedure in Section 2.6.1.3 was repeated with the following change: 400 ppm of kaolinite suspension was added to the 30 ppm roxarsone solution before coagulants/flocculants were added. The table (Table 2.3) above details the coagulants and flocculants used in the various experiments.

2.6.2 Arsenate (V) Removal

2.6.2.1 Arsenate System at ambient temperature

The procedure in Section 2.6.1.1 was repeated with the following change: 500 mL of 30 ppm arsenate (V) solution was poured into the beaker with the stir bar. Table 2.2 details the coagulants and flocculants used in the various experiments.

2.6.2.2 Kaolinite Suspended Solids with Arsenate System at ambient temperature

The procedure in Section 2.6.1.2 was repeated with the following changes: 500 mL of 30 ppm arsenate (V) solution was poured into the beaker with the stir bar and 400 ppm of kaolinite suspension was added to the arsenate (V) solution before coagulants/flocculants were added. The table (Table 2.2) above details the coagulants and flocculants used in the various experiments.

2.6.2.3 Arsenate System at higher temperature

The procedure in Section 2.6.1.3 was repeated with the following changes: 250 mL of 30 ppm of arsenate (V) solution was poured into the beaker with the stir bar. The table above (Table 2.3) details the coagulants and flocculants used in the various experiments.

2.6.2.4 Kaolinite Suspended Solids with Arsenate System at higher temperature

The procedure in Section 2.6.1.4 was repeated with the following changes: 250 mL of 30 ppm arsenate (V) solution was poured into the beaker with the stir bar and 400 ppm of kaolinite suspension was added to the arsenate (V) solution before coagulants/flocculants were added. The table above (Table 2.3) details the coagulants and flocculants used in the various experiments.

2.6.2.5 Statistical Analysis

Jar test studies on roxarsone and arsenate (V) were done in replicates of two (2) and error bars were reported as the standard deviations of the replicates.

2.6.3 Kinetic Studies Evaluation: Equations and "Best fit" criteria

Kinetic studies were conducted using the "*one-pot*" setup at ambient pH and variable temperature (20, 30 and 40 °C). This *one-pot* method was adapted from previous studies reported elsewhere[59,61] for studies focused on adsorption-based processes. The study undertaken herein is the first to study coagulation-flocculation rather than adsorption using an *in-situ* sampling setup. This is an important difference since there is not always a clearly defined solid phase but rather a colloidal phase in the case of kaolinite addition, formation of iron hydroxides and, in some cases, microflocs. The choice of barrier material can be adjusted to the system being studied. Dialysis membranes, with pore sizes of <0.1 µm,[103] can be used for smaller particles and filter paper can be used for larger particles. For instance, Whatman no. 40 filter paper has a pore size of 8 µm.[104]

The solution phase containing the arsenic species was measured by continuous *in-situ* sampling of fixed volumes at variable time intervals during the coagulation/flocculation and settling process. The use of a semi-permeable barrier offers the advantage of retarding the process, which was found to have very rapid floc formation. The barrier material results in separation of the formed flocs from the sampling site, which measures the bulk phase (not flocculated) solution containing arsenic. Sampling was done as described previously.

The kinetic studies conducted using the *one-pot* method examined the effect of the various coagulant/flocculant combinations of the iron (III)-chitosan/alginate system on the removal of roxarsone. This was shown in plots expressed by the amount of roxarsone "adsorbed" per mass of iron (III), represented by Q_t, *vs.* time. Q_t (mg/g) was determined by equation 2-1, where C_o and C_t are the concentrations in mg/L of arsenic initially and at time, t. The V is the volume (in L) of solution of arsenic and m is the mass of the coagulant/flocculant used (in g). In the case of multiple coagulant/flocculants, the mass of iron (III) only was used since it is mainly responsible for the

removal of arsenic. The data was then fitted with either pseudo-first (PFO) or pseudo-second order (PSO)[59] kinetic models expressed by equations (2-2) and (2-3), shown below:

$$Q_t = \frac{(C_o - C_t)V}{m} \quad (2\text{-}1)$$

$$Q_t = Q_e(1 - e^{-k_1 t}) \quad (2\text{-}2)$$

$$Q_t = \frac{Q_e^2 k_2 t}{1 + k_2 t Q_e} \quad (2\text{-}3)$$

The fitted plots determined two important constants, Q_e and k_1/k_2. The former constant, Q_e, was the amount of roxarsone "adsorbed" at pseudo-equilibrium and k_1/k_2 are the rate constants for the PFO and PSO models, respectively. The data was fit with both PFO and PSO models and the "best-fit" criteria was determined by comparing the r-squared values (R^2) and the reduced chi-square values (χ^2), the latter of which is calculated using equation 2-4.

$$\chi^2 = \Sigma\sqrt{\frac{Q_{e,i} - Q_{c,i}}{N}} \quad (2\text{-}4)$$

The χ^2 is the difference between the experimental ($Q_{e,i}$) and calculated ($Q_{c,i}$) uptake values, and N represents the number of experimental data points.

2.6.4 Thermodynamic Studies

From the kinetic studies performed and data plots of the PFO and PSO kinetic models, the rate constants k_1 and k_2 were obtained. The relationship between the rate constant and temperature can be determined by the Arrhenius equation.[105] It is applicable to both gas and condensed phase systems. By using the Eyring equation[105] (eqn. 2-5), the relationship between the reaction rate (through rate constant) and temperature can be determined for the coagulation-flocculation processes since it is used for mixed phase (heterogeneous) reactions. The thermodynamic parameters of the activated complex, $\Delta H^{\ddagger}$ and $\Delta S^{\ddagger}$, can be obtained along with molecular level information on reaction progress. These thermodynamic parameters give insight into the nature of transition state.

$$ln\left(\frac{k_i h}{k_B T}\right) = -\frac{\Delta H^{\ddagger}}{R}\frac{1}{T} + \frac{\Delta S^{\ddagger}}{R} \quad (2\text{-}5)$$

In the above equation, k_i is the rate constant according to the PFO and PSO models, k_B is the Boltzmann constant (1.381×10^{-23} J/K), T is the temperature (K) and h is Planck's constant (6.626×10^{-34}J.s). Plots of $ln\left(\frac{k_i h}{K_B T}\right)$ vs. $\frac{1}{T}$ will constructed and used to determine the relevant

thermodynamic parameters for the removal of roxarsone and arsenate (V) removal through the coagulation-flocculation process.

Chapter 3 RESULTS AND DISCUSSION: OPTIMIZATION COAGULATION-FLOCCULATION STUDIES USING KAOLINITE MODEL SUSPENSIONS USING JAR TEST STUDIES

1.1 Dosage of Coagulant/Flocculant

3.1.1 Dosage of Metal Salts

Conventional systems used for coagulation-flocculation experiments usually consist of a metal salt such as iron (II) chloride ($FeCl_2$), iron (III) chloride ($FeCl_3$) or aluminum sulphate ($Al_2(SO_4)_3$), which is commonly referred to as 'alum'.[28] To enhance the properties of such coagulants, and decrease their negative consequences, two biopolymers (chitosan and alginate) were chosen to complement the metal salts. Previous studies have shown that the use of polymers, whether natural or synthetic, lower dosage requirements overall and thus lower the material cost for the treatment process.[43,76] The primary use of coagulation-flocculation is the removal of colloidal species, which do not settle due to charge repulsion between particles. This study focused on kaolinite clay as a model colloidal system to test the efficiency of colloid removal by lowering the turbidity of such suspended solids.

Three types of metal salts were chosen for the studies that contain Fe(II) ions, Fe(III) ions and Al(III) ions. These metal cations possess a high positive charge density and were easily ionized. To investigate the effect of dosage and the type of salt used in the system, the dosage of medium MW chitosan (MMWC) and high viscosity alginate (HVA) biopolymers were fixed and the dosage of each salt was varied from 15 to 60 ppm in 15 ppm increments. The system was maintained at a pH of ~8.5 and the system was used to carry out Jar tests on 400 ppm kaolinite suspensions. The initial concentration of suspended solids was chosen from previous studies reported in the literature.[50] A controlled study of the settling of kaolinite was conducted by carrying out the jar test procedure without coagulant or biopolymer flocculant. The kaolinite was allowed to settle on its own and this was used for comparison of settling with the metal salt-chitosan/alginate system.

Figure 3.1 shows the effect of alum dosage on turbidity removal. The optimum dosage was determined to be 30 ppm. It should first be noted that the addition of the metal ion/biopolymer system greatly enhanced the turbidity removal as evidenced by the 35 %T from the settling of kaolinite on its own. While the amount of chitosan was constant, the amount of positive charge

changed upon increasing the concentration of metal salt (alum). The results show that an increase in positive charge beyond a certain point causes the continued stabilization of the colloidal particles, as evidenced by less settling.

Figure 3.2 shows the effect of Fe(II) dosage on the turbidity removal. The optimum dosage was evident at 15 ppm, the lowest dosage of four dosages studied. A minimal amount of Fe(II) was required since more Fe(II) ions would introduce an excess of positive charge, which leads to repulsion among the colloidal particles, thus resulting in stabilization. The higher dosages did not show a marked difference in terms of turbidity removal, implying that a 15 ppm dosage of Fe(II) along with a 2.5 ppm dosage of chitosan provides enough positive charge for neutralization of 400 ppm of kaolinite.

By comparing the type of metal salt coagulant, alum and Fe(II) showed better turbidity removal according to measurement of light transmittance (%T). Turbidity was assessed, where the %T value was in the range (90%) for alum and Fe(II), while Fe(III) was 55 %T, with a poorer performance. According to the shape of the %T vs. time plot (Fig. 3.3); kaolinite removal had not leveled out by the 30 min. mark when using Fe(III). This implies that slower kinetics occurred but not necessarily lower uptake of kaolinite. While Fe(III) has a similar charge density to alum (both of which are higher than that of Fe(II)), its solubility is lower than that of Fe(II). Based on studies performed by Baskan *et al.*[30], the formation of insoluble iron hydroxides leads to the adsorption of particles onto the hydroxide mineral surface.[30] Since the hydroxides are formed at a slower rate for Fe(III) then it would take longer to remove the kaolinite particles. The rate of formation of iron (III) hydroxides is faster than that of iron (II) hydroxides. Therefore, since the metal hydroxides are insoluble, there is less unbound Fe(III) available for charge neutralization for reduction of charge and colloidal destabilization.

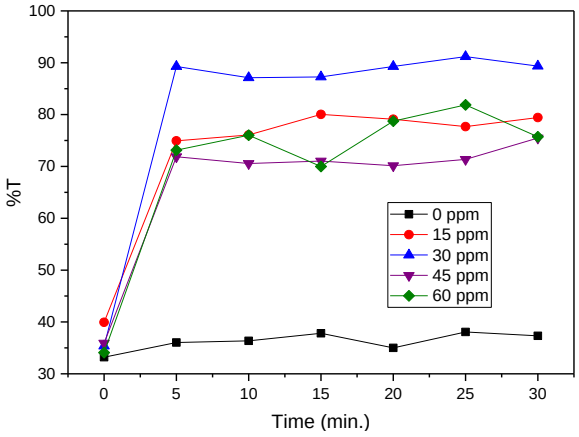

Figure 3.1: Effect of dosage of alum on kaolinite removal (400 ppm) [10 ppm MMWC, 10 ppm HVA]

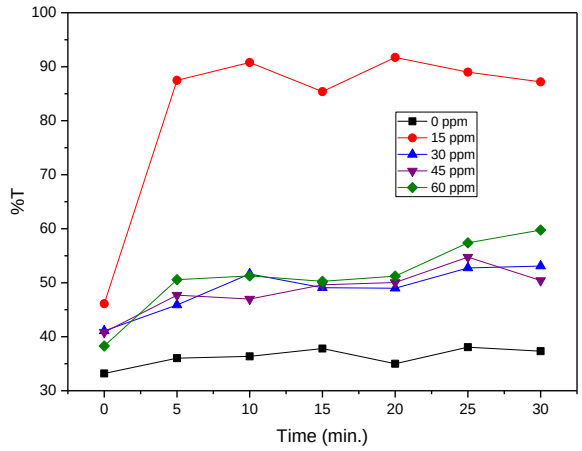

Figure 3.2: Effect of dosage of Fe (II) on kaolinite removal (400 ppm) [10 ppm MMWC, 10 ppm HVA]

The same dosage was proven to be optimal for Fe(III) (*see* Figure 3.3). This dosage was not well defined as that of Fe(II) since the plots showed an upward slope for most dosages rather than a plateau, which may have indicated completion of settling. A comparison of slopes revealed that there was a plateau for the 60 ppm dosage; however, there was no plateau for the other dosages. A dosage of 15 ppm showed the highest %T at the end of settling time, where its settling rate showed a sharper increase while those for 30 and 45 ppm were about to level off at a lower final turbidity level. Overall it can be inferred that the lower dosage of Fe(III) was slower to action, but provided in improved reduction in charge repulsion. It is possible that the formation of solid Fe (III) hydroxide particles reached a critical point (around 20 minutes) where they aggregated to form larger particles, which provided the best surface for adsorption of the kaolinite particles.

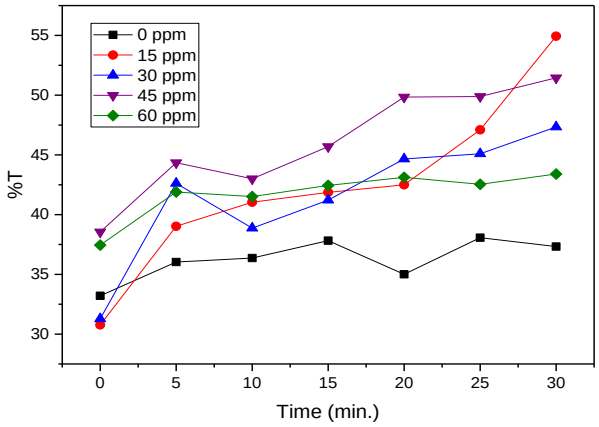

Figure 3.3: Effect of dosage of Fe (III) on kaolinite removal (400 ppm) [10 ppm MMWC, 10 ppm HVA]

3.1.2 Dosage of Chitosan

The amount of chitosan (MMWC and LMWC) was varied from 2.5 to 10 ppm while alginate (HVA and LVA) was kept at 10 ppm and the optimum dosage of metal salts (Section 3.1.1) for removal of kaolinite turbidity was used here (Fig. 3.4, 3.5, 3.6). In general, the results showed that the system worked better at lower dosages (2.5 and 5 ppm) rather than the higher dosages (7.5 and 10 ppm). This can be attributed to an increase in positive charges from the higher amounts of chitosan that destabilize the colloid by first neutralizing the negatively charged colloid then re-stabilizing the colloid by providing an excess of positive charge.

It is of great importance to note that this was not always the observed trend because in some instances chitosan at 7.5 ppm worked quite effectively. However, in all instances 10 ppm chitosan tended to correspond to the lowest %T, indicating that the colloid was re-stabilized. The dosages were varied with each combination of chitosan MW to alginate viscosity. MMWC was combined with LVA and HVA separately. In each instance the dosage was varied and the test was repeated for LMWC. Since chitosan is a linear polymer, the lower the MW, the shorter the chain with fewer amino groups per chain length. This means that LMWC compared to MMWC is expected to have a smaller number of positive charges per chain when dissolved in an acidic medium. For systems with LMWC, the 7.5 ppm dosage showed good flocculating ability because a higher concentration of chitosan was needed to provide enough positive charges for destabilization of the kaolinite. Cooperativity might also play a role in enhancing the attachment of the chitosan chains; the addition of one chitosan chain may alter surface charge on the kaolinite allowing shorter chains to attach themselves to the clay surface. The adsorption of chitosan onto

the kaolinite surface causes cations to be displaced from the counterion layer. This leaves the surface more accessible for further polymer attachment, which may be due to steric and/or electronic effects.

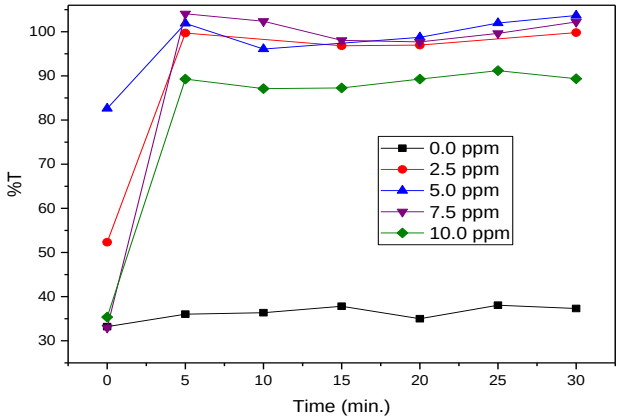

Figure 3.4: Effect of dosage of MMWC on kaolinite removal (400 ppm) [30 ppm Alum, 10 ppm HVA]

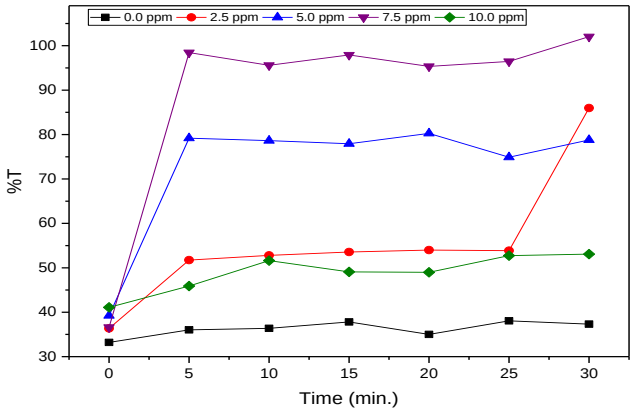

Figure 3.5: Effect of dosage of MMWC on kaolinite removal (400 ppm) [15 ppm Fe (II), 10 ppm HVA]

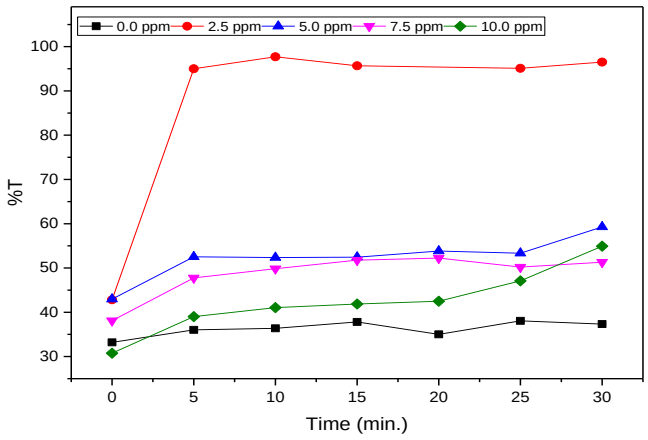

Figure 3.6: Effect of dosage of MMWC on kaolinite removal (400 ppm) [15 ppm Fe (III), 10 ppm HVA]

3.1.3 Dosage of Alginate

The effect of alginate dosage was studied by using the optimal amounts of the salts obtained from previous experiments in Section 3.1.1 and using a constant 10 ppm dosage of chitosan. Alginate dosages were 2.5, 5.0, 7.5 and 10.0 ppm. As with the chitosan, the alginate dosage affected the flocculating ability of the system. Sodium alginate has many carboxyl groups, which allows it to be negatively charged in basic media by deprotonating those groups when pH lies above the pK_a of the conjugate acid (alginic acid). In acidic conditions ($pH < pK_a$), the carboxyl groups are protonated which lowers the number of negatively charged carboxylate groups. The results showed that while the low dosages of alginate were quite effective, higher dosages were also favoured. High dosages of alginate did not stabilize the colloid like the chitosan.

The trend identified was that a higher dosage of alginate was needed when the MMWC was used, implying that more negative charged chains were needed to neutralize the extra positive charges originating from the chitosan cation sites. The kaolinite suspension ranged between pH 8 and 9, where this alkaline pH range contrasted with typical values (pH of 3 – 4) of alginate solutions. This system ultimately became acidic (pH 3 – 3.5) during flocculation. This may have been due to hydronium ions being released when the metal ions were taken up at the exchange sites,[106] onto the edges and the basal (-OH) surfaces,[107] onto kaolinite. The alginate may also cause release of protons when the alginate complexes with the metal ions, and perhaps the kaolinite as well. This would have meant that there were less negative charges on the alginate. A higher dosage

would have somewhat offset this effect and allow the formation of flocs that undergo settling. Results are shown in Fig. 3.7, 3.8 and 3.9.

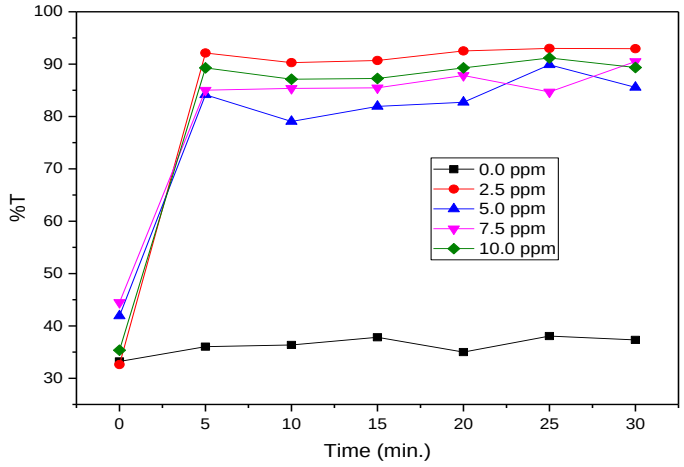

Figure 3.7: Effect of HVA dosage on kaolinite removal (400 ppm) [30 ppm Alum, 10 ppm MMWC]

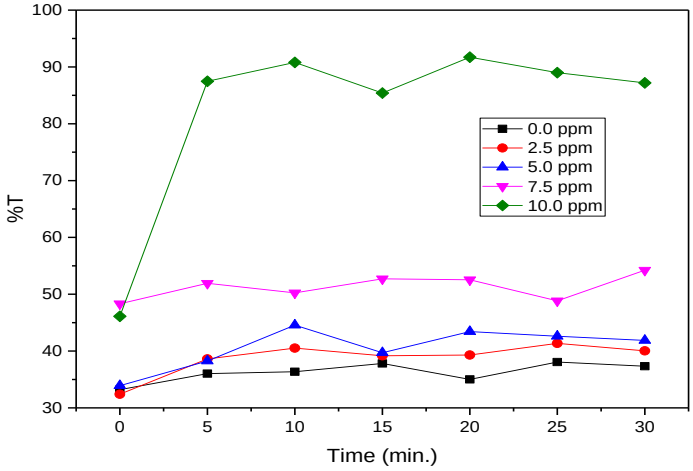

Figure 3.8: Effect of HVA dosage on kaolinite removal (400 ppm) [15 ppm Fe (II), 10 ppm MMWC]

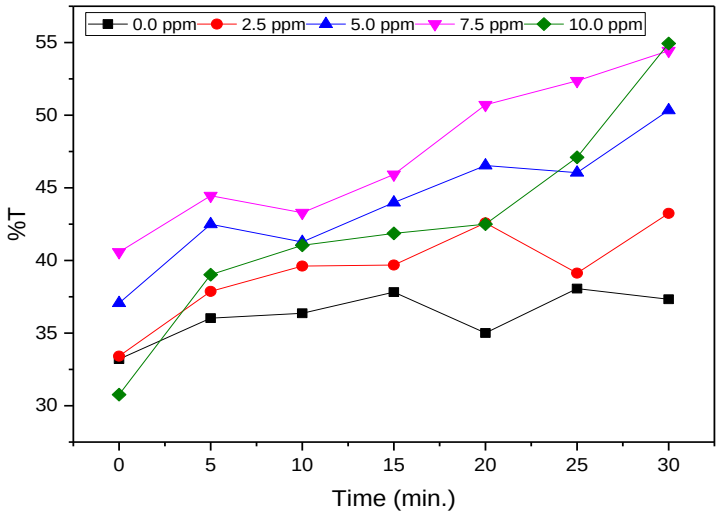

Figure 3.9: Effect of HVA dosage on kaolinite removal (400 ppm) [15 ppm Fe (III), 10 ppm MMWC]

3.2 Effect of pH on Coagulation-Flocculation

The pH of the kaolinite suspension was adjusted using HCl and NaOH to obtain suspensions with various pH (pH 3, 5, 7 and 9). Figure 3.10 shows that the initial pH of the kaolinite suspension did not affect the %T after flocculation was allowed to occur. To discuss this in further detail, consider the kaolinite suspension. Kaolinite consists of aluminates and silicates with Al-OH and Si-OH functional groups. These mineral oxides are arranged in layers with slightly different composition on the edges compared to the faces of the clay particles. These groups impart negative charges on the kaolinite in basic media and protonated groups in acidic media. Due to the negative charges on the alumina sites, kaolinite acts as a cation exchanger. So, the overall charge environment in the kaolinite changes based on the pH. The unadjusted pH of kaolinite is pH 8 – 9, implying that there are many negative charges present on the surface of the kaolinite (deprotonated hydroxyl groups). Additionally, metal ions like Na^+ and K^+ found within the kaolinite are exchanged with H^+ ions from the water molecules, leaving -O- surface sites free, which lead to the higher pH value. These stabilize the colloid. The salts and polymers all contribute to the final pH of the flocculated system and since these are all acidic (chitosan is generally only soluble in acidic aqueous solution or ionic solvent media). Because the chitosan is dissolved in HCl, the free protons from the HCl solution would help to lower the pH of the system. The protons from the coagulant and flocculants seem to undergo some sort of cation exchange with the kaolinite that causes a drop in the pH to around pH 3. At this pH, chitosan remains dissolved and positively charged, which aids in charge neutralization of the colloid.[108] The alginate likely has most of its carboxyl groups protonated, which aids in keeping the amount of negative charges

down, so as not to help re-stabilize the colloid. At a basic pH, the Al^{3+}, Fe^{2+} and Fe^{3+} would begin to form hydroxides, which are insoluble and precipitate out leaving fewer ions in solution to aid in charge neutralization. At lower pH values (below pH 7), there are more metal cations (Al^{3+}, Fe^{2+}, Fe^{3+}) than solid (hydr)oxides[109,110] present in water. These ions would form flocs of kaolinite by the charge neutralization mechanism; that is, the positive ions would cause the electrical double layer to become compressed.

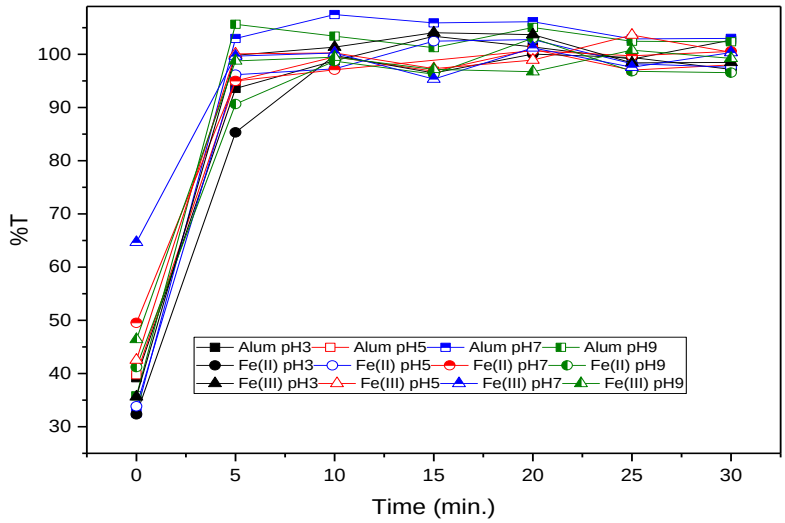

Figure 3.10: Effect of pH on kaolinite removal (400 ppm) [30ppm Alum, 15 ppm Fe (II), 15 ppm Fe (III), 2.5 ppm MMWC, 10 ppm

3.3 Molecular Weight of Chitosan

As mentioned previously, the MW of the chitosan affects the flocculating ability of the system. From the data obtained the following chart was constructed to highlight the effect of MW of chitosan for the removal of turbidity in the suspension. Figure 3.11 below shows that the effect of MW on flocculating varies based on the salt used as a coagulant. First of all, the results on the far-left show that changing the molecular weight of chitosan when alum is used as the coagulant did not significantly affect the %T. The results in the middle show that when Fe(II) is used as the coagulant, changing the MW of the chitosan had a more significant impact on the removal of turbidity. The effect of Al^{3+} when compared to Fe^{2+} has a smaller positive charge density (smaller radius and less charge) so when the LMWC is replaced by the MMWC, the relative decrease in positive charge was inadequate to fully destabilize the colloid.

Overall the %T decreased but the level was the same for the LMWC/LVA and MMWC/HVA combinations. The largest decrease observed was for the LMWC/HVA combination, followed by the MMWC/HVA polymer duo. This contrasting mixture of what are essentially

differing polymer lengths was not favorable. Perhaps in the case of LMWC, any loops and tails that may have formed were short and the polymer chains of the HVA would attach and have excess chain remaining, which may become entangled with itself and less able to bridge other flocs. In the second lowered combination, the alginate used was a LVA. The longer chitosan chain could electrostatically attach to the short alginate chain, thereby leaving less carboxyl groups free for bridging. Then finally, the results to the far right in Fig. 3.11 are similar to those of the alum, which could mean that Fe^{3+} has enough positive charge to fully destabilize the system and allow flocculation to occur. Both Al^{3+} and Fe^{3+} may be bridging points for the kaolinite and alginate by attaching to the clay and has binding sites free for the alginate, similar to chelate effects where the alginate functions similar to a podand.[28]

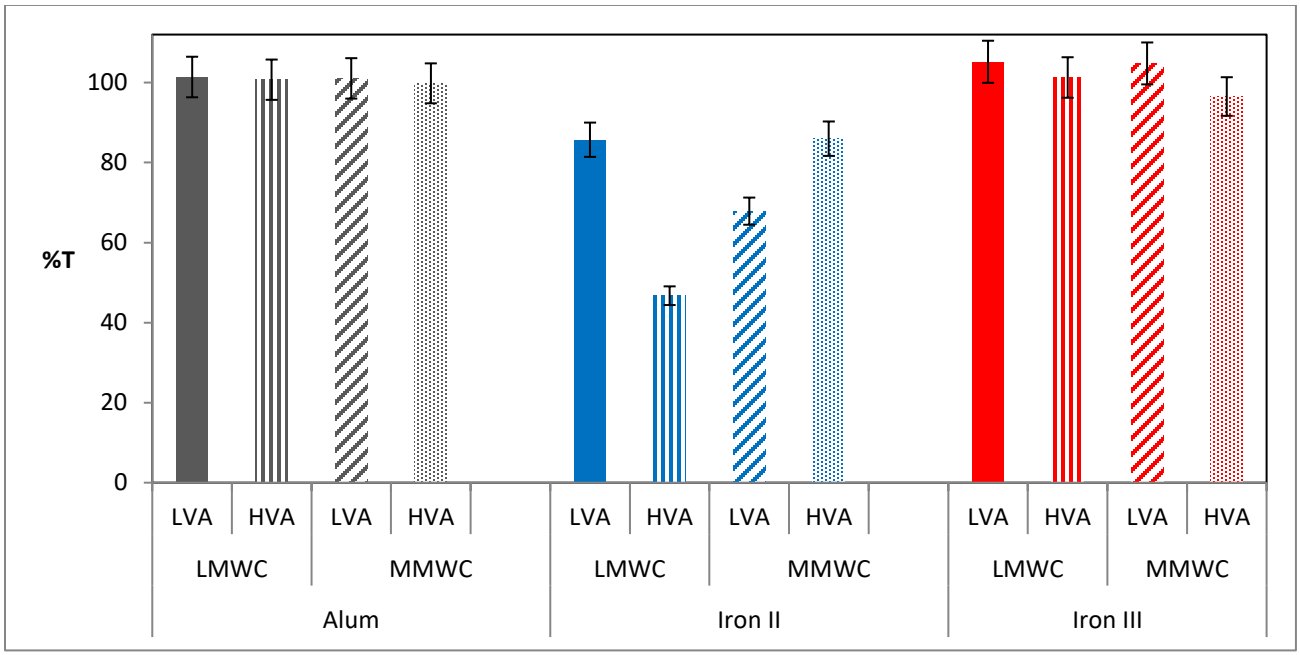

Figure 3.11: Effect of molecular weight of chitosan on kaolinite removal (400 ppm) using jar test studies (LVA – low viscosity alginate, HVA – high viscosity alginate, LMWC – low molecular weight chitosan, MMWC – medium molecular weight chitosan) – Error bars are 5% error of instrument

3.4 Viscosity of Alginate

The viscosity of alginate was chosen to indirectly study the effect of MW of alginate on flocculation. The longer the alginate chain is, the greater its viscosity and vice versa. This would imply that the LVA has shorter chains; therefore, it should have less negative charges per chain compared to a longer chain because it has fewer units. Formation of macroflocs (visible to the eye) on addition of alginate shows that it acts as a bridge between the microflocs (not visible). Since

the alginate is negatively charged (pK_a ~3.5)[65] it probably binds to the positive cation species and/or the chitosan protonated sites to bridge the flocs. The figure (Fig. 3.12) below shows the variation of %T when the alginate viscosity was changed at a constant dosage of 2.5 ppm alginate. Looking at the three different salts, it is seen that viscosity affects each salt differently and also, the lower amount of alginate present significantly affected the results when compared to the previous figure (Fig. 3.11), where alginate was 10 ppm. This shows that it is better to have more alginate present than less. For alum on the far left, the results show that the HVA was the better choice for flocculant compared to the LVA. The shorter alginate chain (low viscosity) might simply have not bridged the microflocs as well the longer chain (high viscosity). For Fe(II), the MMWC did not perform well with either LVA or HVA. This might be due to too much positive charge from the chitosan stabilizing the colloid, or the long chain of chitosan might have become entangled with itself leaving fewer binding sites for the alginate. The LMWC would have less positive charge, which would not be enough to cause stabilization of the colloid through positive charge repulsion. The shorter chains of the LMWC would not be long enough to become much entangled, thereby allowing more binding sites (its protonated amine groups) to be exposed. The HVA outperformed the LVA, which might be due to greater bridging ability due to the longer chain. At 2.5 ppm of alginate, there may have been less entanglement with the long alginate chains amongst themselves.

Finally, iron (III) ion results on the far right all showed lower %T compared to alum and some iron (II). Since Fe^{3+} has a higher positive charge density than Fe^{2+} then it is likely that this caused the colloid to be stabilized instead of destabilized even for the use of LMWC.

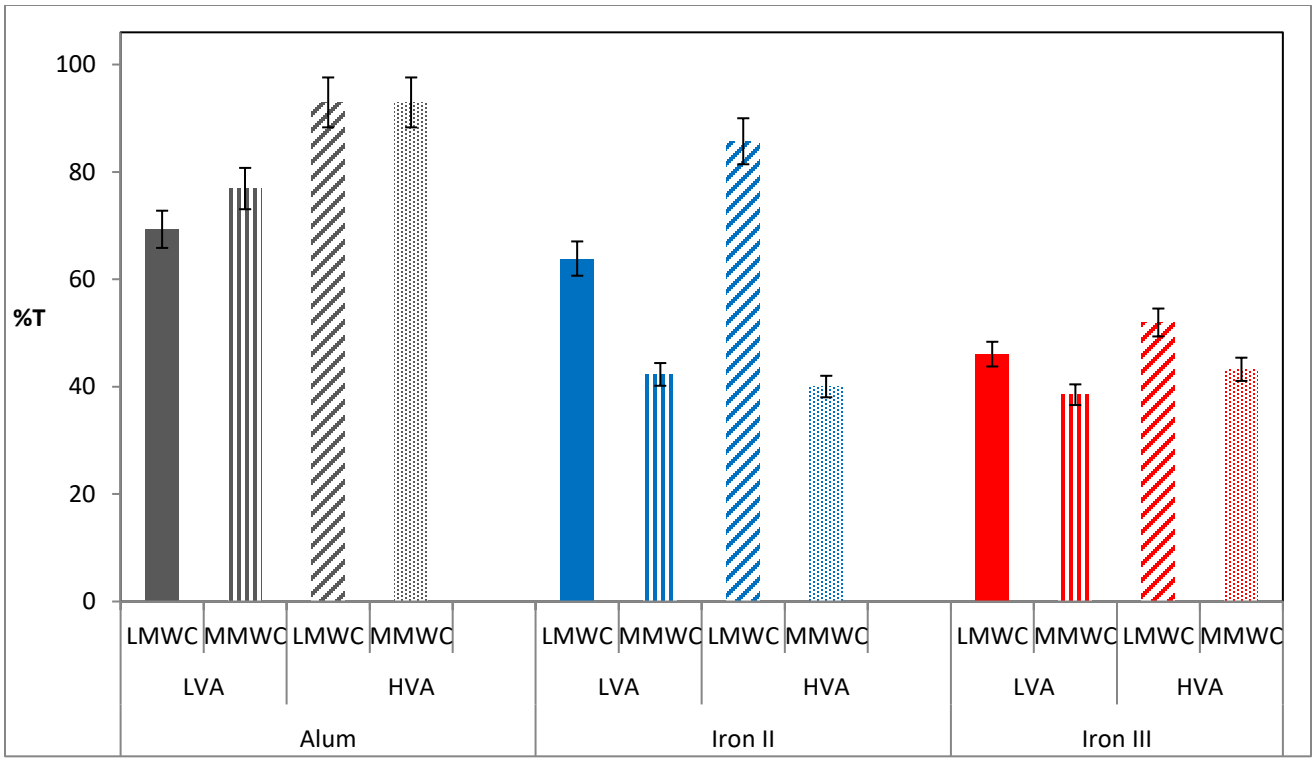

Figure 3.12: Effect of viscosity of alginate on kaolinite removal (400 ppm) using jar test studies – Error bars are 5% error of instrument

3.5 Sequence of Polymer Addition

The system used for coagulation-flocculation was unique in that it used two polymers along with the coagulant metal salt. Because of this, it was important to study the effects, if any, according to the order of polymer addition on the flocculation process. The order chosen firstly involved the addition of chitosan at 0 minutes with slow mixing, followed by alginate at 10 minutes thereafter. This was then compared to adding the alginate at 0 minutes, followed by chitosan at 10 minutes slow mixing. Then both polymers were added at 10 minutes into the slow mixing stage. Finally, the alginate and chitosan were pre-mixed separately (forming a PEC) when 5 minutes of slow mixing stage had elapsed. This pre-mixed polymer combination was added 10 minutes into the slow mix stage. The results of these experiments are shown in Figure 3.13. What can be inferred from the chart is that addition of the polymers separately into the jar, whether it was 10 minutes apart or 0 minutes apart, works better than adding the pre-mixed polymers. From the observed results, the pre-mixed polymers formed a gel and this prevented the polymers from fully self-assembling into the optimal configurations for flocculation. The gel was insoluble in the aqueous

part of the suspension; that is, the polymers were unavailable for charge neutralization and bridging of the clay particles because they were interacting with each other to form a stable complex.

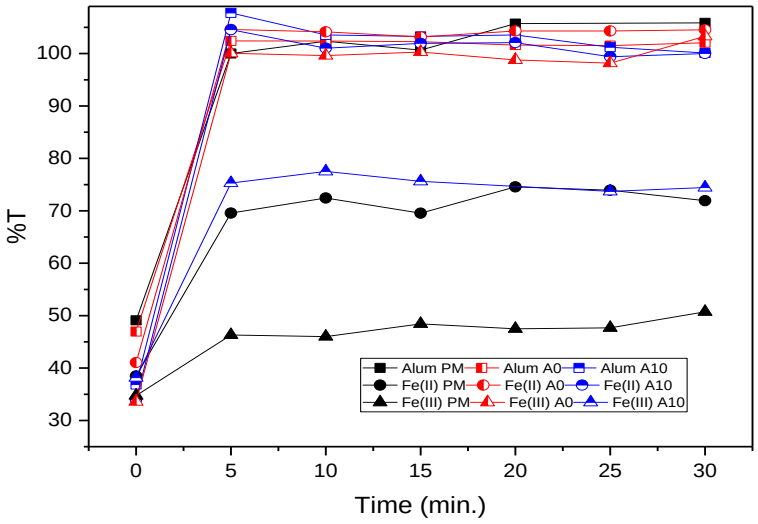

Figure 3.13: Effect of order of addition of biopolymers on kaolinite removal (400 ppm). PM represents pre-mixed chitosan and alginate, A0 represents alginate added at 0 minutes slow mix and A10 represents alginate added at 10 minutes slow mix

3.6 Mechanical Aspects of Jar Test Studies

3.6.1 Effect of Stirring Time

The coagulation-flocculation process is used in many water treatment operations since it is a simple, straightforward process which does not require complex machinery and also, because it requires fewer chemicals. It works quite well once it is optimized for the specific system requiring treatment.[28,33]

The Jar test experiment is used to optimize the coagulation-flocculation process because it allows for the testing of the coagulant-flocculant system but on a relatively small scale, which is very cost effective and works quite well. One of the parameters important to the coagulation-flocculation process is the amount of time that mixing occurs between the system to be treated and the coagulants and/or flocculants. This is usually done in two stages: fast (flash) mixing and slow mixing. The first stage is usually when the coagulant (such as alum) is added and is rapidly incorporated into the treated system in a short span of time. The second stage requires a slower speed for mixing for the formation and maintenance of microflocs. The second stage requires a longer time to allow for larger flocs to develop since the larger flocs settle faster and are more stable.[33]

For this experiment, three different sets of mixing times were chosen to be investigated. The figure (Fig. 3.14) below shows how the variation of fast and slow mixing times affected the alum-polymer system during the Jar test. It is observed that there was no significant difference among the results. For fast mixing, a time of 1, 3 and 5 minutes was chosen to be studied and for slow mixing, 15, 20 and 25 minutes. The results indicate that adequate flash mixing occurred at time intervals as low as 1 minute and ample microfloc formation occurred in as little as 15 minutes for the kaolinite suspension. This is inferred because the results were similar after increasing both times.

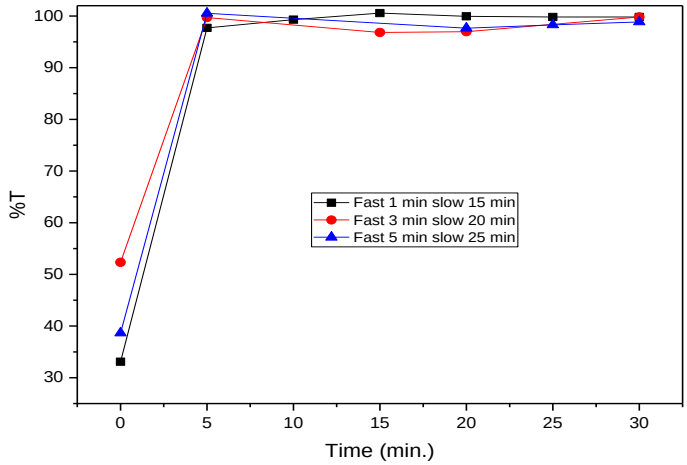

Figure 3.14: Effect of mixing time on kaolinite removal (400 ppm) [30 ppm Alum, 2.5 ppm MMWC, 10 ppm HVA]

3.6.2 Effect of Stirring Speed

Two speeds were investigated for flash mixing: 295 rpm and 150 rpm; two speeds were also investigated for slow mixing: 50 rpm and 25 rpm. From Figure 3.15 there was good settling at all speed combinations, implying that the alum had been properly incorporated into the colloid and that the polymers (added in the second stage) were allowed enough time to form microflocs and macroflocs. The speed was not too fast or the floc would have broken apart. It should be noted however that when the speed of stage two was decreased to 25 rpm from 50 rpm, there was a decrease in the amount of time required to reach a leveling off point in the settling process. From such observations, the flocs produced were bigger hence settling occurred faster.

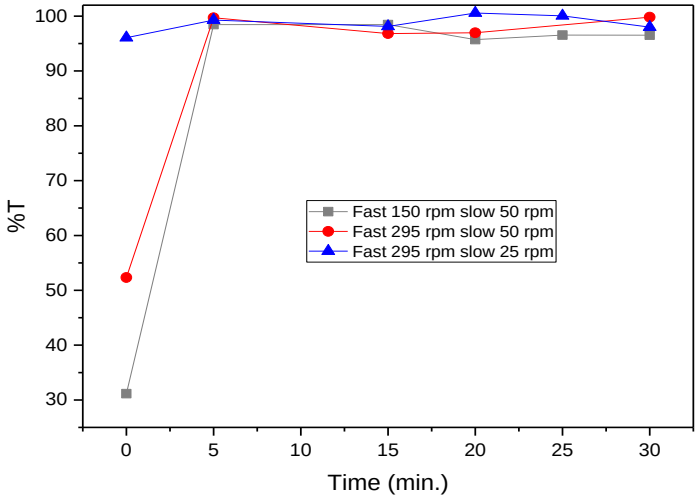

Figure 3.15: Effect of mixing speed on kaolinite removal (400 ppm) [30 ppm Alum, 2.5 ppm MMWC, 10 ppm HVA]

Chapter 4 RESULTS AND DISCUSSION: COAGULATION FLOCCULATION STUDIES FOR ARSENIC REMOVAL USING JAR TEST STUDIES

4.1 Roxarsone Removal

Roxarsone concentration was measured using the Beer-Lambert Law, where a calibration curve (Figure 4.2) was constructed for the determination of the concentration of roxarsone. Measurements were taken at the absorption maximum (λ_{max}) of 244 nm, as shown in Figure 4.1 below. Roxarsone exists as the neutral species and also as the mono-, di- and trivalent anion species in water based on the pH. In order to maintain a uniform species distribution when measuring, a 0.1 M phosphate buffer was employed to analyze the solution at pH 7.

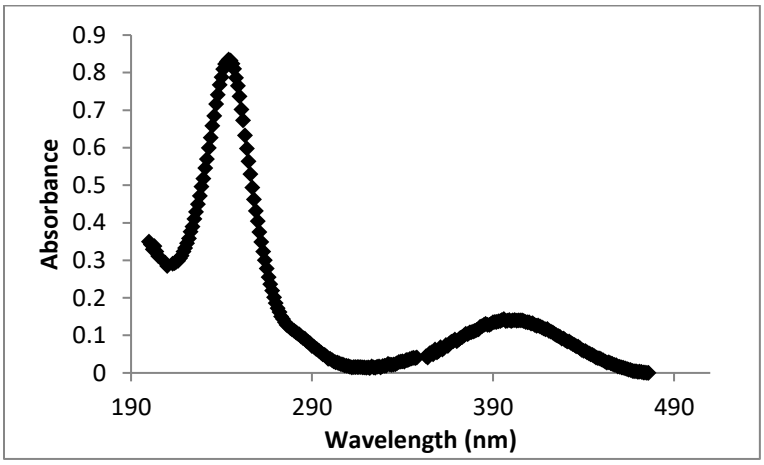

Figure 4.1: Absorbance spectrum for roxarsone in phosphate buffer (pH 7)

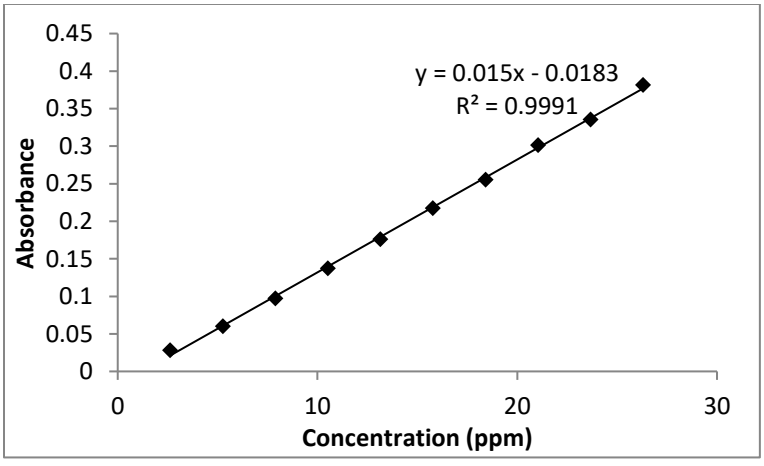

Figure 4.2: Calibration curve for roxarsone in phosphate buffer (pH 7)

4.1.1 Roxarsone Removal at ambient pH

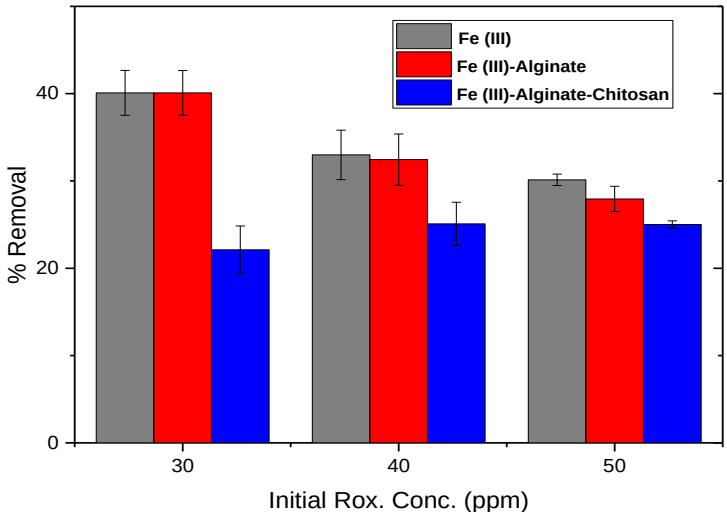

Figure 4.3: Roxarsone removal at various initial concentrations [15 ppm Fe (III), 2.5 ppm MMWC, 10 ppm HVA]

The removal of roxarsone was determined at three different initial concentrations of roxarsone solution and different combinations of coagulant/flocculant. Through preliminary studies, it was determined that the system containing Fe(III) ions showed the most promising roxarsone removal results. The Fe(III)-MMWC/HVA system was under study; however, through visual observation of kaolinite coagulation-flocculation, it was shown that macrofloc formation did not occur until the addition of alginate. For this reason, a simpler dual Fe(III)-alginate system was also investigated. It is well documented in the literature that iron compounds effect significant arsenic removal, so the Fe(III) was studied on its own to determine how much of the removal was due to Fe(III) alone.

The results in Figure 4.3 above show that Fe(III) alone was the cause of the removal of roxarsone and that as the initial amounts of roxarsone increased, the percentage of the species being removed decreased. Fe(III) ions are believed to remove arsenic species by formation of insoluble iron hydroxides, to which arsenic can adsorb onto and aggregate into larger molecules with greater settling ability. Alternatively, the arsenic may be enveloped within the forming iron hydroxide precipitates and be removed from solution. It is possible that both mechanisms occur simultaneously as well. An increase in roxarsone caused a decrease removal, likely due to a lesser number of surface sites for adsorption on to Fe(III) hydroxides as more roxarsone was introduced into the system. The addition of HVA and MMWC showed no enhancement in the removal of

roxarsone. This was evident from the almost identical results for both Fe(III) only and Fe(III)-alginate systems. The addition of MMWC caused an overall lowering of roxarsone removal. It is possible that the MMWC and HVA formed a PEC that enveloped some of the Fe(III) ions, causing less to be available for roxarsone removal. The pH is very important to coagulation-flocculation because it affects the structures of most of the species involved. The pH was steady throughout the experiment at ~3.5; this meant that both HVA and MMWC were charged, allowing for PEC formation to occur. Also, the formation of insoluble iron (III) hydroxides is somewhat limited at this pH.

4.1.2 Kaolinite Suspended Solids with Roxarsone at ambient pH

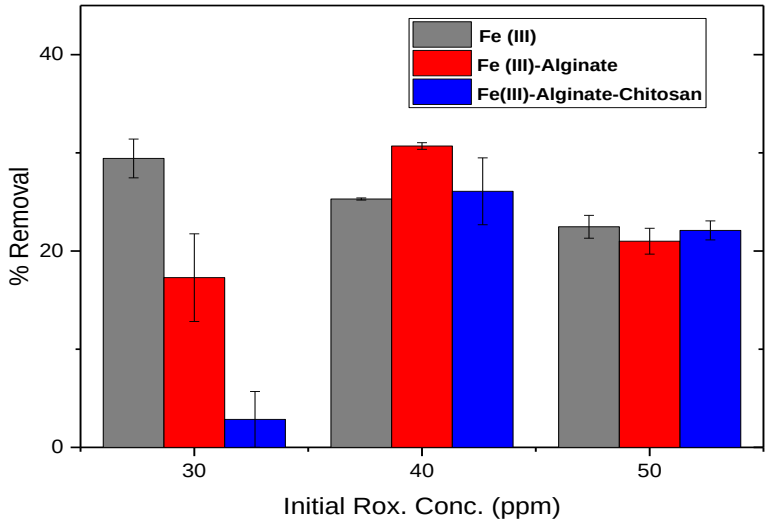

Figure 4.4: Roxarsone removal with 400 ppm kaolinite at various initial concentrations [15 ppm Fe (III), 2.5 ppm MMWC, 10 ppm HVA]

The addition of suspended solids in the form of kaolinite alters the removal of roxarsone (Fig. 4.4). Overall, Fe(III) shows the greatest roxarsone removal ability; however, this ability was lowered at all initial concentrations of roxarsone by about 10% for 30 ppm roxarsone, indicates that kaolinite (with a negative zeta potential) is also negatively charged and may compete to a certain extent for sites on Fe(III) hydroxides. It is possible that kaolinite particles might have also hindered nucleation of Fe(III) into solid particles by allowing less contact between the particles. Arsenic removal was less affected at higher concentration since the active adsorption sites were already filled at the lower concentration. The addition of HVA and MMWC worked in a similar manner when kaolinite was present as when it was absent at 40 and 50 ppm, perhaps due to Fe(III) being the principal species for arsenic removal.

4.1.3 Roxarsone Removal at pH 7

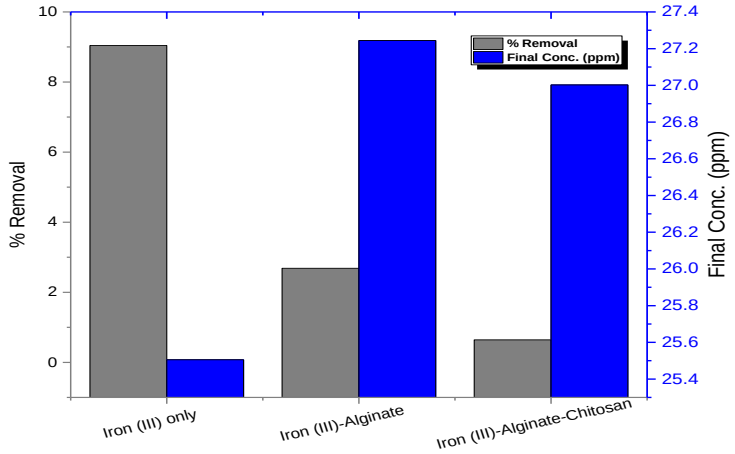

Figure 4.5: Roxarsone removal (30 ppm) at initial pH 7 [15 ppm Fe (III), 2.5 ppm MMWC, 10 ppm HVA]

Roxarsone removal at pH 7 proved to be ineffective, with a maximum removal of 9% using Fe(III) only. Since most water systems tend to exhibit neutral pH, the model system was adjusted to pH 7 to determine its effectiveness at this pH environment (Fig. 4.5). It proved ineffectual likely because Fe (III) hydroxides did not form at this pH value. Also, HVA and MMWC were likely to have precipitated at pH 7, taking Fe(III) ions out of solution rather than roxarsone. At the low concentrations of biopolymers used, the amounts may be insufficient for precipitation of appreciable amounts of roxarsone.

4.1.4 Kaolinite Suspended Solids with Roxarsone at pH 7

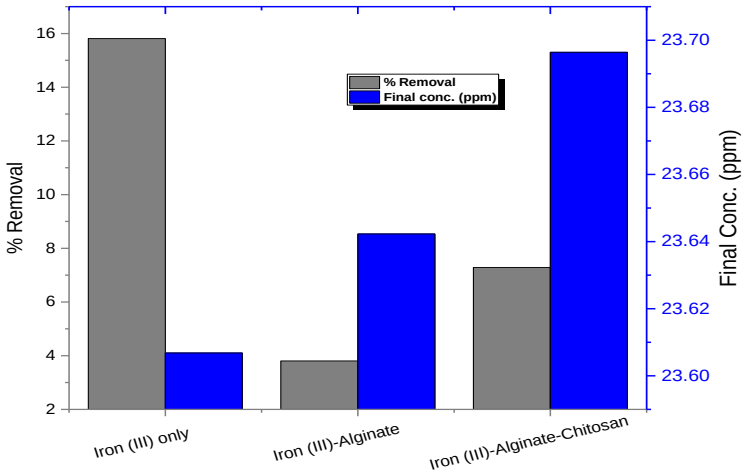

Figure 4.6: Roxarsone removal (30 ppm) with 400 ppm kaolinite at initial pH 7 [15 ppm Fe (III), 2.5 ppm MMWC, 10 ppm HVA]

At pH 7, with the presence of kaolinite, roxarsone removal increased slightly overall but the highest increase was up to 16% using Fe(III) only. Enhanced coagulation-flocculation with the addition of suspended solids may have been due to increased adsorption sites from kaolinite. Results are shown in Fig. 4.6.

4.2 Arsenate (V) Removal

Arsenate (V) solution is colorless, which does not allow for the direct measurement of inorganic arsenate species by UV-Vis spectrophotometry. To use the UV-Vis, the addition of a color developing reagent was employed involving molybdate. The arsenate (V) ions form a blue-colored complex with the molybdate reagent and its λ_{max} is 900 nm, which was determined using its spectrum (not shown). Concentration of As(V) was determined using the calibration curve in Fig. 4.7 by utilizing the Beer-Lambert Law.

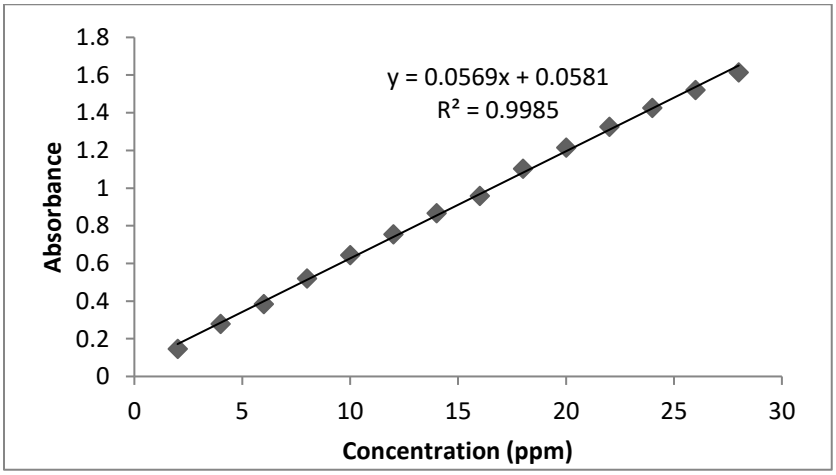

Figure 4.7: Calibration curve for arsenate (V) using molybdate color reagent

4.2.1 Arsenate (V) at Ambient pH

The removal of As(V) using only Fe(III) proved to be about 10% less effective than that of roxarsone. However, using the Fe(III)-MMWC/HVA system, As(V) removal was the same as that of the highest roxarsone removal (%) achieved by Fe (III) addition only. The results, including the study using Fe (III)-alginate, indicates that the addition of two biopolymers caused enhanced removal of inorganic As(V). The pH of the As(V) system was initially *ca.* 6.5 but dropped to *ca.* 3.5 with subsequent addition of coagulant and flocculants. This pH drop would allow both MMWC and HVA to possess an ionic charged and to be able to form a PEC, to enable entrapment of the As(V). The singular use of alginate does not work adequately since it cannot form a PEC. Results are shown in Fig. 4.8.

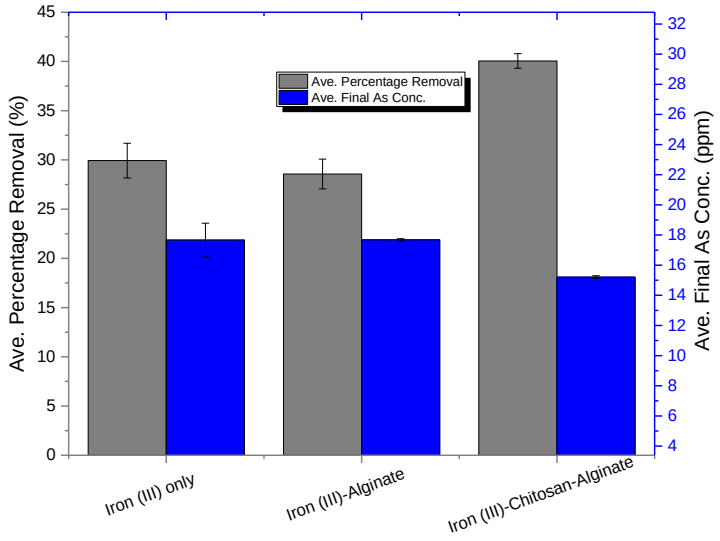

Figure 4.8: Arsenate (V) removal (30 ppm) at initial pH ~6.5 [15 ppm Fe(III), 2.5 ppm MMWC, 10 ppm HVA]

The greater removal observed for roxarsone over inorganic As(V) could be due to the presence of its phenyl ring.

4.2.2 Kaolinite Suspended Solids with Arsenate(V) at Ambient pH

The addition of kaolinite to As(V) seems to have enhanced the removal when using only Fe(III) or combined with alginate (Fig. 4.9). All three systems had an equal amount of removal at 40%. The kaolinite would have added to the amount of negative charges present in the suspension. It is possible that the suspended kaolinite particles may have provided more surfaces for nucleation to occur; hence, the Fe(III) particles could form the insoluble hydroxides in greater amounts. Kaolinite has a pH of ~8 when dispersed in Millipore water, and also a slight buffering effect. It may have kept the pH in the neutral region after addition of Fe(III) solution, which tends to lower pH to 3.5 – 4, thereby allowing for less dissolution of insoluble Fe(III) hydroxides and greater surface area for the adsorption of As(V) removal.

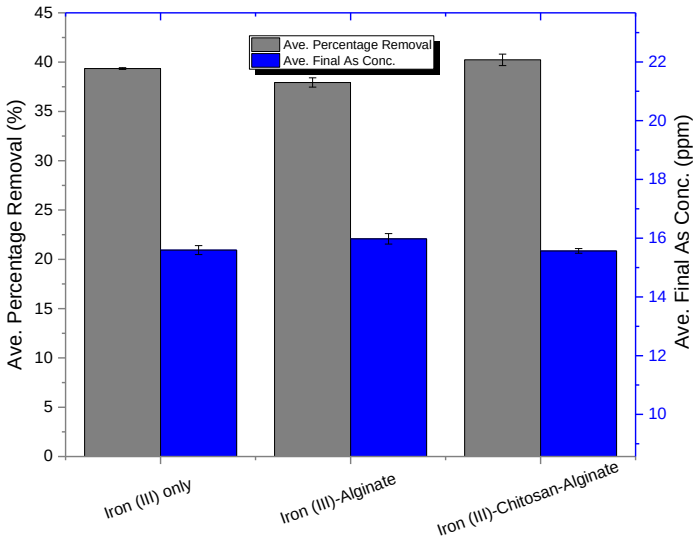

Figure 4.9: Arsenate (V) removal (30 ppm) with 400 ppm kaolinite at initial pH ~6.5 [15 ppm Fe(III), 2.5 ppm MMWC, 10 ppm HVA]

4.2.3 Arsenate (V) at pH 3

The removal of roxarsone was best achieved at *ca.* pH 3.5. Based on this reason, the effect of pH on As(V) removal was investigated at pH 3. Figure 4.10 shows that removal of As(V) was limited at this pH regardless of the coagulant/flocculant combination utilized. It is possible that the low pH caused the Fe(III) ions to remain soluble and not form insoluble hydroxides. This would have accounted for the low As(V) removal due to lack of surface sites for adsorption.

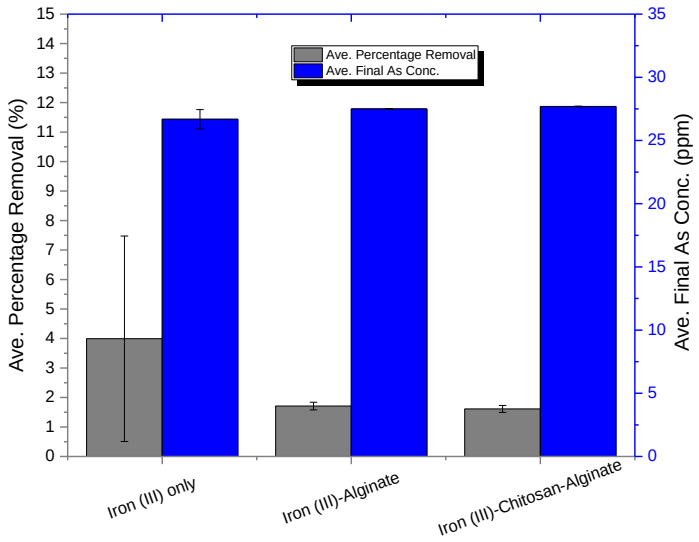

Figure 4.10: Arsenate (V) removal (30 ppm) at pH 3 [15 ppm Fe(III), 2.5 ppm MMWC, 10 ppm HVA]

4.2.4 Kaolinite Suspended Solids with Arsenate (V) at pH 3

Addition of kaolinite improved removal As(V), as shown in the previous study on As(V) removal at ambient pH. A removal of ~20% was determined, as compared to ~2% without kaolinite. The kaolinite would have provided solid particles, where the Fe(III) could nucleate onto and form hydroxides as proposed to adsorb the As(V). Since kaolinite suspension has a pH of *ca.* 8, it may have also caused the overall pH to remain less acidic, allowing for precipitation of the hydroxides. Results are shown in Fig. 4.11.

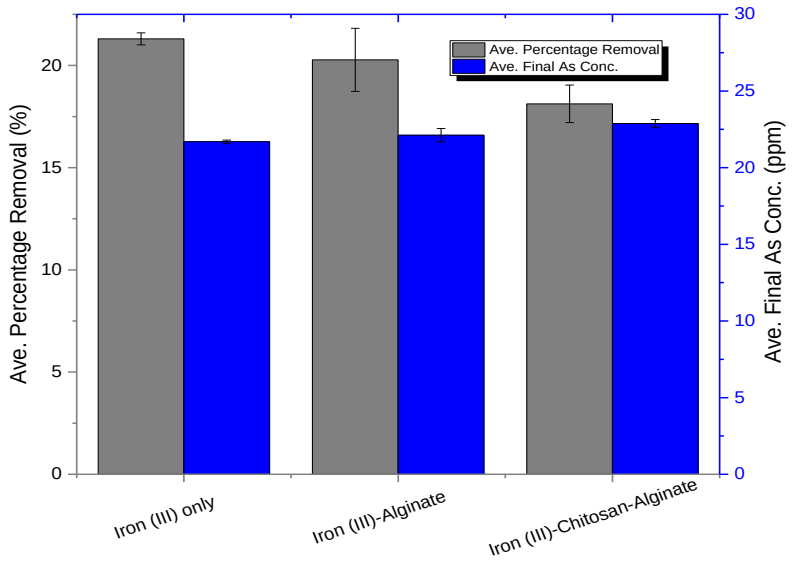

Figure 4.11: Arsenate (V) removal (30 ppm) with 400 ppm kaolinite at pH 3 [15 ppm Fe(III), 2.5 ppm MMWC, 10 ppm HVA]

Chapter 5 *ONE-POT* KINETIC STUDIES

5.1 Roxarsone Studies

5.1.1 Roxarsone Removal at Ambient Temperature

The one pot system was used to study the removal of roxarsone using the various components of the Fe(III)-MMWC/HVA system, both together and individually. With multicomponent systems, it is ideal to investigate each component separately. The one pot study was ideal for this because it allowed for the observation of the *in-situ* change in roxarsone removal with time during the entire coagulation-flocculation process. The results shown in Figure 5.1 below indicate that the Fe(III) species was primarily responsible for roxarsone removal, since plots of each individual component shows the most significant roxarsone removal occurs with Fe(III) only. However, the plot shows an initial high uptake during stirring but after the system is allowed to settle (after 60 min.) there is a rapid decrease, which may have been due to weak binding between roxarsone and Fe(III).

Both MMWC and HVA did not show significant removal (<5%). When Fe(III) was combined with each of the biopolymers, its effectiveness dropped with the addition of the alginate, but MMWC resulted in no apparent change. The combination of MMWC and HVA with Fe(III) caused a slight increase from Fe(III)-HVA. Both plots that contain Fe(III) and alginate showed a peak around the 5 minute mark; this implies that there was binding of roxarsone with Fe(III) initially but when alginate has been added 4 minutes after the roxarsone seems to have become unbound from the Fe(III). The alginate may have a higher affinity for the Fe(III) since it is also negatively charged, comparable to roxarsone. Sreeram *et al.*[108] determined the binding constant for Fe(III)-alginate at acidic pH similar to those of this study (~3.5 – 4.0) as 5.04×10^4 M^{-1}.[15] With such a large binding constant, it shows that the deprotonated carboxyl groups on the alginate are strongly bound to Fe(III). This would account for the decrease in roxarsone binding as a result of the addition of alginate.

The addition of MMWC seems to have a more positive effect when compared to the alginate. When combined with Fe(III), it had a stabilizing effect on uptake, if not an enhancing effect. When alginate was added to the system, it decreased the binding of alginate to Fe(III), allowing Fe(III) to bind with roxarsone. This was done by binding with alginate itself, since at acidic pH MMWC is also positively charged like Fe(III). Being a polymer, it would possess multiple positive charge sites, which has a greater chance of entangling itself with alginate.

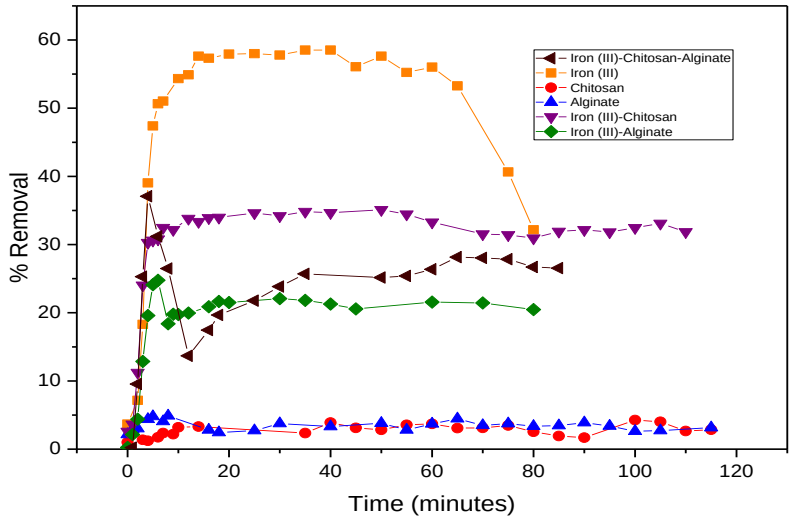

Figure 5.1: Roxarsone removal (30 ppm) using *one-pot* studies [15 ppm Fe(III), 2.5 ppm MMWC, 10 ppm HVA]

5.1.2 Kaolinite Suspended Solids with Roxarsone at Ambient Temperature

From Fig. 5.2, the addition of kaolinite enhanced uptake overall, where *ca.* 10% increase occurred, with the exception of the Fe(III)-MMWC/HVA. Again Fe(III) displayed the best coagulant properties, especially when compared to alginate and MMWC when used as the primary coagulant.

The Fe(III)-biopolymer combination showed that MMWC displayed a stable plateau after the initial increase in roxarsone removal, while the alginate showed a maximum point (*ca.* 4 min.), followed by a drop in roxarsone removal at *ca.* 5 min. The maximum removal was lower with the kaolinite than without it.

When both biopolymers were used, roxarsone removal decreased sharply after settling occurred. There is the characteristic maximum removal point for alginate but it is less pronounced in the presence of kaolinite. It is possible that the MMWC is not able to offset the negative effect of the alginate due to the introduction of excess negative charge upon addition of the kaolinite.

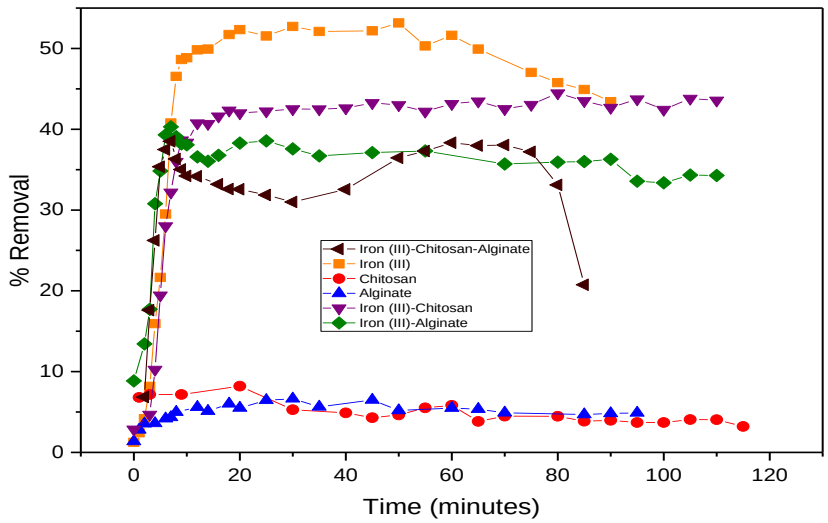

Figure 5.2: Roxarsone removal (30 ppm) with 400 ppm kaolinite using *one-pot* studies [15 ppm Fe(III), 2.5 ppm MMWC, 10 ppm HVA]

5.2 Arsenate Removal Studies

5.2.1 Arsenate(V) at Ambient Temperature

The removal of As(V) showed a much more stable removal profile. The %removal vs. time (Fig. 5.3) plots for Fe(III) and Fe(III)-biopolymer combinations showed a sharp increase followed by a plateau in arsenate (V) removal. The individual MMWC and HVA biopolymer systems showed a slight increase in arsenate (V) removal, followed by steady removal. The Fe(III) system and Fe(III)-MMWC/HVA showed similar removal (%), where the latter was slightly higher and more stable.

The combination of Fe(III) and MMWC showed slightly better uptake when compared to Fe(III)-HVA; the difference is less pronounced than previously encountered and was found to be around 40%. The maximum is not observed in Fig. 5.3, which might indicate that binding between arsenate and Fe(III) is stronger than that of HVA. However, Fe(III)-HVA did show the lowest removal of the Fe(III) containing systems, where the addition of MMWC enhanced the arsenate removal.

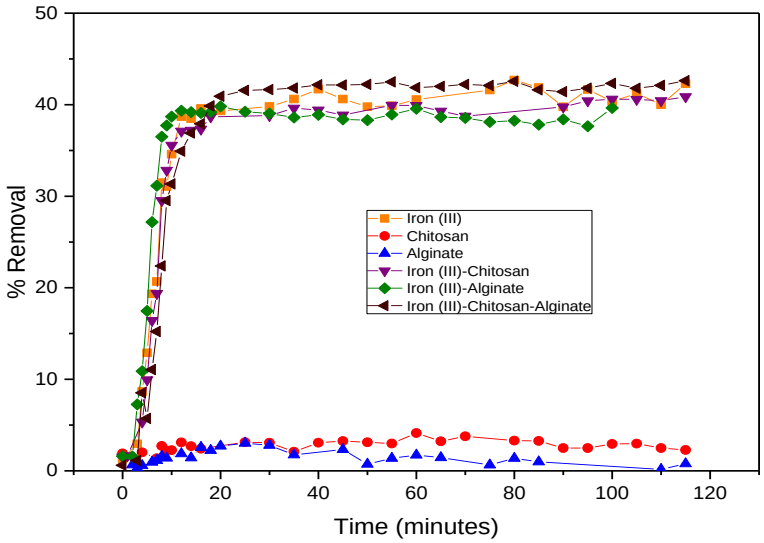

Figure 5.3: Arsenate (V) removal (30 ppm) using *one-pot* studies [15 ppm Fe(III), 2.5 ppm MMWC, 10 ppm HVA]

5.2.2 Kaolinite Suspended Solids with Arsenate(V) at Ambient Temperature

By adding kaolinite to the system, uptake by Fe (III) and Fe (III)-MMWC/HVA increased appreciably at *ca.* 10% for the former and *ca.* 6% for the latter. Fe (III) –MMWC and –HVA both remained at similar uptake values, while the uptake of MMWC and HVA remained low when used as single component biopolymers.

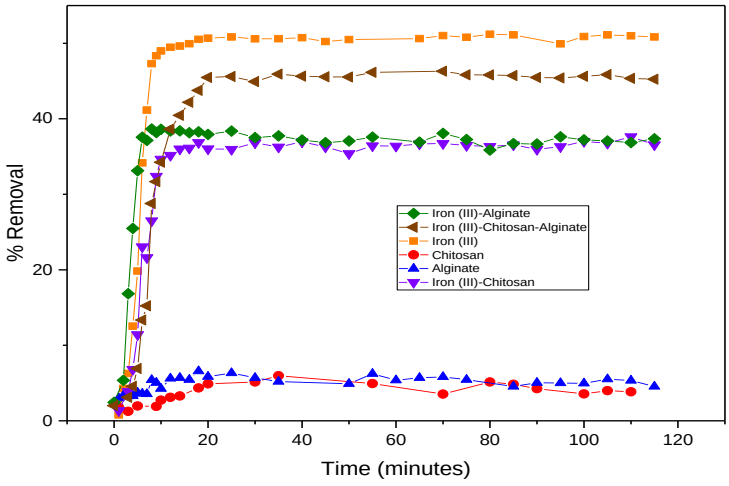

Figure 5.4: Arsenate (V) removal (30 ppm) with 400 ppm kaolinite using *one-pot* studies [15 ppm Fe(III), 2.5 ppm MMWC, 10 ppm HVA]

5.3 Kinetic Studies

Studies on the kinetics of the coagulation-flocculation process were obtained by using the *one-pot* method. The removal (%) was converted to Q_t (refer to eq. 2-1) by using the mass of the main coagulant/flocculant species. In all multi-component systems, iron (III) was used, where the individual component studies proved it to have the most significant removal (%) compared to the biopolymers. Q_t vs. time (t) was plotted and the kinetics of the systems was analyzed using the two kinetic models described in Section 2: PFO and PSO kinetic models. Through an analysis of goodness of fit determination by the use of R^2 and reduced χ^2 values, the better of the two kinetic models was chosen and is used to not only comment on the rate of reaction (through rate constant comparison), but also, molecular level mechanistic action.

5.3.1 Roxarsone removal

5.3.1.1 Using varying coagulant/flocculant species

The kinetic studies conducted using the *one-pot* method examined the effect of the various coagulant/flocculant combinations of the Fe(III)-MMWC/HVA system on the removal of roxarsone.

The fitted plots provided determination of two important constants, k_1/k_2 and their corresponding Q_e values. The latter constant, Q_e, was the amount of roxarsone "adsorbed" at longer time denoted as pseudo-equilibrium and k_1/k_2 are the rate constants for the PFO and PSO models, respectively. The use of adsorption is due to the mechanism proposed by Baskan *et al.*,[31] which suggests adsorption/precipitation of the iron hydroxides as the beginning of the coagulation-flocculation with iron (III) for arsenate (V) removal. MMWC, with its positively charged arrangement at pH 3 – 4, is less likely to precipitate out and more likely to act through charge neutralization (refer to Fig. 1.4A). The results in Fig. 5.13 and Table 5.1 show that PFO proved to display the better fit criterion in all cases, except that of the HVA biopolymer.

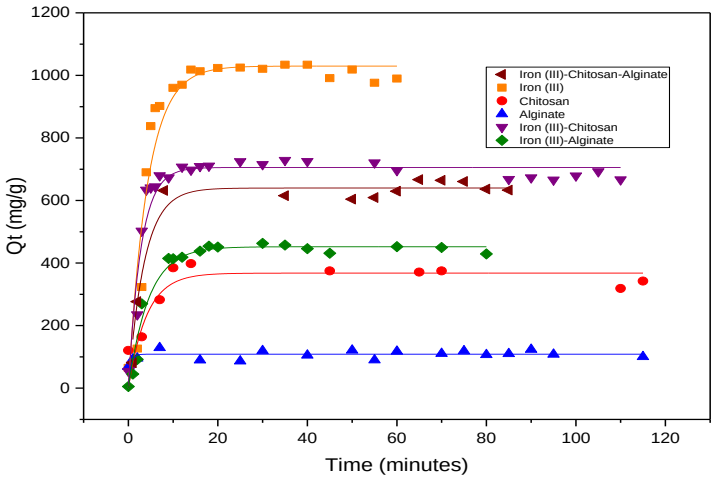

Figure 5.5: Roxarsone (30 ppm) removal fitted with PFO kinetic model at pH ~3.5 at ambient temperature [15 ppm Fe(III), 2.5 ppm MMWC, 10 ppm HVA]

The PFO model indicates that the removal of the roxarsone from the solution and into the flocs occurs in two stages: (i) an initial rapid uptake stage and (ii) a subsequent slow pre-equilibrium stage, where uptake is maintained. The PFO model indicates reversible interactions; whereas, the PSO model describes irreversible interactions, such as chemisorption. Only HVA seems to favor the PSO model in terms of electrostatic attraction, it seems unlikely since the coagulation-flocculation of roxarsone occurs between pH 3 to 4, where both HVA and roxarsone (pK_a values 3.49, 6.38, 9.76)[60] are mostly protonated. However, since the HVA would have a low charge density at this point (and it being HVA) means that it is likely to be very coiled,[51] which may have a strong "trapping" effect due to polymer entanglement and entrapment effects From the Q_e values in Table 5.1, it is seen that Q_e varies with the coagulant/flocculant involving iron (III) has the highest value, followed by iron (III)-MMWC and then iron (III)-MMWC/HVA. This clearly demonstrates the important role of iron (III) because it enhances the removal of roxarsone when used along with HVA, MMWC or both.

In terms of rate, a comparison of k_1 (and k_1 and k_2 in the case of HVA) was carried out. The values of k_1 were quite similar for each of the coagulant/flocculant systems and were on average six times slower than that of the HVA system with the PFO model but five times slower with the PSO model. Since the PSO model was more suitable, it is likely that it takes a longer time to entrap the roxarsone molecules.

Table 5.1: Kinetic parameters for arsenic removal using various coagulant/flocculant systems as described by PFO and PSO kinetic models

Coagulant/Flocculant	Pseudo-First Order			Pseudo-Second Order		
	Q_e	k_1	R^2	Q_e	k_2	R^2
	($mg.g^{-1}$)	(min^{-1})		($mg.g^{-1}$)	($g.mg^{-1}.min^{-1}$)	
Roxarsone						
Iron (III)	1029.7	0.234	0.91	1136.4	2.85E-04	0.84
MMWC	367.8	0.244	0.69	381.7	1.25E-03	0.58
HVA	108.6	1.735	0.81	109.3	4.96E-02	0.80
Iron (III)-MMWC	705.6	0.356	0.93	743.7	7.93E-04	0.84
Iron (III)-HVA	452.1	0.221	0.97	498.2	6.08E-04	0.93
Iron (III)-MMWC-HVA	639.8	0.278	0.96	672.8	5.44E-04	0.91
Roxarsone/kaolinite						
Iron (III)	1110.1	0.157	0.91	1258.5	1.52E-04	0.84
MMWC	495.5	1.000	0.95	513.0	7.90E-03	0.94
HVA	155.1	0.372	0.66	160.9	4.98E-03	0.69
Iron (III)-MMWC	935.4	0.169	0.92	1001.9	2.75E-04	0.85
Iron (III)-HVA	838.3	0.320	0.86	879.9	5.84E-04	0.79
Iron (III)-MMWC-HVA	433.1	0.164	0.92	464.8	5.46E-04	0.85
Arsenate (V)						
Iron (III)	855.7	0.138	0.93	927.5	2.20E-04	0.87
MMWC	379.3	0.266	0.86	393.9	1.42E-03	0.73
HVA	47.0	0.201	0.45	49.2	7.41E-03	0.33
Iron (III)-MMWC	829.0	0.181	0.98	883.1	3.63E-04	0.95
Iron (III)-HVA	819.9	0.198	0.77	870.0	4.05E-04	0.59
Iron (III)-MMWC-HVA	822.4	0.092	0.86	931.6	1.20E-04	0.79
Arsenate (V)/kaolinite						
Iron (III)	963.4	0.246	0.94	1017.5	4.46E-04	0.82
MMWC	648.4	0.083	0.97	763.2	1.25E-04	0.94
HVA	167.1	0.390	0.62	171.9	4.96E-03	0.67
Iron (III)-MMWC	885.1	0.198	0.93	930.4	4.01E-04	0.85
Iron (III)-HVA	819.0	0.222	0.96	868.6	3.63E-04	0.92
Iron (III)-MMWC-HVA	929.5	0.140	0.99	981.6	2.90E-04	0.95

5.3.1.2 Variable temperature effects

The kinetic study at variable temperature on roxarsone removal was studied using the *one-pot* method via a circulating bath system. Fe(III) and Fe(III)-MMWC/HVA were chosen for the study at ambient temperature (20 °C), 30 °C and 40 °C. The value of Q_e decreased with an increase in temperature when both Fe(III) and Fe(III)-MMWC/HVA were used, as shown in Table 5.2. The PFO kinetic model was found to be a better fit for the data, except for Fe(III)-MMWC/HVA at 40 °C. From a comparison of the k_1 values, the rates are similar to each other but the iron (III) at 20 °C was around four times faster. The addition of MMWC and HVA decreased the uptake across all temperatures, which may have been due to limiting the availability of access to the Fe(III). HVA has an especially high affinity for Fe(III), as evidenced by the Fe(III)-alginate binding constant of 10^4 M^{-1}.[108]

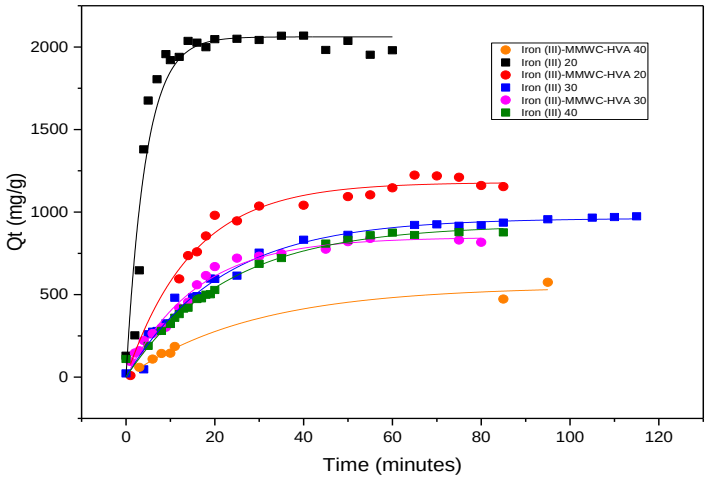

Figure 5.6: Roxarsone (30 ppm) removal at pH ~3.5 at various temperatures fitted with PFO model [15 ppm Fe(III), 2.5 ppm MMWC, 10 ppm HVA]

5.3.2 Roxarsone removal with kaolinite

5.3.2.3 Using varying coagulant/flocculant species

The addition of kaolinite to roxarsone caused an overall increase in the Q_e (Table 5.1). The highest Q_e was found for Fe(III) and Fe(III)-MMWC, which was similar to the results of roxarsone only removal, with the exception of Fe(III)-MMWC/HVA system, that was found to have a decreased roxarsone removal with addition of the colloid. In terms of rate, the PFO model was favored by all systems, with the exception of HVA addition without Fe(III). Similar to roxarsone removal, the HVA took up roxarsone at a slower rate (*ca.* 47 times slower) according to the favored PSO model. Kaolinite has many groups that give it a negatively charged surface, which may cause

repulsion with the HVA with a more open structure of HVA. This morphology would be less capable of entrapping roxarsone species.

Table 5.2: Kinetic parameters at various temperatures for arsenic removal using various coagulant/flocculant systems as described by PFO and PSO kinetic models

Coagulant/Flocculant		Pseudo-First Order			Pseudo-Second Order		
	T	Q_e	k_1	R^2	Q_e	k_2	R^2
	(K)	($mg.g^{-1}$)	(min^{-1})		($mg.g^{-1}$)	($g.mg^{-1}.min^{-1}$)	
Roxarsone							
Iron (III)	293.15	2061.4	0.228	0.91	2287.3	1.37E-04	0.84
	303.15	963.1	0.047	0.98	1182.2	4.02E-05	0.98
	313.15	921.5	0.044	0.99	1213.7	3.24E-05	0.98
Iron (III)-MMWC/HVA	293.15	1180.0	0.068	0.97	1389.5	5.87E-05	0.97
	303.15	846.8	0.064	0.98	1054.4	6.09E-05	0.97
	313.15	549.5	0.035	0.98	732.2	3.87E-05	0.98
Roxarsone/kaolinite							
Iron (III)	293.15	2292.9	0.149	0.89	2689.7	6.24E-05	0.83
	303.15	1074.1	0.068	0.99	1262.9	6.09E-05	0.98
	313.15	884.0	0.071	0.99	1027.1	8.14E-05	0.98
Iron (III)-MMWC/HVA	293.15	1393.8	0.214	0.93	1495.7	1.94E-04	0.88
	303.15	669.8	0.054	0.98	852.1	5.98E-05	0.96
	313.15	615.5	0.094	0.95	691.5	1.79E-04	0.87
Arsenate (V)							
Iron (III)	293.15	1686.8	0.184	0.99	1761.0	2.46E-04	0.98
	303.15	930.7	0.140	0.98	1022.4	1.88E-04	0.97
	313.15	858.0	0.169	0.98	930.2	2.60E-04	0.95
Iron (III)-MMWC/HVA	293.15	1696.8	0.143	1.00	1780.4	1.80E-04	0.97
	303.15	769.5	0.132	0.98	849.9	2.02E-04	0.95
	313.15	815.0	0.134	0.94	900.1	1.98E-04	0.86
Arsenate (V)/kaolinite							
Iron (III)	293.15	1927.4	0.195	0.96	2047.6	1.60E-04	0.88
	303.15	765.2	0.125	0.99	846.0	1.93E-04	0.97
	313.15	717.6	0.149	0.99	788.9	2.62E-04	0.96
Iron (III)-MMWC/HVA	293.15	1878.2	0.112	0.92	2043.2	7.89E-05	0.87
	303.15	783.9	0.148	0.99	851.3	2.45E-04	0.96
	313.15	827.7	0.214	0.95	877.7	4.05E-04	0.87

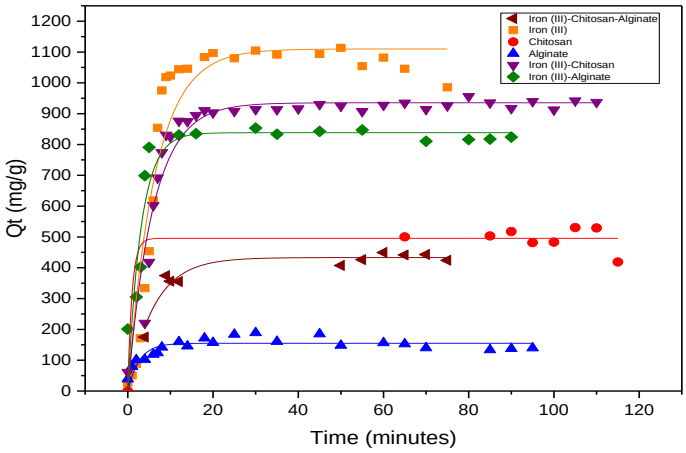

Figure 5.7: Roxarsone (30 ppm) removal with kaolinite (400 ppm) at pH ~3.5 at ambient temperature fitted with PFO kinetic model [15 ppm Fe(III), 2.5 ppm MMWC, 10 ppm HVA]

5.3.2.4 Variable temperature effects

The kaolinite addition to roxarsone shows similar trends as that of roxarsone only, where the value of Q_e decreased with increasing temperature. At the lowest two temperatures, greater uptake was shown by the Fe(III) alone and Fe(III)-MMWC/HVA system showed higher uptake only at the lowest temperature with the addition of kaolinite. The PFO model was favored overall and had the highest rate at the lowest temperature condition for both Fe(III) and Fe(III)-MMWC/HVA.

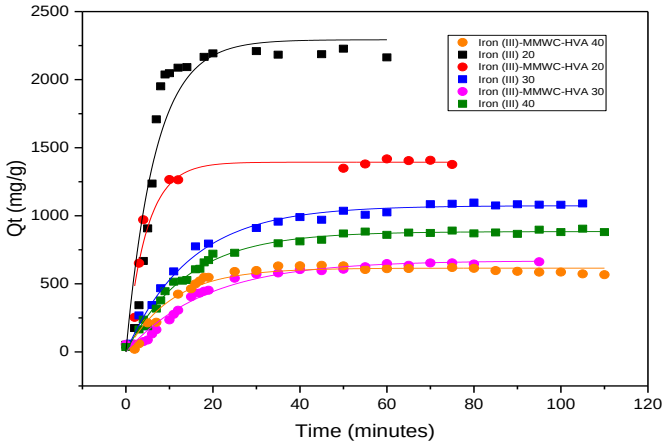

Figure 5.8: Roxarsone (30 ppm) removal with kaolinite (400 ppm) at pH ~3.5 at various temperatures fitted with PFO model [15 ppm Fe(III), 2.5 ppm MMWC, 10 ppm HVA]

5.3.3 Arsenate removal

5.3.3.1 Using varying coagulant/flocculant species

While the removal of arsenate (V) was the highest with Fe(III), it was similar to the Q_e values (Table 5.1) of the other systems that incorporated iron (III). HVA showed the lowest uptake followed by MMWC; however, MMWC showed a much better affinity for arsenate (V). The PFO kinetic model was proven to provide the best fit to the experimental data. On average, the rate constants were similar for arsenate (V) as that of roxarsone removal.

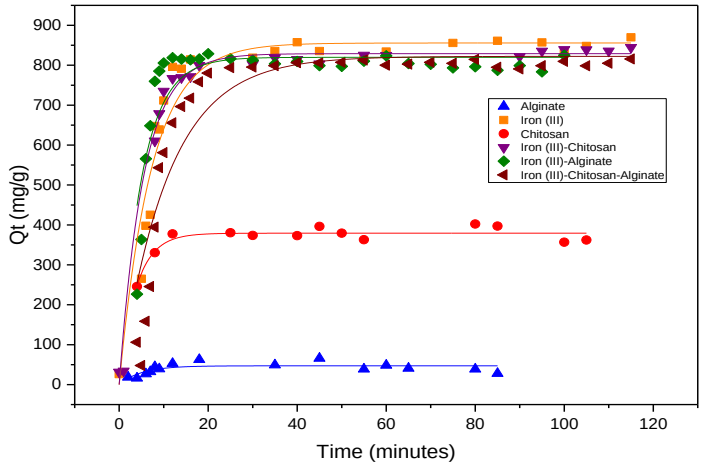

Figure 5.9: As(V) (30 ppm) removal at pH 6.5 at ambient temperature fitted with PFO model [15 ppm Fe(III), 2.5 ppm MMWC, 10 ppm HVA]

5.3.3.2 Varying temperature effects

Table 5.2 summarizes the Q_e and k_1 values for the removal of arsenate (V) at 20 °C, 30 °C and 40 °C. The increase in temperature caused a decrease in uptake of arsenate (V) when using only Fe(III) as a coagulant. The addition of MMWC and HVA affects the trend as evidenced by a lower Q_e value at 30 °C rather than 40 °C. The best removal was obtained at the lowest temperature, similar to Fe(III) only. The PFO model was fitted to the data and the k_1 values ranged from 0.13 to 0.18.

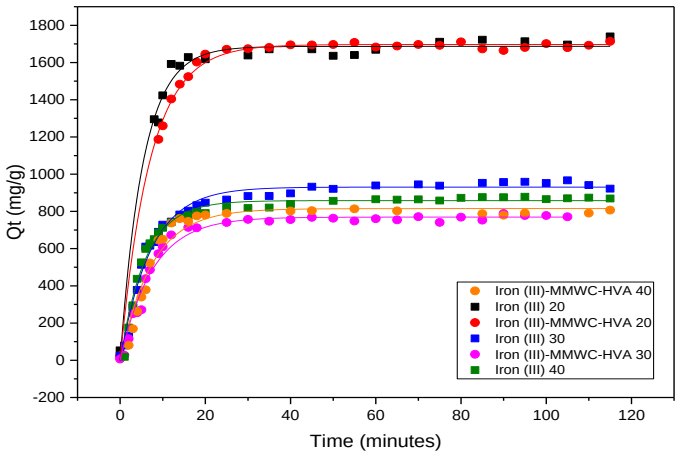

Figure 5.10: As (V) (30 ppm) removal at pH ~6.5 at various temperatures fitted with PFO model [15 ppm Fe(III), 2.5 ppm MMWC, 10 ppm HVA]

5.3.4 Arsenate removal with kaolinite

5.3.4.1 Using varying coagulant/flocculant species

Kaolinite addition showed a similar trend as that of the removal of arsenate (V) without kaolinite, where the Fe(III) addition showed the highest removal. The other Fe(III) containing systems also performed well. The kaolinite seems to have greatly increased the removal of arsenate (V) with MMWC and to a smaller extent with HVA. The kinetic model best suited to data fitting was PFO for all systems but HVA. The k_1 values ranged from 0.08 - 0.25 $min.^{-1}$, and k_2 was 0.00496 $g.mg^{-1}.min^{-1}$. Kaolinite enhanced uptake of arsenate (V) with all coagulant/flocculant systems.

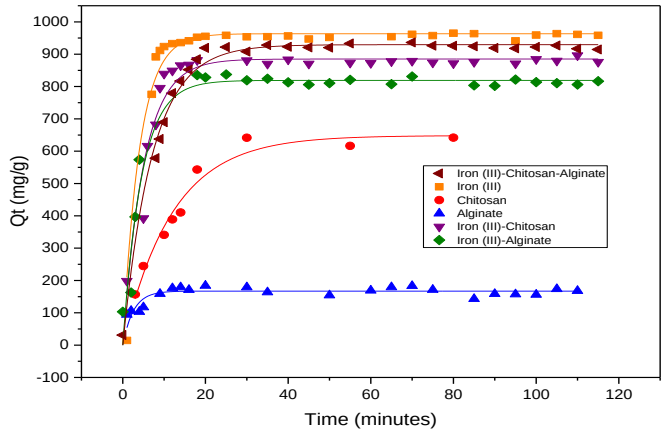

Figure 5.11: As (V) (30 ppm) removal with kaolinite (400 ppm) at pH ~6.5 at ambient temperature fitted with PFO kinetic model [15 ppm Fe(III), 2.5 ppm MMWC, 10 ppm HVA]

5.3.4.2 Variable temperature effects

The effect of temperature on arsenate (V) removal with kaolinite was studied using only Fe(III) and Fe(III)-MMWC/HVA. The increase in temperature caused a decrease in uptake using Fe(III) alone but with Fe(III)-MMWC/HVA there was no clear trend. The highest uptake was at 20 °C but the lowest uptake was at 30 °C, rather than 40 °C for the removal of arsenate (V) with kaolinite. The PFO kinetic model was found to provide the best fit to the data, where all k_1 values fell between 0.11 – 0.22 min.$^{-1}$. Overall the addition of kaolinite caused an increase in arsenate (V) uptake but not with iron (III) only at 30 °C and 40 °C.

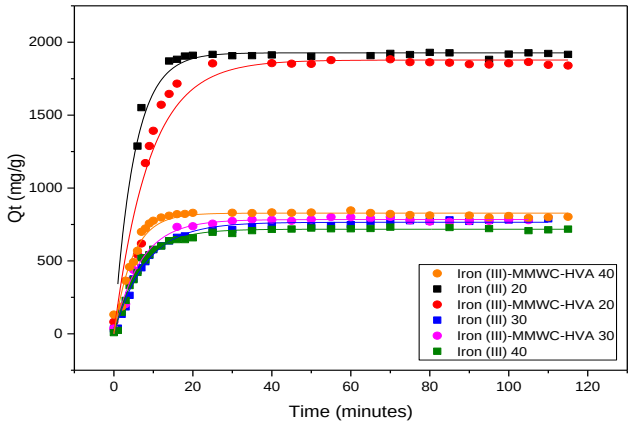

Figure 5.12: As(V) removal (30 ppm) with kaolinite (400 ppm) at various temperatures at pH ~6.5 fitted with PFO model [15 ppm Fe(III), 2.5 ppm MMWC, 10 ppm HVA]

5.4 Thermodynamic Studies

The Eyring equation (eq. 2-5) was used to calculate the thermodynamic parameters of the coagulation-flocculation process as listed in Table 5.3, along with the Gibbs activation energy (eq. 5-1) and Arrhenius equations (eq. 5-2), which were used for determination of $\Delta G^{\ddagger}$ and E_a, respectively.

$$\Delta G^{\ddagger} = \Delta H^{\ddagger} - T\Delta S^{\ddagger} \qquad (5\text{-}1)$$

$$lnk_i = \frac{-E_a}{R}\left(\frac{1}{T}\right) + lnA \qquad (5\text{-}2)$$

The removal of organic arsenic versus inorganic arsenic, with and without kaolinite, show varied negative "apparent" E_a values, with the exception of arsenate (V) removal with kaolinite using the Fe(III)-MMWC/HVA system. The term "apparent" applies to the E_a when the process cannot be accounted for with the simple transition state theory. Processes that involve composite

kinetic steps, such as reactions involving hydration steps, tend to show apparent E_a values, which can be negative.[111] An increase of the temperature of the system causes a decrease in arsenic removal. This negative value indicates that the coagulation-flocculation process occurs in a series of steps and through stable intermediates. This is a reasonable suggestion as the formation of iron hydroxides are proposed to occur before and during "adsorption" of the arsenic, implying that the formation of iron hydroxide-As complexes may induce formation of more species, in a cooperative binding process. The mostly negative $\Delta H^{\ddagger}$ indicates an exothermic binding taking place during the process. A negative $\Delta S^{\ddagger}$ implies that as the process is taking place, the organization of the system is increasing, likely due to the Fe (III) binding to the arsenic, and in certain cases, the MMWC and HVA as well. It should be noted that the entropy is slightly higher when the biopolymers are present, which may be an indication of their lesser role in binding arsenic. The processes for arsenic removal, based on $\Delta G^{\ddagger}$, implies a non-spontaneous process, with perhaps the energy being added to the system via the stirring process.

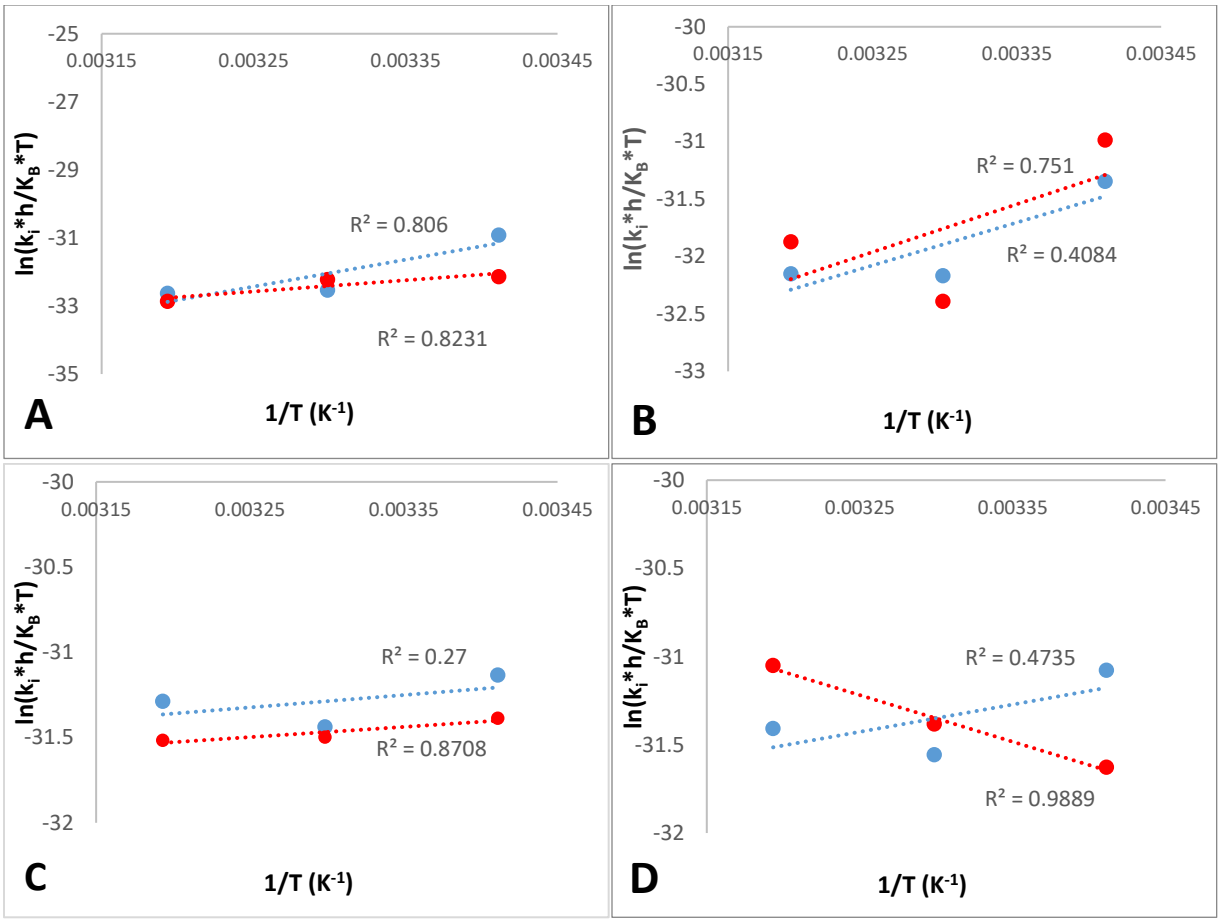

Figure 5.13: Eyring plots for arsenic uptake at variable temperatures based on PFO kinetic models: (A) Roxarsone removal, (B) Roxarsone removal with kaolinite, (C) Arsenate (V) removal and (D) Arsenate (V) removal with kaolinite, (●) represents iron (III) only and (●) represents Fe (III)-MMWC/HVA

Table 5.3: Thermodynamic parameters for arsenic removal using coagulation-flocculation based on rate constants obtained using the PFO kinetic model at various temperature

Coagulant/Flocculant	$\Delta H^{\ddagger}$	$\Delta S^{\ddagger}$	T	$\Delta G^{\ddagger}$	E_a
	(kJ.mol^{-1})	(J.K^{-1}.mol^{-1})	(K)	(kJ.mol^{-1})	(kJ.mol^{-1})
Roxarsone					
Iron (III)	-65.71	-483.2	293.15	75.93	-63.20
			303.15	80.77	
			313.15	85.60	
Iron (III)-MMWC/HVA	-27.47	-360.1	293.15	114.18	-24.95
			303.15	119.01	
			313.15	123.84	
Roxarsone/kaolinite					
Iron (III)	-34.64	-378.3	293.15	76.26	-28.54
			303.15	80.04	
			313.15	83.83	
Iron (III)-MMWC/HVA	-31.06	-367.6	293.15	79.26	-32.12
			303.15	83.83	
			313.15	87.41	
Arsenate (V)					
Iron (III)	-6.03	-280.0	293.15	76.06	-3.52
			303.15	78.86	
			313.15	81.66	
Iron (III)-MMWC/HVA	-4.98	-278.1	293.15	77.11	-2.46
			303.15	79.91	
			313.15	82.71	
Arsenate (V)/kaolinite					
Iron (III)	-12.87	-303.1	293.15	75.99	-10.35
			303.15	79.02	
			313.15	82.05	
Iron (III)-MMWC/HVA	21.97	-188.1	293.15	110.83	24.49
			303.15	113.86	
			313.15	116.89	

Chapter 6 CONCLUSIONS AND FUTURE WORK

6.1 Conclusions

The investigation of the removal of organic (roxarsone) and inorganic (arsenate; As(V)) arsenic species encompassed several questions to be addressed through this thesis research:

- **Do the parameters of dosage, metal salt type, pH, MW and viscosity affect the removal of colloidal materials using a metal salt-chitosan/alginate system?**

Overall, the various parameters studied were shown to affect the removal of colloidal kaolinite suspended solids but to differing extents. In coagulation-flocculation studies the dosage of the coagulants and flocculants are crucial to the optimizing the process. The coagulants (traditional metal salts) had an optimal dosage at 30 ppm (alum) and 15 ppm (Fe(II) and Fe(III)), while the flocculants had an optimal dosage of 2.5 – 5 ppm (chitosan) and 7.5 – 10 ppm (alginate), and were found to depend on the MW and viscosity of the two biopolymers.

The MW of chitosan was varied to determine the effects of longer chains/higher charge density (MMWC) and shorter chains/lower charge density (LMWC). The charge density (and ionic strength) affects the conformation of the polymer by rendering it as a coiled or extended structure.[51] The higher the charge density of the biopolymer, the more open the structure due to minimization of charge repulsion along the polymer backbone. Overall, the MMWC compensated for a lack of positive charge from the metal salts, especially Fe(II). The LMWC was favored when there was enough positive charge from the metal ions where an excess of positive charge leads to re-stabilization of the colloidal suspension.

The viscosity of alginate was also studied and it functions similarly to the role of MW in chitosan. The greater viscosity with increasing MW occurs due to increased chain entanglement and dispersion forces. The charge on the alginate at greater pH values above its pK_a of *ca.* pH 3 to 4 was negative, which was the opposite of the chitosan and metal salt. The general result was a higher dosage (7.5 to 10 ppm) of alginate being favored over the lower dosages (2.5 to 5 ppm). This would be primarily due to its function as the bridge between microflocs. The higher dosage would be better for bridging and entrapping the flocs. A 10 ppm dosage was favored for lower positive charges from the coagulant and chitosan.

The pH of the kaolinite was adjusted from its value of ~8.5 to 3, 5, 7 and 9 and the coagulation-flocculation was investigated. In this instance, the pH does not greatly affect the removal of kaolinite. This was attributed to the slight buffering capacity of the kaolinite, and came from its cation exchange capacity. The cations in the kaolinite, such as Na^+, exchange with the H^+ ions and maintain the pH constant. Since the pH remains at ~3 for all of the Jar tests, the initial pH of the kaolinite does not greatly affect the process.

The order of polymer addition was assessed since two biopolymers were used and this might give insight into their mechanism of action. The combination with Fe(III), highlighted the importance of alginate and chitosan being added separately rather than pre-mixed to form a PEC. It is likely that the polymers formed a PEC through electrostatic forces and this entangled structure left them mostly unavailable for bridging, resulting in reduced turbidity, according to the measured transmittance (%T) of the solution.

Finally, both the stirring time and speed of the Jar test apparatus was adjusted to evaluate the effect on coagulation-flocculation. The stirring time was important because it allowed the suspension to mix with the coagulants and flocculants. The mixing times were found to be adequate for kaolinite removal, with 3 minutes of fast mixing and 20 minutes of slow mixing. The fast mixing (295 rpm) was sufficient to incorporate the coagulant (metal salts) with the kaolinite suspension, and the slow mixing (25 rpm) allowed for proper floc formation. The use of a lower mixing speed (25 rpm) was shown to have better results over the 50 rpm mixing. The higher mixing speed may have caused mechanical damage and dispersed the self-assembled flocs.

- **How does the addition of colloidal materials affect the removal of roxarsone using the metal salt-chitosan/alginate system?**

The study of roxarsone removal was carried out with and without kaolinite at conditions of ambient pH and pH 7. These conditions better helped to mimic natural water source conditions and further investigated the role of pH in arsenic removal. Since many water systems possess neutral pH, a pH value of 7 was chosen for this reason and to match the ambient pH of the arsenate (V) system *ca.* pH 7. This aids in the comparison of the removal of both organic and inorganic forms of arsenic.

Without kaolinite, the roxarsone removal ranged from 20 – 40% at ambient pH (~3). Fe(III) by itself removed the most roxarsone, while addition of HVA and MMWC hindered the removal. When HVA was added solely to the Fe (III), there was less reduction in removal of roxarsone. The roxarsone concentration was varied at initial values of 30, 40 and 50 ppm with a corresponding drop in the level of removal (%). The presence of the biopolymers hindered uptake on the Fe(III), possibly due to competitive affinity for Fe(III), or the self-assembly of MMWC with HVA.

Addition of kaolinite influences the roxarsone removal in the Jar test. At 30 ppm roxarsone removal decreased upon addition of kaolinite. It was less pronounced in the case of higher roxarsone concentration. At 30 ppm roxarsone with kaolinite, Fe(III) alone, Fe(III)-HVA and Fe(III)-MMWC/HVA showed a drop of *ca.* 5%, 20% and 35%, respectively. But at 40 ppm and 50 ppm roxarsone, the levels were similar in the presence and absence of kaolinite, except for when Fe(III) alone was used at 40 ppm roxarsone (10% drop recorded with kaolinite addition).

The change in pH from *ca.* 3 to 7 caused a drastic decrease in the uptake of roxarsone, and likely due to the change in speciation of Fe(III). An interesting observation showed that the addition of kaolinite at pH 7 slightly enhanced the roxarsone uptake.

- **How does the addition of colloidal materials affect the removal of arsenate using the metal salt-chitosan/alginate system?**

There was a reversal in removal capacity when considering the arsenate anion species, where the Fe(III)-MMWC/HVA has the highest removal (%) and sole addition of Fe(III) and Fe(III)-HVA having a 10% lower removal at *ca.* 30%. The overall range of removal was 30 – 40% arsenate (V). Addition of kaolinite affected the removal of arsenate in a positive manner. The presence of kaolinite appears to enhance the removal using Fe(III) and Fe(III)-HVA to 40%, which is similar to the uptake using the Fe(III)-MMWC/HVA system. The removal studies were carried out at ambient pH, which in the case of arsenate (V) was *ca.* pH 7.

The pH for arsenate (V) was then adjusted to pH 3, similar to that of roxarsone. The pH drop had a negative effect on arsenate (V) removal overall. The range was ~2 – 4%, with Fe(III) having the highest value but also the greatest error. The kaolinite addition enhanced uptake at pH 3 from *ca.* 2% to 20%. The increase was proportional, where the presence or absence of kaolinite revealed

that Fe(III) had the highest uptake. By contrast, Fe(III)-MMWC/HVA had lowest uptake in the presence or absence of kaolinite.

The kaolinite at acidic pH provides surface sites for iron (III) particles to nucleate. The presence of kaolinite may have increased the pH which aids the precipitation of iron hydroxides.

- **Which of the components are responsible for roxarsone removal and how do they affect the kinetics of the reaction?**

The kinetics of the coagulation-flocculation of roxarsone with the Fe(III)-MMWC/HVA system was explored. This study was done using the unique "*one-pot*" method at variable temperature (20, 30 and 40 °C). The *one-pot* method uses a filter paper barrier to separate the roxarsone to be sampled from the mixed system containing the coagulants and flocculants. The barrier provided a way to attenuate the fast process and monitor the progress of the reaction *in situ*. This method is a very unique approach to the study of coagulation-flocculation since most studies focus on the kinetics for coagulation-flocculation progress by studying the final turbidity rather than the actual kinetic process.

The kinetics of coagulation-flocculation process show relatively fast uptake of the roxarsone that is typical for this type of process. The *one-pot* method was used to study combinations of coagulant-flocculant systems. The separation of these systems helped to elucidate the importance of the Fe(III), MMWC, HVA and their component combinations.

The sole addition of Fe(III) performed the best for roxarsone relative to the biopolymers which caused a decrease in the level of removal. The reduction in performance due to the biopolymers relates to the binding onto available surface sites with Fe(III) hydroxides. Charge neutralization plays a likely role, especially in the case of chitosan. However, chitosan was more likely to involve charge neutralization since there is a very small amount (2.5 ppm MMWC) of it and the pH is acidic (favoring dissolution of chitosan). Precipitation of chitosan is likely to be very minimal at these conditions. HVA functions likely by entrapping the roxarsone particles within its coils. The high viscosity of the alginate contributes and the protonated nature of the alginate in acidic solution since fewer negatively charged carboxyl groups exist. The charged groups increase repulsion among the alginate coils and spread them out into an extended configuration.

- **Which of the components are responsible for arsenate removal and how do they affect the kinetics of the reaction?**

The removal of arsenate (V) using Fe(III) has been studied through the process of adsorption and fewer studies are available on coagulation-flocculation processes. As mentioned previously, studies by Baskan *et al.*[30] have proposed a similar sort of adsorption mechanism that occurs when using Fe(III) to remove arsenate (V) even through coagulation-flocculation. These studies relate to the removal of arsenate (V) with Fe(III), MMWC and HVA show that the positively charged Fe(III) and MMWC are better suited to arsenate (V) removal. The Q_e values of arsenate (V) removal are very similar to that of roxarsone, which indicate that the aromatic group attached does not greatly affect removal efficiency. The addition of kaolinite resulted in similar behaviour when introduced to roxarsone and arsenate (V) by enhancing removal of the two species. The Fe(III) and the HVA alone provided better removal of roxarsone, and removal of arsenate (V) was lower. Overall, the Q_e and k_1 values are very similar across the various contaminant species, both with and without kaolinite.

6.2 New Insight on Arsenic Removal using Coagulation-Flocculation

Studies in the literature report on the role of Fe(III) for the removal of arsenic species in water and wastewater. Baskan *et al.*[29–31] provided a mechanism of action for the removal of arsenate (V) using coagulation-flocculation using Fe(III). This work examined the addition of biopolymers (chitosan and alginate) on the role of enhanced uptake of arsenic and a reduction of the amounts of coagulants/flocculants required for dosing. The further addition of kaolinite served to mimic natural waters with colloidal species present, which is often the case in lakes, ponds and other water bodies where arsenic may be generally present.

Investigations into arsenic removal showed that there is little difference between the removal of roxarsone and arsenate (V) using the Fe(III)-MMWC/HVA system for coagulation-flocculation. The main difference between roxarsone and arsenate (V) is the aromatic ring that contains hydroxyl and nitro groups attached to the arsenate (V) group, in place of one of the hydroxyl groups. It can be inferred that the $-AsO_3H_2$ group binds to the Fe(III) rather than the aromatic group of the roxarsone. The addition of kaolinite was shown to enhance arsenic uptake for roxarsone and arsenate (V). This is more apparent in studies related to the *one-pot* method. The addition of the biopolymers seems better suited to colloid removal rather than arsenic because

Fe(III) does an excellent job on its own through charge neutralization and some amount of adsorption onto iron hydr(oxides). However, since many natural systems contain arsenic and colloidal materials, the Fe(III)-MMWC/MMWC will be beneficial for removal of suspended solids.

6.3 Future Work

Some aspects of this research could benefit from extending further studies of the type presented herein. One limitation of the Fe(III)-MMWC/HVA system is the level of removal *ca.* 40%. Comparison with other systems for arsenic removal show much higher removal efficiencies. However, the quantities of coagulant/flocculant species used for removal were very low and the amount of arsenic was higher (~30 ppm) in this research, as compared with other studies or those found in typical aquatic environments. The WHO sets the acceptable limit for arsenic in drinking water at below 10 ppb and natural waters studied usually have arsenic levels below the ppm level. For example, rivers and lakes can range from 10 µg/L to 5 mg/L due to anthropogenic contamination.[7] Factors, such as dosage of Fe(III) and the biopolymers may be adjusted and further removal studies can be conducted over variable arsenic concentration.

The flocs formed during the coagulation-flocculation process, especially with kaolinite present, are usually quite large and a potential source for further insight into the nature of the flocs through spectroscopic characterization. The nature of the floc refers to the components that contribute to their formation and the types of binding that occur. This will lead to an improved understanding of the mechanism of the floc formation process. It has been posited that the biopolymer(s) self-assembles onto the solid iron (III) hydroxides where spectroscopic methods such as Scanning Electron Microscopy (SEM) and Dynamic Light Scattering (DLS) may reveal the mode of binding. Infrared (IR) spectroscopy and X-ray absorption spectroscopy (XAS) may also be used for further elucidation of binding within the flocs.

Studies on the type of complexation between Fe(III) and arsenate (V) have been done.[112,113] The general consensus is an inner-sphere complex between Fe(III) and arsenate (V). This was determined by electrophoretic mobility (EM), Fourier Transform Infrared (FTIR) and Raman spectroscopy, sorption studies and the use of surface complexation models, such as the constant capacitance model.[112] These methods can be applied to the Fe(III)-MMWC/HVA system for a more detailed study into the molecular structure of the flocs formed. Controlled formation of larger

sized flocs may be achieved by increasing the Fe(III) concentration and ageing of the Fe(III) chloride solution at variable timescale.

The investigation reported herein was conducted using model arsenic and kaolinite system in Millipore water. This was done to minimize the contribution of ionic species, which was proven to influence the uptake of contaminants, structure of biopolymers, etc. The utility of this work was not meant to be limited to model systems. Further studies using real environmental samples from natural water sources, such as industrial tailing ponds, are essential to affirming the *proof-of-concept* of the coagulation-flocculation treatment process. These studies would also help to elucidate the role of competitive ions in the removal of arsenic, whether they are a help or hindrance.

REFERENCES

(1) Patnaik, P. Handbook of Inorganic Chemicals; McGraw-Hill: New York, 2003; pp 61–63.

(2) Arsenic http://www.rsc.org/periodic-table/element/33/arsenic (accessed Apr 11, 2016).

(3) Manning, B. A.; Goldberg, S. Adsorption and Stability of Arsenic(III) at the Clay Mineral−Water Interface. *Environ. Sci. Technol.* **1997**, *31* (7), 2005–2011.

(4) Bissen, M.; Frimmel, F. H. Arsenic — a Review. Part I: Occurrence, Toxicity, Speciation, Mobility. *Acta Hydrochim. Hydrobiol.* **2003**, *31* (1), 9–18.

(5) Chiban, M.; Zerbet, M.; Carja, G.; Sinan, F. Application of Low-Cost Adsorbents for Arsenic Removal: A Review. *J. Environ. Chem. Ecotoxicol.* **2012**, *4* (5), 91–102.

(6) Sarkar, A.; Paul, B. The Global Menace of Arsenic and Its Conventional Remediation - A Critical Review. *Chemosphere* **2016**, *158*, 37–49.

(7) Smedley, P. L.; Kinniburgh, D. G. *Source and Behaviour of Arsenic in Natural Waters Importance of Arsenic in Drinking Water*; Geneva, Switzerland, 2001.

(8) Lloyd, N. C.; Morgan, H. W.; Nicholson, B. K.; Ronimus, R. S. The Composition of Ehrlich's Salvarsan: Resolution of a Century-Old Debate. *Angew. Chem. Int. Ed. Engl.* **2005**, *44* (6), 941–944.

(9) Hu, J.; Tong, Z.; Hu, Z.; Chen, G.; Chen, T. Adsorption of Roxarsone from Aqueous Solution by Multi-Walled Carbon Nanotubes. *J. Colloid Interface Sci.* **2012**, *377* (1), 355–361.

(10) Brown, B. L. The Sorption of Roxarsone, an Organoarsenical Animal Feed Additive. **2003**, 1–95.

(11) Hu, C.; Chen, Q.; Liu, H.; Qu, J. Coagulation of Methylated Arsenic from Drinking Water: Influence of Methyl Substitution. *J. Hazard. Mater.* **2015**, *293*, 97–104.

(12) Bentley, R.; Chasteen, T. G. Microbial Methylation of Metalloids: Arsenic, Antimony, and Bismuth. *Microbiol. Mol. Biol. Rev.* **2002**, *66* (2), 250–271.

(13) Gupta, R. C. (Ramesh C. Handbook of Toxicology of Chemical Warfare Agents; Elsevier/Academic Press, 2009; p 1147.

(14) Pontoni, L.; Fabbricino, M. Use of Chitosan and Chitosan-Derivatives to Remove Arsenic from Aqueous Solutions—a Mini Review. *Carbohydr. Res.* **2012**, *356*, 86–92.

(15) Roy, P.; Saha, A. Metabolism and Toxicity of Arsenic: A Human Carcinogen. *Curr. Sci.* **2002**, *82* (1), 38–45.

(16) Jain, C. K.; Ali, I. Arsenic: Occurrence, Toxicity and Speciation Techniques. *Water Res.* **2000**, *34* (17), 4304–4312.

(17) Mohan, D.; Pittman, C. U. Arsenic Removal from Water/wastewater Using adsorbents—A Critical Review. *J. Hazard. Mater.* **2007**, *142* (1), 1–53.

(18) Smedley, P. .; Kinniburgh, D. . A Review of the Source, Behaviour and Distribution of Arsenic in Natural Waters. *Appl. Geochemistry* **2002**, *17* (5), 517–568.

(19) Crecelius, E. A.; Johnson, C. J.; Hofer, G. C. Contamination of Soils near a Copper Smelter by Arsenic, Antimony and Lead. *Water. Air. Soil Pollut.* **1974**, *3* (3), 337–342.

(20) Romero, L.; Alonso, H.; Campano, P.; Fanfani, L.; Cidu, R.; Dadea, C.; Keegan, T.; Thornton, I.; Farago, M. Arsenic Enrichment in Waters and Sediments of the Rio Loa (Second Region, Chile). *Appl. Geochemistry* **2003**, *18* (9), 1399–1416.

(21) Azcue, J. M.; Nriagu, J. O. Impact of Abandoned Mine Tailings on the Arsenic Concentrations in Moira Lake, Ontario. *J. Geochemical Explor.* **1995**, *52* (1–2), 81–89.

(22) Schwarzenbach, R. P.; Egli, T.; Hofstetter, T. B.; von Gunten, U.; Wehrli, B. Global Water Pollution and Human Health. *Annu. Rev. Environ. Resour.* **2010**, *35* (1), 109–136.

(23) Chapelle, F. H.; Lovley, D. R. Competitive Exclusion of Sulfate Reduction by Fe(lll)-Reducing Bacteria: A Mechanism for Producing Discrete Zones of High-Iron Ground Water. *Ground Water* **1992**, *30* (1), 29–36.

(24) Amini, M.; Abbaspour, K. C.; Berg, M.; Winkel, L.; Hug, S. J.; Hoehn, E.; Yang, H.; Johnson, C. A. Statistical Modeling of Global Geogenic Arsenic Contamination in Groundwater. *Environ. Sci. Technol.* **2008**, *42* (10), 3669–3675.

(25) Pourbaix Diagrams https://www.wou.edu/las/physci/ch412/pourbaix.htm (accessed Apr 11, 2016).

(26) IARC Working Group on the Evaluation of Carcinogenic Risks to Humans. Arsenic, Metals, Fibres, and dusts.No Title. *IARC Monogr. Eval. Carcinog. Risks Hum.* **2012**, *100*, 11–465.

(27) Lage, C. R.; Nayak, A.; Kim, C. H. Arsenic Ecotoxicology and Innate Immunity. *Integr. Comp. Biol.* **2006**, *46* (6), 1040–1054.

(28) Renault, F.; Sancey, B.; Badot, P.-M.; Crini, G. Chitosan for Coagulation/flocculation Processes – An Eco-Friendly Approach. *Eur. Polym. J.* **2009**, *45* (5), 1337–1348.

(29) Baskan, M. B.; Pala, A. A Statistical Experiment Design Approach for Arsenic Removal by

Coagulation Process Using Aluminum Sulfate. *Desalination* **2010**, *254* (1), 42–48.

(30) Baskan, M. B.; Pala, A. Determination of Arsenic Removal Efficiency by Ferric Ions Using Response Surface Methodology. *J. Hazard. Mater.* **2009**, *166* (2), 796–801.

(31) Baskan, M. B.; Pala, A.; Türkman, A. Arsenate Removal by Coagulation Using Iron Salts and Organic Polymers. *Ekoloji* **2010**, *74* (19), 69–76.

(32) Singh, R.; Singh, S.; Parihar, P.; Singh, V. P.; Prasad, S. M. Arsenic Contamination, Consequences and Remediation Techniques: A Review. *Ecotoxicol. Environ. Saf.* **2015**, *112*, 247–270.

(33) Wilson, L. D. Overview of Coagulation-Flocculation Technology. *Water Cond. Purific. Mag.* **2014**, *56* (4), 28–34.

(34) Thirunavukkarasu, O. S.; Viraraghavan, T.; Subramanian, K. S.; Tanjore, S. Organic Arsenic Removal from Drinking Water. *Urban Water* **2002**, *4* (4), 415–421.

(35) Ramesh, A.; Hasegawa, H.; Maki, T.; Ueda, K. Adsorption of Inorganic and Organic Arsenic from Aqueous Solutions by Polymeric Al/Fe Modified Montmorillonite. *Sep. Purif. Technol.* **2007**, *56* (1), 90–100.

(36) Cheng, Z.; Van Geen, A.; Louis, R.; Nikolaidis, N.; Bailey, R. Removal of Methylated Arsenic in Groundwater with Iron Filings. *Environ. Sci. Technol.* **2005**, *39* (19), 7662–7666.

(37) Lafferty, B. J.; Loeppert, R. H. Methyl Arsenic Adsorption and Desorption Behavior on Iron Oxides. *Environ. Sci. Technol.* **2005**, *39* (7), 2120–2127.

(38) Banerjee, K.; Helwick, R. P.; Gupta, S. A Treatment Process for Removal of Mixed Inorganic and Organic Arsenic Species from Groundwater. *Environ. Prog.* **1999**, *18* (4), 280–284.

(39) Leupin, O. X.; Hug, S. J. Oxidation and Removal of Arsenic (III) from Aerated Groundwater by Filtration through Sand and Zero-Valent Iron. *Water Res.* **2005**, *39* (9), 1729–1740.

(40) Meng, X.; Bang, S.; Korfiatis, G. P. Effects of Silicate, Sulfate, and Carbonate on Arsenic Removal by Ferric Chloride. *Water Res.* **2000**, *34* (4), 1255–1261.

(41) Košutić, K.; Furač, L.; Sipos, L.; Kunst, B. Removal of Arsenic and Pesticides from Drinking Water by Nanofiltration Membranes. *Sep. Purif. Technol.* **2005**, *42* (2), 137–144.

(42) Hering, J.; Chen, P.; Wilkie, J.; Elimelech, M. Arsenic Removal from Drinking Water during Coagulation. *J. Environ. Eng.* **1997**, *123* (8), 800–807.

(43) Farid, H.; Bijan, B.; Ebrahimi, A.; Amin, M. M. Arsenic Removal by Coagulation Using Ferric Chloride and Chitosan from Water. *Int J Env Heal. Eng* **2013**, *1* (9), 1–6.

(44) Zouboulis, A.; Katsoyiannis, I. Removal of Arsenates From Contaminated Water By Coagulation–Direct Filtration. *Sep. Sci. Technol.* **2002**, *37* (12), 2859–2873.

(45) Lenoble, V. Arsenite Oxidation and Arsenate Determination by the Molybdene Blue Method. *Talanta* **2003**, *61* (3), 267–276.

(46) Dhar, R. K.; Zheng, Y.; Rubenstone, J.; van Geen, A. A Rapid Colorimetric Method for Measuring Arsenic Concentrations in Groundwater. *Anal. Chim. Acta* **2004**, *526* (2), 203–209.

(47) Chun, J.; Lee, H.; Lee, S.-H.; Hong, S.-W.; Lee, J.; Lee, C.; Lee, J. Magnetite/mesocellular Carbon Foam as a Magnetically Recoverable Fenton Catalyst for Removal of Phenol and Arsenic. *Chemosphere* **2012**, *89* (10), 1230–1237.

(48) Yoon, S.-H.; Oh, S.-E.; Yang, J. E.; Lee, J. H.; Lee, M.; Yu, S.; Pak, D. Titanium Dioxide Photocatalytic Oxidation Mechanism of As(III). *Environ. Sci. Technol.* **2009**, *43* (3), 864–869.

(49) Aryal, M.; Ziagova, M.; Liakopoulou-Kyriakides, M. Study on Arsenic Biosorption Using Fe(III)-Treated Biomass of Staphylococcus Xylosus. *Chem. Eng. J.* **2010**, *162* (1), 178–185.

(50) Li, J.; Jiao, S.; Zhong, L.; Pan, J.; Ma, Q. Optimizing Coagulation and Flocculation Process for Kaolinite Suspension with Chitosan. *Colloids Surfaces A Physicochem. Eng. Asp.* **2013**, *428*, 100–110.

(51) Bratby, J. Coagulation and Flocculation in Water and Wastewater Treatment; Uplands Press Ltd.: Croydon, 1980; pp 56–76.

(52) Petzold, G.; Schwarz, S. Polyelectrolyte Complexes in Flocculation Applications. In *Polyelectrolyte Complexes in the Dispersed and Solid State II: Application Aspects*; Müller, M., Ed.; Springer Berlin Heidelberg: Berlin, Heidelberg, 2014; pp 25–65.

(53) Li, J.; Song, X.; Pan, J.; Zhong, L.; Jiao, S.; Ma, Q. Adsorption and Flocculation of Bentonite by Chitosan with Varying Degree of Deacetylation and Molecular Weight. *Int. J. Biol. Macromol.* **2013**, *62*, 4–12.

(54) Taubaeva, R.; Meszaros, R.; Musabekov, K.; Barany, S. Electrokinetic Potential and Flocculation of Bentonite Suspensions in Solutions of Surfactants, Polyelectrolytes and

Their Mixtures. *Colloid J.* **2015**, *77* (1), 91–98.

(55) Biggs, S.; Habgood, M.; Jameson, G. J.; Yan, Y. Aggregate Structures Formed via a Bridging Flocculation Mechanism. *Chem. Eng. J.* **2000**, *80* (1), 13–22.

(56) Aragonés-Beltrán, P.; Mendoza-Roca, J. A.; Bes-Piá, A.; García-Melón, M.; Parra-Ruiz, E. Application of Multicriteria Decision Analysis to Jar-Test Results for Chemicals Selection in the Physical–chemical Treatment of Textile Wastewater. *J. Hazard. Mater.* **2009**, *164* (1), 288–295.

(57) Clark, T.; Stephenson, T. Development of a Jar Testing Protocol for Chemical Phosphorus Removal in Activated Sludge Using Statistical Experimental Design. *Water Res.* **1999**, *33* (7), 1730–1734.

(58) Satterfield, Z. Jar Testing. *Natl. Environ. Serv. Cent. Tech Br.* **2005**, *5* (1), 2–4.

(59) Mohamed H. Mohamed; Wilson, L. D. Kinetic Uptake Studies of Powdered Materials in Solution. *Nanomaterials* **2015**, *5*, 969–980.

(60) Kwon, J. H.; Wilson, L. D.; Sammynaiken, R. S. Sorptive Uptake Studies of an Aryl-Arsenical with Iron Oxide Composites on an Activated Carbon Support. *Materials (Basel).* **2014**, *7* (3), 1880–1898.

(61) Xue, C.; Wilson, L. D. Kinetic Study on Urea Uptake with Chitosan Based Sorbent Materials. *Carbohydr. Polym.* **2016**, *135*, 180–186.

(62) Mahaninia, M. H.; Wilson, L. D. Phosphate Uptake Studies of Cross-Linked Chitosan Bead Materials. *J. Colloid Interface Sci.* **2017**, *485*, 201–212.

(63) Dolatkhah, A. S.; Wilson, L. D. Magnetite/Polymer Brush Nanocomposites with Switchable Uptake Behavior Toward Methylene Blue. *ACS Appl. Mater. Interfaces* **2016**, *8* (8), 5595–5607.

(64) Fox, D. I.; Stebbins, D. M.; Alcantar, N. A. Combining Ferric Salt and Cactus Mucilage for Arsenic Removal from Water. *Environ. Sci. Technol.* **2016**, *50* (5), 2507–2513.

(65) Younes, I.; Rinaudo, M. Chitin and Chitosan Preparation from Marine Sources. Structure, Properties and Applications. *Mar. Drugs* **2015**, *13* (3), 1133–1174.

(66) Pillai, C. K. S.; Paul, W.; Sharma, C. P. Chitin and Chitosan Polymers: Chemistry, Solubility and Fiber Formation. *Prog. Polym. Sci.* **2009**, *34* (7), 641–678.

(67) Rinaudo, M. Chitin and Chitosan: Properties and Applications. *Prog. Polym. Sci.* **2006**, *31* (7), 603–632.

(68) Yuan, Y.; Chesnutt, B. M.; Haggard, W. O.; Bumgardner, J. D. Deacetylation of Chitosan: Material Characterization and in Vitro Evaluation via Albumin Adsorption and Pre-Osteoblastic Cell Cultures. *Materials (Basel).* **2011**, *4* (12), 1399–1416.

(69) Park, J. K.; Chung, M. J.; Choi, H. N.; Park, Y. Il. Effects of the Molecular Weight and the Degree of Deacetylation of Chitosan Oligosaccharides on Antitumor Activity. *Int. J. Mol. Sci.* **2011**, *12* (1), 266–277.

(70) Park, J. K.; Chung, M. J.; Choi, H. N.; Park, Y. Il. Effects of the Molecular Weight and the Degree of Deacetylation of Chitosan Oligosaccharides on Antitumor Activity. *Int. J. Mol. Sci.* **2011**, *12* (1), 266–277.

(71) Zheng, H.; Zhu, G.; Jiang, S.; Tshukudu, T.; Xiang, X.; Zhang, P.; He, Q. Investigations of Coagulation–flocculation Process by Performance Optimization, Model Prediction and Fractal Structure of Flocs. *Desalination* **2011**, *269* (1), 148–156.

(72) Singh, R. P.; Tripathy, T.; Karmakar, G. P.; Rath, S. K.; Karmakar, N. C.; Pandey, S. R.; Kannan, K.; Jain, S. K.; Lan, N. T. Novel Biodegradable Flocculants Based on Polysaccharides. *Curr. Sci.* **2000**, *78* (7), 798–803.

(73) Dutta, P. K.; Duta, J.; Tripathi, V. S. Chitin and Chitosan: Chemistry, Properties and Applications. *J. Sci. Ind. Res. (India).* **2004**, *63* (1), 20–31.

(74) Jain, D.; Banerjee, R. Comparison of Ciprofloxacin Hydrochloride-Loaded Protein, Lipid, and Chitosan Nanoparticles for Drug Delivery. *J. Biomed. Mater. Res. B. Appl. Biomater.* **2008**, *86* (1), 105–112.

(75) Hejazi, R.; Amiji, M. Chitosan-Based Gastrointestinal Delivery Systems. *J. Control. Release* **2003**, *89* (2), 151–165.

(76) Bárány, S.; Meszaros, R.; Marcinova, L.; Skvarla, J. Effect of Polyelectrolyte Mixtures on the Electrokinetic Potential and Kinetics of Flocculation of Clay Mineral Particles. *Colloids Surfaces A Physicochem. Eng. Asp.* **2011**, *383* (1), 48–55.

(77) Guibal, E.; Van Vooren, M.; Dempsey, B. A.; Roussy, J. A Review of the Use of Chitosan for the Removal of Particulate and Dissolved Contaminants. *Sep. Sci. Technol.* **2006**, *41* (11), 2487–2514.

(78) Vandenbossche, M.; Jimenez, M.; Casetta, M.; Traisnel, M. Remediation of Heavy Metals by Biomolecules: A Review. *Crit. Rev. Environ. Sci. Technol.* **2015**, *45* (15), 1644–1704.

(79) Vandenbossche, M.; Jimenez, M.; Casetta, M.; Bellayer, S.; Bourbigot, S.; Traisnel, M.

Sorption of Heavy Metals on a Chitosan-Grafted-Polypropylene Nonwoven Geotextile. **2011**, *5003*, 1–4.

(80) Draget, K. I.; Smidsrød, O.; Skjåk-Bræk, G. Alginates from Algae. In *Polysaccharides and Polyamides in the Food Industry. Properties, Production and Patents.*; Steinbuchel, A., Rhee, S. K., Eds.; Wiley-VCH GmbH & Co.: Weinheim, 2005; pp 1–26.

(81) McHugh, D. J. A Guide to the Seaweed Industry. In *FAO Fisheries Technical Paper*; 2003; p 105.

(82) McHugh, D. J. Production, Properties and Uses of Alginate http://www.fao.org/3/a-x5822e/x5822e04.htm (accessed Apr 11, 2017).

(83) Lee, K. Y.; Mooney, D. J. Alginate: Properties and Biomedical Applications. *Prog. Polym. Sci.* **2012**, *37* (1), 106–126.

(84) Chuah, H. .; Lin-Vien, D.; Soni, U. Poly(trimethylene Terephthalate) Molecular Weight and Mark–Houwink Equation. *Polymer (Guildf).* **2001**, *42* (16), 7137–7139.

(85) Onsøyen, E. Alginates. In *Thickening and Gelling Agents for Food*; Imeson, A. P., Ed.; Springer US: Boston, MA, 1997; pp 22–44.

(86) Donati, I.; Paoletti, S. Material Properties of Alginates. In *Alginates: Biology and Applications. Microbiology Monographs*; Rehm, B. H. A., Ed.; Springer Berlin Heidelberg: Berlin, Heidelberg, 2009; pp 1–46.

(87) Ramsay, J. A.; Mok, W. H. W.; Luu, Y.-S.; Savage, M. Decoloration of Textile Dyes by Alginate-Immobilized Trametes Versicolor. *Chemosphere* **2005**, *61* (7), 956–964.

(88) Chen, J.-P.; Lin, Y.-S. Decolorization of Azo Dye by Immobilized Pseudomonas Luteola Entrapped in Alginate–silicate Sol–gel Beads. *Process Biochem.* **2007**, *42* (6), 934–942.

(89) Qin, Y.; Hu, H.; Luo, A. The Conversion of Calcium Alginate Fibers into Alginic Acid Fibers and Sodium Alginate Fibers. *J. Appl. Polym. Sci.* **2006**, *101* (6), 4216–4221.

(90) Thu, B.; Bruheim, P.; Espevik, T.; Smidsrød, O.; Soon-Shiong, P.; Skjåk-Bræk, G. Alginate Polycation Microcapsules: I. Interaction between Alginate and Polycation. *Biomaterials* **1996**, *17* (10), 1031–1040.

(91) Nazzaro, F.; Orlando, P.; Fratianni, F.; Coppola, R. Microencapsulation in Food Science and Biotechnology. *Curr. Opin. Biotechnol.* **2012**, *23* (2), 182–186.

(92) Escudero, C.; Fiol, N.; Villaescusa, I.; Bollinger, J.-C. Arsenic Removal by a Waste Metal (Hydr)oxide Entrapped into Calcium Alginate Beads. *J. Hazard. Mater.* **2009**, *164* (2), 533–

541.

(93) Lim, S.-F.; Zheng, Y.-M.; Zou, S.-W.; Chen, J. P. Uptake of Arsenate by an Alginate-Encapsulated Magnetic Sorbent: Process Performance and Characterization of Adsorption Chemistry. *J. Colloid Interface Sci.* **2009**, *333* (1), 33–39.

(94) Lim, S. F.; Chen, J. P. Synthesis of an Innovative Calcium-Alginate Magnetic Sorbent for Removal of Multiple Contaminants. *Appl. Surf. Sci.* **2007**, *253* (13), 5772–5775.

(95) Listiarini, K.; Tan, L.; Sun, D. D.; Leckie, J. O. Systematic Study on Calcium–alginate Interaction in a Hybrid Coagulation-Nanofiltration System. *J. Memb. Sci.* **2011**, *370* (1), 109–115.

(96) Michaels, A. S. Polyelectrolytes Complexes. *Ind. Eng. Chem.* **1965**, *57* (10), 32–40.

(97) Sæther, H. V.; Holme, H. K.; Maurstad, G.; Smidsrød, O.; Stokke, B. T. Polyelectrolyte Complex Formation Using Alginate and Chitosan. *Carbohydr. Polym.* **2008**, *74* (4), 813–821.

(98) Russel, W. B.; Saville, D. A.; Schowalter, W. R. Colloidal Dispersions; Cambridge University Press: Cambridge, 1989; pp 310–328.

(99) Becherán-Marón, L.; Peniche, C.; Argüelles-Monal, W. Study of the Interpolyelectrolyte Reaction between Chitosan and Alginate: Influence of Alginate Composition and Chitosan Molecular Weight. *Int. J. Biol. Macromol.* **2004**, *34* (1), 127–133.

(100) Li, X.; Xie, H.; Lin, J.; Xie, W.; Ma, X. Characterization and Biodegradation of Chitosan–alginate Polyelectrolyte Complexes. *Polym. Degrad. Stab.* **2009**, *94* (1), 1–6.

(101) Han, J.; Zhou, Z.; Yin, R.; Yang, D.; Nie, J. Alginate–chitosan/hydroxyapatite Polyelectrolyte Complex Porous Scaffolds: Preparation and Characterization. *Int. J. Biol. Macromol.* **2010**, *46* (2), 199–205.

(102) Wibowo, S.; Velazquez, G.; Savant, V.; Torres, J. A. Surimi Wash Water Treatment for Protein Recovery: Effect of Chitosan–alginate Complex Concentration and Treatment Time on Protein Adsorption. *Bioresour. Technol.* **2005**, *96* (6), 665–671.

(103) Spectrum Labs. Pore Size http://spectrumlabs.com/dialysis/PoreSize.html (accessed Apr 11, 2017).

(104) Sigma-Aldrich. Whatman quantitative filter paper, Grade 40 http://www.sigmaaldrich.com/catalog/product/aldrich/z241318?lang=en&region=CA (accessed Apr 11, 2017).

(105) Chang, R. Physical Chemistry for the Biosciences; University Science Books: Sausalito, California, 2005; pp 333–340.

(106) Srivastava, P.; Singh, B.; Angove, M. Competitive Adsorption Behavior of Heavy Metals on Kaolinite. *J. Colloid Interface Sci.* **2005**, *290* (1), 28–38.

(107) Ma, C.; Eggleton, R. A. Cation Exchange Capacity of Kaolinite. *Clay Clay Miner.* **1999**, *47* (2), 174–180.

(108) Sreeram, K. J.; Yamini Shrivastava, H.; Nair, B. U. Studies on the Nature of Interaction of iron(III) with Alginates. *Biochim. Biophys. Acta - Gen. Subj.* **2004**, *1670* (2), 121–125.

(109) Beverskog, B.; Puigdomenech, I. Revised Pourbaix Diagrams for Iron at 25–300 °C. *Corros. Sci.* **1996**, *38* (12), 2121–2135.

(110) McCafferty, E. Introduction to Corrosion Science; Springer New York, 2010; p 96.

(111) Kwon, J. H.; Wilson, L. D.; Sammynaiken, R. Sorptive Uptake of Selenium with Magnetite and Its Supported Materials onto Activated Carbon. *J. Colloid Interface Sci.* **2015**, *457*, 388–397.

(112) Goldberg, S.; Johnston, C. T. Mechanisms of Arsenic Adsorption on Amorphous Oxides Evaluated Using Macroscopic Measurements, Vibrational Spectroscopy, and Surface Complexation Modeling. *J. Colloid Interface Sci.* **2001**, *234* (1), 204–216.

(113) Sherman, D. M.; Randall, S. R. Surface Complexation of arsenic(V) to iron(III) (Hydr)oxides: Structural Mechanism from Ab Initio Molecular Geometries and EXAFS Spectroscopy. *Geochim. Cosmochim. Acta* **2003**, *67* (22), 4223–4230.